LA-UR-01-273 January, 2001

Applications of Non-Reactive Compressible Fluids

Ralph Menikoff, rtm@lanl.gov

Theoretical Division, mail stop B214

Los Alamos National Laboratory

Los Alamos, New Mexico 87544

U. S. A.

PREFACE

Compressible fluid flow is modeled by a system of partial differential equations (PDEs) that express the conservation laws of mass, momentum and energy. The PDEs must be supplemented by an equilibrium equation of state (EOS) which characterizes the material properties of the fluid. For a thermodynamically consistent EOS the PDEs are hyperbolic. Consequently, an important aspect of fluid flow is its non-linear wave behavior. These lectures focus on the wave structure of fluid flow in both one and two dimensions.

The perspective presented here results from working with James Glimm and collaborators on the development of the front tracking algorithm. However, the understanding of the wave structure is important in its own right. In particular, for a well-posed initial value problem, the wave structure places stronger constraints on the EOS then is imposed by thermodynamics. Constriants on the EOS are important for all numerical algorithms since their solutions must reflect those of the PDEs they are approximating.

There is a tendency among those performing numerical calculations to treat an EOS as a given. This is due to the complex physical phenomena needed in order to understand the construction of a model EOS and its domain of validity. Uncritically accepting an EOS that violates the constraints imposed by the wave structure can result in a calculation being numerical unstable or giving a qualitatively incorrect solution for the intended application.

Simple wave patterns can be used as building blocks to obtain an understanding of more complicated flows. This is particularly useful for applications when analytic solutions are not available. The wave structure provides an important consistency check on the most singular part of the solution to the fluid flow and can be used for assessing the accuracy of a calculation.

The understanding of the topics presented is the result of joint work with several colleagues. In particular, it is a pleasure to acknowledge the contributions of Bradley Plohr, John Grove and Klaus Lackner.

These lecture notes are based on a two week coarse taught at the **Ecole d'Eté d'Analyse Numérique**, sponsored by C.E.A., I.N.R.I.A. and E.D.F. The summer school focused on **Problèmes Hyperboliques et Applications aux Ecoulements Réactifs et Non-Réactifs**. It was held at the **Centre d'Etudes du Bréau** (outside Paris, France) from 28 June – 9 July, 1993. I wish to express my appreciatation to the organizers of the summer school for their hospitality.

Ralph Menikoff

Los Alamos, NM

CONTENTS

IN PREPARATION

Notation

c	sound speed
g	dimensionless inverse specific heat
t	time coordinate
u	particle velocity
x	spatial coordinate

E	specific internal energy
H	enthalpy, $E + PV$
M	Mach number, u/c
P	pressure
S	specific entropy
T	temperature
V	specific volume

Quasi-linear hyperbolic system of PDEs

$$\partial_t \vec{w} + \partial_x \vec{F}(\vec{w}) = 0$$

DF	derivative of flux function
$\vec{L}$	left eigenfunction of **DF**
$\vec{R}$	right eigenfunction of **DF**
$R_\pm$	Riemann invariants

Greek Symbols

γ	adiabatic exponent
λ	characteristic velocity
ρ	material density
σ	wave speed
Γ	Grüneisen coefficient

Other Symbols

$\mathcal{E}$	total specific energy, $E + \frac{1}{2}\,u^2$
$\mathcal{G}$	fundamental derivative of fluid dynamics
d/dt	convective derivative, $\partial_t + u\partial_x$

Lecture 1
Compressible Fluid Equations

Fluid flow is a theory for a continuous medium, and is modeled by a system of partial differential equations (PDEs). These equations can be written in different forms to emphasis different aspects of the problem. In this lecture we review the various forms of the equations for fluid flow in one-dimension. We assume an **ideal fluid** in which transport effects (such as viscosity, heat conduction and radiation) are neglected.

1.1 Conservation Form

Physical principles lead to integral equations that express the conservation of mass, momentum and energy; see Ex. 1.1. The integral equations are equivalent to the PDEs in conservation form

$$\partial_t \begin{pmatrix} \rho \\ \rho u \\ \rho(\frac{1}{2}u^2 + E) \end{pmatrix} + \partial_x \begin{pmatrix} \rho u \\ \rho u^2 + P \\ \rho(\frac{1}{2}u^2 + E)u + Pu \end{pmatrix} = - \begin{pmatrix} 0 \\ \rho \partial_x \Phi \\ \rho u \partial_x \Phi \end{pmatrix} \tag{1.1}$$

where

u = particle velocity,
ρ = mass density,
E = specific internal energy,
P = pressure,
Φ = gravitational potential energy.

In conservation form the PDEs consist of the sum of terms involving the time derivative of a density for a conserved quantity, the spatial derivative of a flux and a source term. Source terms do not contain any partial derivatives of the dependent variables; $\Phi(x)$ is assumed to be independent of the fluid variables. Henceforth, we assume that the effect

of gravity is small and the source terms can be neglected. However, the dominant effect for multi-dimensions can frequently be approximated as a geometric source term for quasi 1-D fluid flow; see Exs. 1.2 and 1.3.

The fluid equations must be supplemented by a constitutive relation that specifies the material properties. The constitutive relation of a fluid is called an **equation of state** (EOS). For the ideal fluid flow equations only an incomplete EOS is needed; $P(V, E)$ where $V = 1/\rho$ is specific volume. A simple example is an ideal gas EOS

$$P = (\gamma - 1)E/V \tag{1.2}$$

where $\gamma > 1$. The EOS for realistic materials are described later in more detail.

Mathematically, the conservation form of the fluid flow equations are an example of a **System of Quasi-Linear Hyperbolic PDEs** of the form

$$\partial_t \vec{w} + \partial_x \vec{F}(\vec{w}) = \vec{0} \ , \tag{1.3}$$

where $\vec{w}$ and $\vec{F}$ are vectors with N components. These equations (i) are linear in derivatives, (ii) have a non-linear flux function, $\vec{F}(\vec{w})$, and (iii) are hyperbolic when the linearized equations are hyperbolic; *i.e.*, the PDEs can be written as

$$\partial_t \vec{w} + \mathbf{DF} \cdot \partial_x \vec{w} = \vec{0} \ , \tag{1.3a}$$

and the derivative matrix of the flux function,

$$\mathbf{DF}_{ij} = \partial F_i / \partial w_j \ , \tag{1.4a}$$

has a complete set of eigenvectors with real eigenvalues. Thus, **DF** can be expressed as

$$\mathbf{DF} = \sum_i \lambda_i \, \vec{R}_i \otimes \vec{L}_i \tag{1.4b}$$

where λ_i are the eigenvalues, and $\vec{R}_i$ and $\vec{L}_i$ are right and left eigenvectors normalized such that $(\vec{L}_i, \vec{R}_j) = \delta_{i,j}$. The right eigenvectors can be though of as a matrix with one column and the left eigenvectors as a matrix with one row.

It follows from Eqs. (1.3a) and (1.4b) that

$$\vec{L}_i \cdot (\partial_t + \lambda_i \partial_x) \, \vec{w} = 0 \ , \tag{1.5a}$$

for $i = 1, 2, \cdots, N$. Hence,

$$(\partial_t + \lambda_i \partial_x)\,(\vec{L}_i \cdot \vec{w}) = \vec{w} \cdot (\partial_t + \lambda_i \partial_x)\,\vec{L}_i \ . \tag{1.5b}$$

We note, for a linear flux function, $\vec{L}_i(x,t) =$ constant and the right hand side vanishes. In this case the system of PDEs reduces to N scalar wave equations, with wave speeds λ_i. For this reason, the eigenvalues of **DF** are called **characteristic velocities**. Subsequently, we will see that the characteristic velocities play an important role in the analysis of both non-linear waves and numerical algorithms.

Remark 1.1: The term characteristic is sometimes used to denote a typical scale. As an example of this usage, for viscous fluids the dimensionless Reynolds number is defined as $Re = UL/\nu$, where U and L are characteristic velocity and length scales for the flow of interest, and ν is the kinematic viscosity. In contrast, the term characteristic velocity in the context of hyperbolic PDEs has a precise meaning; namely, a wave speed for the linearized equations.

For a non-linear flux function, the wave speeds λ_i can not be treated as globally constant. This leads to non-linear wave behavior in the solution of the PDEs. In these lectures, the non-linear wave properties are derived in the context of fluid flow. The properties for compressible fluid flow which can be abstracted and applied in general to Quasi-Linear Hyperbolic PDEs are summarized below:

0. $\vec{L}_i$ and λ_i are functions of $\vec{w}$ and hence of x and t.
1. A solution to the Cauchy problem with smooth initial data does <u>not necessarily</u> remain smooth. Discontinuities called shock waves can form in a finite time; see Exs. 1.6 and 1.7. A discontinuous solution to the PDEs in the sense of a distribution is known as a **weak solution**. This is in contrast to a classical smooth solution to the PDEs.
2. Conservation form enables weak solutions to be well defined. The jump in $\vec{w}$ across a shock wave is not arbitrary. Moreover, the wave speed is related to the magnitude of the discontinuity. This will be discussed in the next lecture.

3. Weak solutions are not unique. The PDEs must be supplemented with additional constraints, which for applications must be determined by the underlying physics. The additional constraints select out the admissible shock waves. This will be discussed in the next lecture.

Numerical algorithms to solve PDEs must be compatible with the structure of the solutions. The qualitative wave structure depends on general properties of the flux function. For the fluid equations, the flux function is determined by the EOS. The effect of the EOS on the wave structure will be discussed in great detail in Lecture 4.

Systems of conservation laws frequently occur in physics, and are often modeled by quasi-linear hyperbolic PDEs. Important examples of such systems are: (i) Steady supersonic two-dimensional flow (discussed later in more detail); (ii) Buckley–Leveret equations for 3 phase flow used in oil reservoir simulations; (iii) Magneto-hydrodynamics; (iv) Elastic flow in a solid. The general properties of the solution to the fluid flow equations that are derived in these lectures, also apply to these other systems. Fluid flow is a particularly nice physical system since there are many applications and experiments that can be used as a guide for developing an intuition and understanding for the properties of quasi-linear hyperbolic PDEs.

1.2 Euler's Equations

By simple algebraic manipulations, the fluid equations (1.1) can be recast in the non-conservative form

$$(d/dt)\begin{pmatrix}\rho\\ u\\ E\end{pmatrix} = -\begin{pmatrix}\rho\partial_x u\\ (1/\rho)\partial_x P\\ (P/\rho)\partial_x u\end{pmatrix} \tag{1.6}$$

where $(d/dt) = \partial_t + u\partial_x$ is the **convective derivative**, *i.e.*, the derivative along a particle path. For $(d/dt)\,u$ one subtracts from the momentum equation u times the mass equation, and for $(d/dt)E$ one subtracts from the energy equation the sum of E times the mass equation plus u times the average momentum component in Eqs. (1.1) and (1.6). This form of the PDEs for fluid flow is known as the Euler equations.

The Euler equations are useful for smooth flows. Since they specify the time derivatives ($\partial_t \rho$, $\partial_t E$ and $\partial_t u$), they can be used to solve the initial value problem: Given $\rho(x)$, $E(x)$ and $u(x)$ at time t_0, find the time evolution of the fluid for $t \geq t_0$. Boundary condition for the fluid equations are discussed in the next section. Euler's equations are not suited for determining solutions with shock waves. At a discontinuity, the right hand side of Eq. (1.6) has the form of the product of a step function with a δ-function. As a distribution this product is not well defined.

Invariance properties of fluid flow are easily seen from the Euler equations. In particular, the equations are **Galilean invariant**; *i.e.*, invariant under the transformation $x' = x + u_0 t$, $t' = t$ and $u' = u - u_0$. The fluid equations are also invariant under the **scale transformation** $x' = x/\alpha$, $t' = t/\alpha$ and $u' = u$, for any $\alpha > 0$. Formally, the fluid equations are time reversal invariant; *i.e.*, $t' = -t$ and $u' = -u$. However, we will show that shock waves or discontinuous solutions must break time reversal invariance. The invariance properties play an important role in the derivation of the elementary waves in the next lecture.

The fluid variables have dimensions. One is free to choose independently units for length, time and mass. It is important for numerical algorithms to use a compatible set of units for which no conversion factors are needed for specific energy density in the form E, u^2, or P/ρ. Standard sets of compatible units are given in Table 1. We note that a convenient reference pressure is a bar (0.987 atmosphere), and that both the MKS unit, $\mathrm{Pa} = \mathrm{N/m^2} = 10^{-5}\,\mathrm{b}$, and the cgs unit, $\mathrm{dyne/cm^2} = 10^{-6}\,\mathrm{b}$, are very small. The high pressure units in Table 1 are convenient for high explosives such as TNT.

In general the fluid equation are not invariant under an arbitrary change of units unless the equation of state is also transformed; $P'(V', E') = P(V, E)$. This is because EOS parameters typical have dimensions. However, an ideal gas equation of state, $P = (\gamma - 1)\rho E$, has no dimensional parameters. It has the special property that it is

	MKS units	high pressure units	
length	m	mm	cm
time	s	μs	μs
mass	kg	mg	g
derived units			
force	N (Newton)	kN	10^{12} dynes $= 10^7$ N
energy	J (Joule)	J	10^{12} ergs $= 10^5$ J
fluid variables			
ρ	kg/m^3	mg/mm^3 $= 10^3$ kg/m^3	g/cm^3 $= 10^3$ kg/m^3
u	m/s	mm/μs $= 10^3$ m/s	cm/μs $= 10^4$ m/s
E	J/kg	J/mg $= 10^6$ J/kg	Mb $\cdot$ cm^3/g $= 10^8$ J/kg
P	Pa (Pascal $=$ N/m^2)	GPa $= 10^9$ Pa	Mb $= 10^{11}$ Pa

Table I: Compatible units for fluid flow variables.

invariant under the general scale transformation

$$\left.\begin{aligned} x' &= x/\ell \\ t' &= t/\tau \\ \rho' &= \ell^3\rho/\mu \end{aligned}\right\} \quad \text{and} \quad \left\{\begin{aligned} u' &= (\tau/\ell)u \\ E' &= (\tau/\ell)^2 E \\ P' &= (\ell\tau^2/\mu)\rho \end{aligned}\right.$$

for any positive ℓ, τ and μ corresponding to the choice of units for length, time or mass. Therefore, the Euler equations with an ideal gas EOS are invariant under an arbitrary change of units. As a consequence, in this special case, the fluid equations have non-trivial **similarity solutions**. Two important similarity solutions are the Taylor-Sedov blast wave and the Guderley converging shock; see for example [Whitham, 1974] Sec. 6.16, or [Zel'dovich & Raizer, 1966] chpt. XII.

Entropy is an important physical quantity. Its time evolution can be derived from Euler's equations as follows. Substituting the first component into the third component of Eq. (1.6), the energy equation is equivalent to

$$(d/dt)E = -P(d/dt)V \ . \tag{1.7}$$

Comparing with the **fundamental thermodynamic identity**

$$dE = -PdV + TdS \ , \tag{1.8}$$

where

T= temperature,
S= specific entropy,

we deduce that the energy equation is equivalent to

$$(d/dt)S = 0 \ . \tag{1.9}$$

Hence, entropy is constant along particle paths. This implies that the flow is adiabatic; *i.e.*, there is no heat transfer between fluid elements. Moreover, for a smooth flow of an ideal fluid there is no dissipation. In the next lecture we will see that dissipation is required when smooth solutions break down. Furthermore, the needed dissipation leads to the loss of time reversal invariance for weak solutions.

1.3 Characteristic Equations

For an **isentrope** (constant entropy)

$$dE/dV = -P(V, E) \ . \tag{1.10}$$

Hence along a particle path the pressure is a function of only one variable, $P = P_S(V)$. Therefore, for smooth flow the derivative of ρ can be replaced with the derivative of P

$$(d/dt)\rho = \frac{1}{c^2}(d/dt)P \ , \tag{1.11}$$

where the **sound speed** c is defined by

$$\begin{aligned} c^2 &= \partial P/\partial\rho|_S = -V^2\, \partial P/\partial V|_S \\ &= -V^2\, (\partial P/\partial V|_E + \partial E/\partial V|_S \cdot \partial P/\partial E|_V) \\ &= V^2\, (-\partial P/\partial V|_E + P \cdot \partial P/\partial E|_V) \end{aligned} \tag{1.12}$$

Thermodynamic stability requires that the isentropic compressibility is positive, and implies that $c^2 \geq 0$. Shortly, we will see that this is both a necessary and sufficient condition for the fluid equations to be hyperbolic.

Weak disturbances (acoustic waves) propagate at the sound speed. This can be seen by linearizing the fluid equations. The substitutions

$$\rho = \rho_0 + \delta\rho \ ,$$

$$P = P_0 + \delta P \ ,$$

$$u = \delta u \ ,$$

into the fluid equations results to leading order in the wave equation

$$(\partial^2/\partial t^2 + c^2\partial^2/\partial x^2)\, \delta P = 0 \ .$$

Thus, the wave speeds for the linearized equations of a stationary fluid are $\pm c$.

Substituting Eq. (1.11) into Eq. (1.6) leads to the characteristic form of the fluid equations:

$$\begin{aligned} \frac{d}{dt}S = 0\,, &\quad \text{where } (d/dt) = \partial_t + u\partial_x\,; \\ \frac{1}{\rho c}\frac{d}{dt^+}P + \frac{d}{dt^+}u = 0\,, &\quad \text{where } (d/dt^+) = \partial_t + (u+c)\partial_x\,; \\ \frac{1}{\rho c}\frac{d}{dt^-}P - \frac{d}{dt^-}u = 0\,, &\quad \text{where } (d/dt^-) = \partial_t + (u-c)\partial_x\,. \end{aligned} \tag{1.13}$$

For a general system of quasi-linear hyperbolic PDEs, the characteristic form is equivalent to Eq. (1.5a). Hence for the fluid equations, the three characteristic velocities are

$$\lambda = u - c,\ u,\ u + c \ . \tag{1.13a}$$

Thus, the thermodynamic constraint, $c^2 \geq 0$, implies that the fluid equations are hyperbolic. The characteristics velocities $\lambda = u \pm c$ are associated with acoustic waves, and the characteristic velocity $\lambda = u$ with a particle trajectory. Acoustic waves propagate, relative to the fluid, at the sound speed.

For homentropic flow (S = constant, independent of x and t), the characteristic equations can be simplified by introducing the **Riemann invariants**

$$\begin{aligned} R_\pm &= u \pm \int^P dP/(\rho c)\Big|_{S=\text{constant}} \\ &= u \mp \int^V \rho c\, dV\Big|_{S=\text{constant}} . \end{aligned} \tag{1.14}$$

The PDEs then reduce to the ODEs:

$$\begin{aligned} R_+ &= \text{constant}, \quad \text{on } dx/dt = u + c\,; \\ R_- &= \text{constant}, \quad \text{on } dx/dt = u - c\,. \end{aligned} \tag{1.15}$$

For non-homentropic flow, the characteristic equations (1.13) imply that for each characteristic the fluid variables satisfy a constraint called a **compatibility relation**:

$$\begin{aligned} S &= \text{constant}\,, \quad \text{on } dx/dt = u\,; \\ dP/du &= -\rho c\,, \qquad \text{on } dx/dt = u + c\,; \\ dP/du &= \quad \rho c\,, \qquad \text{on } dx/dt = u - c\,. \end{aligned} \tag{1.16}$$

As an example of these concepts, consider an ideal gas EOS, $PV = (\gamma - 1)\, E$ where $\gamma > 1$. The important quantities that have been introduced can be computed analytically and are given by (see Ex. 1.5):

$$\begin{aligned} c^2 &= \gamma PV\ ; \\ P/P_0 &= (V_0/V)^\gamma\,, \quad \text{for } S = \text{constant}\,; \\ R_\pm &= u \pm \frac{2}{\gamma - 1} c\ . \end{aligned} \tag{1.17}$$

We have noted that $c^2 \geq 0$ and the characteristic form implies that the fluid equations are hyperbolic. When $c^2 > 0$, the eigenvalues are distinct and the fluid equations are **strictly hyperbolic**. The sound speed can only vanish (i) when $V \to \infty$ at the interface of the free expansion of a gas into a vacuum, or (ii) due to a phase transition at the triple point. In addition, geometric source terms for quasi one-dimensional flow (*e.g.*, cylindrical or

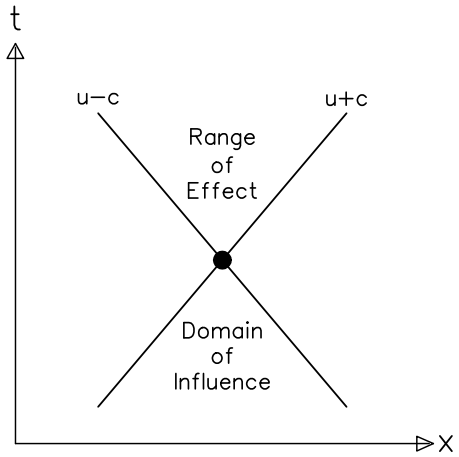

FIGURE 1.1

Domain of influence and range of dependence.

spherical converging flow, see, Ex. 1.2 and 1.3) have the effect of an additional characteristic velocity. Resonant wave phenomena can occur when characteristic velocities coincide; see *e.g.*, [Friedman, 1961] and [Isasaacson & Temple, 1992]. For other systems, the loss of strict hyperbolicity results in additional complications to the wave structure; see *e.g.*, [Isaacson *et al.*, 1988].

The characteristic form of the equations have several important implications:

1. The characteristic equations reduce the PDEs to coupled ODEs and are the basis of numerical algorithms for computing smooth flows, **method of characteristics**. For homentropic flow, the Riemann invariants can be used as coordinates. In this case the method of characteristics is particularly simple and is capable of giving very accurate solutions. When characteristics cross, smooth solutions break down and shock waves are formed.
2. Acoustic signals propagate along characteristics. The finite wave speeds lead to the concepts of a **domain of influence** and a **range of effect**, see Fig. 1.1. We note that the same concepts occur in relativity. The speed of light is the analog of the characteristic speed, the domain of influence corresponds to the backward light cone and the range of effect to the forward light cone. Moreover, spacelike points are

independent of each other. For numerical algorithms, the domain of influence leads to a time step limitation. When violated, explicit algorithms may become unstable and implicit algorithms may loss accuracy. Conversely, an unnecessarily small time step may lead to excessive numerical diffusion.

3. The flow of information along characteristics determines the boundary conditions required for a well-posed initial value problem. One quantity may be specified at a boundary for each characteristic propagating into the computational region. Thus, the number of boundary conditions ranges from 0, for supersonic flow out of the domain, upto 3 for supersonic flow into the domain. Because the characteristics depend on the flow, the number of conditions may not be the same at all boundaries. Furthermore, at a given boundary the number of conditions can vary in time. As an example, consider a converging-diverging nozzle. For subsonic flow at the nozzle entrance, two conditions are required. If the flow remains subsonic throughout the nozzle, one boundary condition is required at the exit. On the other hand, if the nozzle flow is transonic then the flow is supersonic at the nozzle exit and no conditions are needed. For supersonic flow into the nozzle, three conditions are required at the nozzle entrance. If the flow into the nozzle chokes then a shock wave forms and propagates out the nozzle entrance. The flow becomes subsonic and the number of boundary conditions at the nozzle entrance is reduced to two. Boundary conditions incompatible with the flow leads to numerical errors generated at the boundary and propagating into the interior of the computational domain.

For smooth flows, the three forms of the fluid equations are equivalent. Neither the Euler equations nor the characteristic equations are suitable for dealing with discontinuous solutions. In this course, we focus on the non-linear wave structure of compressible fluid flow. For this purpose the conservation form of the equations is crucial. The conservation form is also the basis for numerical algorithms that accurately describe shock waves.

General references:

1. [Courant & Friedrichs, 1948]
2. [Garabedean, 1986] chpt. 2

Exercises

1.1 The integral form of the conservation laws for fluid flow in 3-D are

$$\frac{d}{dt}\int_\Omega d\mathcal{V}\,\rho \qquad + \qquad \oint_{\partial\Omega} dA\,\hat{n}\cdot(\rho\vec{u}) \qquad = 0 \qquad (1E.1)$$

$$\frac{d}{dt}\int_\Omega d\mathcal{V}\,\rho\vec{u} \qquad + \qquad \oint_{\partial\Omega} dA\,\hat{n}\cdot(\rho\vec{u}\otimes\vec{u}-\boldsymbol{\sigma}) \qquad = 0 \qquad (1E.2)$$

$$\frac{d}{dt}\int_\Omega d\mathcal{V}\,\rho\left(\tfrac{1}{2}u^2+E\right) + \oint_{\partial\Omega} dA\,\hat{n}\cdot\left(\rho\left(\tfrac{1}{2}u^2+E\right)\vec{u}-\boldsymbol{\sigma}\cdot\vec{u}+\vec{q}\right) = 0 \qquad (1E.3)$$

for an arbitrary region Ω, with surface $\partial\Omega$ and outward normal $\hat{n}$,

where $\vec{u}$ is the velocity, the **stress tensor** is

$$\boldsymbol{\sigma} = -P\,\mathbf{I} + \boldsymbol{\sigma}' \qquad (1E.4)$$

with viscous stress $\boldsymbol{\sigma}'$ and the heat flux is $\vec{q}$. For Newtonian fluids, the viscous stress is expressed in terms of the deformation tensor $\mathbf{D} = \frac{1}{2}[\nabla\vec{u} + (\nabla\vec{u})^T]$ as

$$\boldsymbol{\sigma}' = 2\eta\left[\mathbf{D} - \tfrac{1}{3}\mathrm{Tr}\,(\mathbf{D})\,\mathbf{I}\right] + \xi\,\mathrm{Tr}\,(\mathbf{D})\,\mathbf{I}\ , \qquad (1E.5)$$

where η is the coefficient of **shear viscosity** and ξ is the coefficient of **bulk viscosity**, and the heat flux is

$$\vec{q} = -\kappa\nabla T\ , \qquad (1E.6)$$

where κ is coefficient of **thermal conductivity**.

A) Derive the equivalent differential equations for the conservation laws. The integral form of the conservation laws are clearly independent of the choice of coordinates. What is the manifestation of this invariance for the differential equations?

B) Is an incomplete EOS sufficient? Are the PDEs hyperbolic?

C) For incompressible flow, $\nabla \cdot \vec{u} = 0$, and constant viscosity coefficient η, show that the momentum equation reduces to the Navier-Stokes equation

$$\partial_t \vec{u} + (\vec{u} \cdot \nabla)\, \vec{u} = -\frac{1}{\rho}\, \nabla P + \nu\, \nabla^2 \vec{u}\ , \qquad (1E.7)$$

where $\nu = \eta/\rho$ is the **kinematic viscosity**.

D) Show that the equation for entropy is

$$\rho T (d/dt) S = \Upsilon - \nabla \cdot \vec{q}\ , \qquad (1E.8)$$

or in conservation form

$$\partial_t (\rho S) + \nabla \cdot \left(\rho S \vec{u} + \frac{\vec{q}}{T} \right) = \frac{\Upsilon}{T} + \kappa \left| \frac{\nabla T}{T} \right|^2\ , \qquad (1E.9)$$

where

$$\begin{aligned} \Upsilon = \sigma'_{jk} D_{jk} \ &= \ {}^2\!/_3\, \eta \Big[(D_{11} - D_{22})^2 + (D_{22} - D_{33})^2 + (D_{33} - D_{11})^2 \Big] \\ &\quad + 4\,\eta\, (D_{12}^2 + D_{23}^2 + D_{31}^2) + \xi\, (D_{11} + D_{22} + D_{33})^2\ . \qquad (1E.10) \end{aligned}$$

When the coefficients η, ξ and κ are positive show that $\Upsilon \geq 0$, and hence the total irreversible entropy ($dS \geq dQ/T$) can only increase.

1.2 For cylindrically or spherically symmetric flow, show that the 3-D fluid equations, with radial velocity component u, reduce to

$$\partial_t \begin{pmatrix} \rho \\ \rho u \\ \rho(\frac{1}{2}u^2 + E) \end{pmatrix} + \partial_r \begin{pmatrix} \rho u \\ \rho u^2 + P \\ \rho(\frac{1}{2}u^2 + E + PV)u \end{pmatrix} = -\frac{\alpha}{r} \begin{pmatrix} \rho u \\ \rho u^2 \\ \rho(\frac{1}{2}u^2 + E + PV)u \end{pmatrix} (1E.11)$$

where $\alpha = 0, 1, 2$ for planar, cylindrical and spherical geometry.

A) Do the source terms affect the entropy, *i.e.*, is $dE/dt = -P dV/dt$?

B) Do the source terms affect the characteristic velocities?

C) Do the source terms affect the Riemann invariants?

1.3 For a duct with cross sectional area A, show that the 1-D fluid flow equations are

$$\partial_t \begin{pmatrix} \rho A \\ \rho A u \\ \rho A(\frac{1}{2}u^2 + E) \end{pmatrix} + \partial_z \begin{pmatrix} \rho A u \\ \rho A u^2 + PA \\ \rho A(\frac{1}{2}u^2 + E + PV)u \end{pmatrix} = \begin{pmatrix} 0 \\ P\partial_z A \\ -P\partial_t A \end{pmatrix} \qquad (1E.12)$$

With $A = z^\alpha$ and $\alpha = 0, 1, 2$, show that the duct flow equations are equivalent to the 1-D fluid flow equations for planar, cylindrical and spherical geometry.

1.4 Let the Lagrangian mass coordinate be defined by $dm = \rho dx$.

A) Show that

$$(\partial_t + u\partial_x)\, m = 0 \ . \qquad (1E.13)$$

Moreover, under the transformation $(x, t) \to (m, \tau)$ with $\tau = t$ show that

$$\begin{aligned} \partial_x &= \rho\partial_m \\ \partial_t + u\partial_x &= \partial_\tau \end{aligned} \qquad (1E.14)$$

B) Derive the 1-D fluid flow equations in Lagrangian coordinates

$$\partial_\tau \begin{pmatrix} V \\ u \\ \frac{1}{2}u^2 + E \end{pmatrix} + \partial_m \begin{pmatrix} -u \\ P \\ Pu \end{pmatrix} = \vec{0} \ , \qquad (1E.15)$$

with the auxiliary equation

$$\partial_\tau x(m, \tau) \equiv u \ . \qquad (1E.16)$$

C) Show that the characteristic velocities are $\lambda = 0, \pm\rho c$.

1.5 Along an isentrope for an ideal gas, $P = (\gamma - 1)E/V$, show that

A) $P(\rho) = (\rho/\rho_0)^\gamma P_0$.

B) $c^2 = \gamma PV = (\rho/\rho_0)^{\gamma-1} c_0^2$.

C) $\int \frac{dP}{\rho c} = \frac{2}{\gamma - 1} c$.

D) Suppose $E = C_v T$, where the specific heat C_v is constant. Show that the specific entropy is

$$S = C_v \ln\left(\frac{PV^\gamma}{P_0 V_0^\gamma}\right) + S_0 \ . \qquad (1E.17)$$

1.6 Consider a right facing simple wave: S is constant and the left Riemann invariant $R_\ell = u - \int dP/(\rho c)$ is constant.

A) Show that $u + c$ is a function of the right Riemann invariant $R_r = u + \int dP/(\rho c)$ and hence the right propagating characteristic is a straight line in the x–t plane.

B) Show that a right facing simple wave has the form $u = F(\xi)$, where $\xi = x - \lambda(\xi)\, t$ and $\lambda(\xi) = u + c$ with F an arbitrary function.

C) Show that a shock forms, $\partial_x u = \infty$, if $1 + \lambda' t = 0$.

Now consider a semi-infinite shock tube, $0 \le x < \infty$, bounded on the left by a piston and containing a fluid with an ideal gas EOS. Suppose the fluid is initially at rest and at $t = 0$ the piston starts moving to the right with constant acceleration, a.

D) Show that the right facing characteristics first cross at $t = \frac{2}{\gamma+1} \cdot \frac{c_0}{a}$.

E) Show that a shock forms ahead of the piston a distance $\Delta x = \frac{2}{\gamma+1} \cdot \frac{c_0^2}{a}$.

1.7 Consider a fluid layer of thickness Δx. Suppose the fluid is initially at rest and is accelerated by a pressure imposed at its boundary. Show that a shock will form in the layer if the boundary pressure grows faster than

$$\frac{dP}{dt} > \frac{(\rho c)^2}{\rho_0\, \Delta x} \cdot \left.\frac{dP}{d(\rho c)}\right|_S \quad . \tag{1E.18}$$

1.8 Consider a semi-infinite shock tube, $-\infty < x < 0$, bounded on the right with a movable piston. Suppose the piston can be treated as a mass layer with mass per unit area M, and the fluid has an ideal gas EOS. If the fluid is initially at rest show that the piston velocity is given by

$$U(\xi) = \frac{2c_0}{\gamma - 1}\left[1 - \xi^{-\left(\frac{\gamma-1}{\gamma+1}\right)}\right] \ , \tag{1E.19}$$

where

$$\xi(t) = 1 + \left(\frac{\gamma+1}{2\gamma}\right) \cdot \left(\frac{\rho_0 c_0 t}{M}\right) \ . \tag{1E.20}$$

1.9 Consider steady-state flow.

A) Derive Bernoulli's relation

$$\tfrac{1}{2}\,u^2 + E + PV = \text{constant}\ . \tag{1E.21}$$

B) For an ideal gas EOS, show that Bernoulli's relation can be written as

$$\tfrac{1}{2}\,u^2 + \frac{1}{\gamma-1}c^2 = \tfrac{1}{2}\Big(\frac{\gamma+1}{\gamma-1}\Big)c_*^2\ . \tag{1E.22}$$

Furthermore, show that the flow is supersonic when $u > c_*$ and subsonic when $u < c_*$.

Solutions

1.1 The integral form expresses the physical conservation laws for mass, momentum and energy. Each conservation law is the sum of two terms: (i) the time derivative of a density and (ii) the surface integral of a flux. Numerical algorithms based on **control volumes** use the integral form of the conservation laws.

A) Since the volume Ω is time independent

$$(d/dt)\int_\Omega d\mathcal{V} f = \int_\Omega d\mathcal{V}\,\partial_t f \ . \tag{1S.1}$$

The surface integral can be replaced by a volume integral using the divergence theorem

$$\oint_{\partial\Omega} dA\,(\hat{n}\cdot\vec{F}) = \int_\Omega d\mathcal{V}\,\nabla\cdot\vec{F}\ . \tag{1S.2}$$

Since the integral vanishes for all Ω, the integrand must also vanish. This leads to the differential fluid equations in conservative form

$$\partial_t\rho + \nabla\cdot(\rho\vec{u}) = 0\ , \tag{1S.3}$$

$$\partial_t(\rho\vec{u}) + \nabla\cdot(\rho\vec{u}\otimes\vec{u}+P\mathbf{I}) = \nabla\cdot\boldsymbol{\sigma}'\ , \tag{1S.4}$$

$$\partial_t\big(\rho\,(\tfrac{1}{2}u^2+E)\big) + \nabla\cdot\big(\rho\,(\tfrac{1}{2}u^2+E)\,\vec{u}+P\vec{u}\big) = \nabla\cdot(\boldsymbol{\sigma}'\cdot\vec{u}-\vec{q})\ . \tag{1S.5}$$

Under change of coordinates, the velocity transforms as a vector and the momentum flux as a tensor. Hence, using tensor calculus the differential form of the conservation laws can be converted from cartesian coordinates into any desired coordinate system; see *e.g.*, Ex. 1.2. For a detailed analysis of the tensorial nature of the fluid equations see *e.g.*, [Aris, 1989], or in modern differential geometry notation see *e.g.*, [Marsden & Hugehes, 1983].

For later use, we note that the equations can be written in terms of the convective derivative $(d/dt) = \partial_t + \vec{u} \cdot \nabla$. In addition, subtracting off a multiple of the mass equation from the momentum and energy equations lead to the equations

$$(d/dt)\,\rho = -\rho \nabla \cdot \vec{u}\ , \tag{1S.6}$$

$$\rho\,(d/dt)\,(\vec{u}) = -\nabla P + \nabla \cdot \boldsymbol{\sigma}'\ , \tag{1S.7}$$

$$\rho\,(d/dt)\left(\tfrac{1}{2}u^2 + E\right) = -\nabla \cdot (P\vec{u}) + \nabla \cdot (\boldsymbol{\sigma}' \cdot \vec{u}) - \nabla \cdot \vec{q}\ . \tag{1S.8}$$

B) The heat flux is specified in terms of the temperature. Hence, an incomplete EOS is not sufficient when heat diffusion is important. With viscosity and heat conduction included, the fluid equations are parabolic. However, when the coefficients are small, heat conduction and viscosity only have a large effect for steep gradients. In the next lecture it is shown when short length scales are not of interest that the steep gradients can be accounted for by the Hugoniot jump conditions for shock waves. Consequently, on the time scale of interest for may applications the motion of a fluid is well approximated by weak solutions to the hyperbolic PDEs for ideal fluid flow.

C) The form of the momentum equations derived at the end of part A is

$$\rho\,(\partial_t + \vec{u} \cdot \nabla)\,\vec{u} = -\nabla P + \nabla \cdot \boldsymbol{\sigma}'\ . \tag{1S.9}$$

When η and ξ are constants, the viscous contribution to the momentum equation can be expressed as

$$\nabla \cdot \boldsymbol{\sigma}' = \eta \nabla^2 \vec{u} + (\xi + {}^1\!/_3\,\eta)\,\nabla(\nabla \cdot \vec{u})\ . \tag{1S.10}$$

In the incompressible case, the $\nabla \cdot \vec{u}$ terms drop out and the momentum equation reduces to

$$\rho\,(\partial_t + \vec{u} \cdot \nabla)\,\vec{u} = -\nabla P + \eta \nabla^2 \vec{u}\ . \tag{1S.11}$$

Dividing by ρ leads to the standard form of the Navier-Stokes equation.

D) The momentum and energy equations derived at the end of part A are

$$\rho(d/dt)\,\vec{u} \quad + \quad \nabla P \quad = \nabla\cdot\boldsymbol{\sigma}'\ , \tag{1S.12}$$

$$\rho\,(d/dt)\left(\tfrac{1}{2}u^2+E\right)+\nabla\cdot(P\vec{u})=\nabla\cdot(\boldsymbol{\sigma}'\cdot\vec{u})-\nabla\cdot\vec{q}\,. \tag{1S.13}$$

Multiplying the momentum equation by $\vec{u}$ and subtracting from the energy equation gives

$$\rho\,(d/dt)E+P\nabla\cdot\vec{u}=\nabla\cdot(\boldsymbol{\sigma}'\cdot\vec{u})-(\nabla\cdot\boldsymbol{\sigma}')\cdot\vec{u}-\nabla\cdot\vec{q}\,. \tag{1S.14}$$

Eliminating $\nabla\cdot\vec{u}$ using the mass equation and substituting $\rho=1/V$ yields

$$\rho\Big[(d/dt)E+P(d/dt)V\Big]=\nabla\cdot(\boldsymbol{\sigma}'\cdot\vec{u})-(\nabla\cdot\boldsymbol{\sigma}')\cdot\vec{u}-\nabla\cdot\vec{q}\,. \tag{1S.15}$$

Using the thermodynamic identity $TdS=dE+PdV$, Eq. (1E.8) follows by substituting for σ' and straight forward but tedious algebraic manipulations to show that

$$\nabla\cdot(\boldsymbol{\sigma}'\cdot\vec{u})-(\nabla\cdot\boldsymbol{\sigma}')\cdot\vec{u}=\sigma'_{ij}\,\partial_i u_j=\Upsilon\ . \tag{1S.16}$$

The conservation form of the entropy equation follows from mass conservation and the algebraic identity

$$\begin{aligned}\nabla\cdot(\vec{q}/T)&=(\nabla\cdot\vec{q})/T-(\vec{q}\cdot\nabla T)/T^2\\&=(\nabla\cdot\vec{q})/T+\kappa\left|\nabla T/T\right|^2\ .\end{aligned} \tag{1S.17}$$

In conservation form we note that there is both a reversible change in entropy from the heat flux $dQ/T=\nabla\cdot(\vec{q}/T)$ and an irreversible entropy change from the dissipation. There is a contribution to the dissipation from both viscous stresses Υ/T and heat conduction $\kappa\left|\nabla T/T\right|^2$. The dissipation increases entropy since it is the sum of squares and hence positive definite.

1.2 The tensor form of the differential equations for the conservation laws derived in Ex. 1.1A are invariant under coordinate transformation. Furthermore, if the flow is initially radial symmetric and the boundary conditions are radially symmetric then the flow remains radially symmetric. Therefore, to derive the equations for cylindrical or spherical symmetric flow, we may assume the velocity has the form $\vec{u} = u(r,t)\,\hat{r}$. First, let us consider spherically symmetric flow. In spherical coordinates

$$\nabla = \hat{r}\partial_r + \frac{\hat{\theta}}{r}\partial_\theta + \frac{\hat{\phi}}{r\sin\theta}\partial_\phi \ , \tag{1S.18}$$

where θ is the polar angle and ϕ is the azimuthal angle. We note as a result of the curved coordinates that

$$\partial_r\hat{r} = 0 \ , \quad \partial_\theta\hat{r} = \hat{\theta} \ , \quad \text{and} \quad \partial_\phi\hat{r} = \sin\theta\hat{\phi} \ . \tag{1S.19}$$

Hence,

$$\nabla\cdot(u\hat{r}) = (\nabla u)\cdot\hat{r} + u\,(\nabla\cdot\hat{r}) = \partial_r u + 2u/r \ . \tag{1S.20}$$

Using these relations it is straight forward algebra to transform the 3-D equations. For example, the momentum flux is

$$\begin{aligned}\nabla\cdot(\rho\vec{u}\otimes\vec{u}) &= (\nabla\rho\cdot\vec{u})\,\vec{u} + \rho\,(\nabla\cdot\vec{u})\,\vec{u} + \rho\,(\vec{u}\cdot\nabla)\,\vec{u} \\ &= (\partial_r\rho)\,u^2\hat{r} + \rho\left(\nabla\cdot(u\hat{r})\right)u\hat{r} + \rho\,(u\partial_r)\,(u\hat{r}) \\ &= \left(\partial_r\Big(\rho u^2\Big) + \frac{2}{r}\rho u^2\right)\hat{r} \ . \end{aligned} \tag{1S.21}$$

In addition,

$$\nabla(P\mathbf{I}) = \nabla P = (\partial_r P)\,\hat{r} \ . \tag{1S.22}$$

Thus, the effect of spherical coordinates on the flux is merely to add geometrical source terms proportional to $2/r$. Similarly, in cylindrical geometry one excludes the contribution from $\partial_\phi\hat{r}$ and the additional terms from the flux are proportional to $1/r$. For planar symmetry, there are no additional terms since the coordinates are not curved.

A) In Ex. 1.1 D, the time derivative of the entropy was derived for the 3-D equations. Since cylindrical and spherical symmetry flow are a reduction of the 3-D equations, without dissipation terms smooth flows conserve entropy. Hence, for both cylindrically and spherically symmetric flow $(d/dt)E = -P(d/dt)V$.

B) Going through the analogous algebraic transformation for the characteristics merely adds geometric source terms

$$\frac{d}{dt}S = 0\,, \qquad \text{where } (d/dt) = \partial_t + u\partial_x\,; \tag{1S.23}$$

$$\frac{1}{\rho c}\frac{d}{dt^+}P + \frac{d}{dt^+}u = -\frac{\alpha}{r}uc\,, \quad \text{where } (d/dt^+) = \partial_t + (u+c)\partial_x\,; \tag{1S.24}$$

$$\frac{1}{\rho c}\frac{d}{dt^-}P - \frac{d}{dt^-}u = -\frac{\alpha}{r}uc\,, \quad \text{where } (d/dt^-) = \partial_t + (u-c)\partial_x\,. \tag{1S.25}$$

Thus, the geometric source terms do not affect the characteristic velocities.

C) Due to the source terms, even for isentropic flow, the Riemann invariants are not constant on characteristics. In particular, rarefaction waves, which are described in the next lecture, can no longer be scale invariant. The method of characteristics can still be applied, but the contribution from the source terms must be included in the compatibility relations.

1.3 Duct flow is a quasi 1-D approximation in which the leading order 2-D effects are accounted for by the variation in cross sectional area of the stream tube. The conserved quantities of mass, momentum and energy are given by

$$\text{mass} = \int dz\, A\rho\ , \tag{1S.26}$$

$$\text{momentum} = \int dz\, A\rho\, u\ , \tag{1S.27}$$

$$\text{energy} = \int dz\, A\rho\,(\tfrac{1}{2}u^2 + E)\ . \tag{1S.28}$$

Therefore, the mass per unit length or ρA rather than ρ is the relevant quantity which enters into the conservation form on the left hand side of the equations. In addition, the

duct wall adds momentum $P\partial_z A$ and energy $-P\partial_t A$ to the fluid. These appear as source terms on the right hand side of Eq. (1E.12).

The cross sectional area for planar, cylindrically and spherically symmetric flow is proportional to z^α with $\alpha = 0, 1$ and 2 respectively. In this case, $\partial_t A = 0$. Applying the derivative rule to the product in the flux and dividing the equation by A leads to the 1-D fluid equations with a geometric source term proportional to $\partial_z A/A = \alpha/z$. The source terms are exactly the same as derived in Ex. 1.2.

1.4 The mass coordinate is defined by

$$m(x,t) = \int_{x_0(t)}^{x} \rho(x,t)dx \ , \tag{1S.29}$$

where $x_0(t)$ is the trajectory of a reference particle which initially at $t = 0$ is at $x = x_0$.

A)

$$(\partial_t + u\partial_x)\, m(x,t) = \int_{x_0(t)}^{x} \partial_t \rho(x,t)\, dx - (dx_0(t)/dt)\rho(x_0(t),t) + (u\rho)\,(x,t) \tag{1S.30}$$

By mass conservation

$$\begin{aligned}\int_{x_0(t)}^{x} \partial_t \rho(x,t)\, dx &= -\int_{x_0(t)}^{x} \partial_x(\rho u)\, dx \\ &= -(\rho u)(x,t) + (\rho u)\,(x_0(t),t) \ .\end{aligned} \tag{1S.31}$$

From the definition of a particle trajectory

$$(d/dt)x_0(t) = u(x_0(t),t) \ . \tag{1S.32}$$

Combining these equations we find

$$(\partial_t + u\partial_x)m(x,t) = 0 \ . \tag{1S.33}$$

Under the transformation $(x,t) \to (m,\tau)$ with

$$\begin{aligned}\tau &= t \\ m &= m(x,t)\end{aligned} \tag{1S.34}$$

Eq. (1E.14) follows immediately.

B) From the definition $\rho = V^{-1}$

$$(d/dt)\rho = -V^{-2}(d/dt)V \ . \tag{1S.35}$$

Substituting Eq. (1E.14) into the Euler equations, Eq. (1.6), leads to the Lagrangian form of the fluid equations. The auxiliary equation, $\partial_\tau x(m,\tau) = u$ follows from the transformation and corresponds to a particle trajectory. The Lagrangian equations are convenient for analysis. However, in numerical computations it is important that mass be exactly conserved. Usually, the equation for $\partial_\tau x$ is used in place of the equation for $\partial_\tau V$ and V is calculated for each cell as a finite difference $V = \Delta x/\Delta m$.

C) Using the transformation in part B, the characteristic equations, Eq. (1.13) are transformed to

$$\partial_\tau S = 0 \ , \tag{1S.36}$$

$$\frac{1}{\rho c}\big(\partial_\tau + \rho c\partial_m\big)P + \big(\partial_\tau + \rho c\partial_m\big)u = 0 \ , \tag{1S.37}$$

$$\frac{1}{\rho c}\big(\partial_\tau - \rho c\partial_m\big)P - \big(\partial_\tau - \rho c\partial_m\big)u = 0 \ . \tag{1S.38}$$

Thus, the characteristic velocities are $\lambda = 0, \pm\rho c$. In effect, the particle trajectory corresponds to $\lambda = 0$. Moreover, the Lagrangian sound speed is ρc.

1.5 **A)** An isentrope is defined by Eq. (1.10). Applied to the ideal equation of state we have

$$dE = -PdV \ , \tag{1S.39}$$

$$dE/E = -(\gamma - 1)dV/V \ , \tag{1S.40}$$

$$E(V)/E_0 = (V/V_0)^{-(\gamma-1)} \ . \tag{1S.41}$$

Then using the EOS to replace E with P we obtain

$$P(V)/P_0 = (V_0/V)^\gamma = (\rho/\rho_0)^\gamma \ . \tag{1S.42}$$

B) From Eq. (1.12) and part A

$$\begin{aligned} c^2 &= \partial_\rho P|_S \\ &= \gamma\,(\rho/\rho_0)^\gamma\, P_0 V \\ &= \gamma P V\ . \end{aligned} \tag{1S.43}$$

Hence $(c/c_0)^2 = E/E_0$ and from part A it follows that

$$c^2 = (\rho/\rho_0)^{\gamma-1}\, c_0^2\ . \tag{1S.44}$$

Without computing $P(V)$ on the isentrope, the sound speed can also be obtained by applying the relation $c^2 = V^2\,(-\partial_V P|_E + P\partial_E P|_V)$ directly to the EOS.

C)

$$\begin{aligned} \int dP/(\rho c) &= \int d\rho\,(\partial_\rho P)_S\,(\rho c)^{-1} \\ &= \int d\rho\, c/\rho = \int d\rho\, c_0 \rho^{\frac{1}{2}(\gamma-3)}/\rho_0^{\frac{1}{2}(\gamma-1)} \\ &= [2/(\gamma-1)]\, c\ . \end{aligned} \tag{1S.45}$$

Hence the Riemann invariants are

$$R_\pm = u \pm [2/(\gamma-1)]\, c\ . \tag{1S.46}$$

D) Substituting $C_v T = E = PV/(\gamma-1)$ into the thermodynamic identity $TdS = dE + PdV$ we find

$$dS = C_v\Big(\frac{dP}{P} + \gamma\frac{dV}{V}\Big) = C_v\, d\ln\Big(PV^\gamma\Big)\ . \tag{1S.47}$$

Integrating then gives S as a function of P and V.

1.6 Note, the right and left Riemann invariants correspond to R_+ and R_- in Eq. (1.15).

A) Take the sum and difference of the Riemann invariants

$$R_r + R_\ell = 2\,u \ , \tag{1S.48}$$

$$R_r - R_\ell = 2\int dP/(\rho c) \ . \tag{1S.49}$$

Two quantities determine the thermodynamic state. When S is constant, $\int dP/(\rho c)$ determines the state. Therefore, R_r, R_ℓ and S completely determine the hydrodynamic state. For a right facing simple wave R_ℓ and S are constant. Therefore, the state of the wave is a function of only R_r. From the characteristic equation, R_r is constant along the curve $dx/dt = u + c$. Since $u + c$ is a function of R_r, it is constant along a right propagating characteristic. Hence, each right facing characteristic is a straight line.

B) By part A, all fluid variables are functions of R_r and are constant along a right facing characteristic. Let us parametrize the right facing characteristics by $\xi = x - \lambda(R_r)t$, where $\lambda = u + c$. Since ξ is in a one-one correspondence with R_r we can parametrize the simple wave with the variable ξ. Then all the variables are functions of ξ. In particular, the characteristic speed $\lambda(\xi)$ and the particle velocity $u = F(\xi)$.

C) By part B, $\xi = x - \lambda(\xi)\,t$. Hence,

$$\begin{aligned}\partial_x\xi &= 1 - \Big(\partial_x\lambda(\xi)\Big)t \\ &= 1 - \lambda'\cdot(\partial_x\xi)\,t \ ,\end{aligned} \tag{1S.50}$$

where $\lambda' = d\lambda/d\xi$. Therefore,

$$\partial_x\xi = 1/(1+\lambda' t) \ . \tag{1S.51}$$

The derivative of the particle velocity is

$$\partial_x u = F'\partial_x\xi = F'/(1+\lambda' t) \ . \tag{1S.52}$$

Hence, smooth solutions break down $\partial_x u = \infty$ if $1 + \lambda' t = 0$.

D) The strategy is to determine the velocity, $F(\xi)$ in part B, from the piston boundary condition, and then apply the criterion in part C. From Ex 1.5 C, the left Riemann invariant is $u - 2c/(\gamma-1)$. Hence,

$$c = c_0 + \tfrac{1}{2}(\gamma-1)\,u\ . \tag{1S.53}$$

On the piston trajectory

$$x = \tfrac{1}{2}at^2\ , \tag{1S.54}$$

$$u = a\,t\ , \tag{1S.55}$$

$$\begin{aligned}\lambda &= u + c = c_0 + \tfrac{1}{2}(\gamma+1)\,u \\ &= c_0 + \tfrac{1}{2}(\gamma+1)\,at\ ,\end{aligned} \tag{1S.56}$$

$$\begin{aligned}\xi &= x - \lambda t \\ &= -\tfrac{1}{2}\gamma\,at^2 - c_0 t\ .\end{aligned} \tag{1S.57}$$

We note that $\lambda \geq c_0$ and $\xi \leq 0$ for $t \geq 0$. Moreover, both λ and ξ are monotonic and hence $\xi(\lambda)$ is a well defined function. Eliminating t, we find λ and ξ are related by

$$\frac{\gamma}{2a}\left[\frac{\lambda - c_0}{\frac{1}{2}(\gamma+1)}\right]^2 + \frac{c_0}{a}\left[\frac{\lambda - c_0}{\frac{1}{2}(\gamma+1)}\right] + \xi = 0\ . \tag{1S.58}$$

Taking the derivative we find

$$\frac{d\xi}{d\lambda} = -\frac{2}{\gamma+1}\frac{c_0}{a}\Big[1 + \frac{2\gamma}{\gamma+1}(\lambda/c_0 - 1)\Big]\ . \tag{1S.59}$$

From part C, $\partial_x u = \infty$ and the characteristics first cross at a time

$$t_* = \min_{\lambda \geq c_0}\big(-d\xi/d\lambda\big)\ . \tag{1S.60}$$

The minimization is necessary because one doesn't know *a priori* which characteristics are the first to cross. The minimum is achieved at $\lambda_* = c_0$ and $t_* = \frac{2}{\gamma+1}\cdot\frac{c_0}{a}$.

E) From part D, the characteristic first crosses at $\lambda_* = c_0$ which corresponds to $\xi_* = 0$. The characteristic cross at a position

$$x_* = \xi_* + \lambda_* t_* = \frac{2}{\gamma+1} \cdot \frac{c_0^2}{a} \ . \tag{1S.61}$$

1.7 Suppose the pressure is imposed on the left boundary. Then the flow is a right facing simple wave as in Ex. 1.6. As an alternative to the approach used in Ex. 1.6 D, a geometric approach based on the crossing of characteristics in the Lagrangian mass coordinate of Ex. 1.4 is used to determine if a shock will form. We can assume the fluid layer corresponds to the interval $0 \le m \le \rho_0 \Delta x$. In mass coordinates the characteristic velocity is $\lambda = \rho c$. It follows in an analogous manner to Ex. 1.6 A that the right propagating characteristics are straight lines in the m–t plane. Therefore, the characteristic launched at the boundary at time t_0 is given by

$$m(t_0, t) = \lambda(t_0) \cdot (t - t_0) \ . \tag{1S.62}$$

The characteristics cross when

$$\frac{\partial m}{\partial t_0} = 0 \ . \tag{1S.63}$$

This occurs at

$$\frac{m}{\lambda} = t - t_0 = \frac{\lambda}{\lambda'} \ . \tag{1S.64}$$

The characteristics cross within the fluid layer if

$$\rho_0 \, \Delta x > m = \lambda^2/\lambda' \ . \tag{1S.65}$$

Since a simple wave is isentropic

$$\lambda' = \left.\frac{d(\rho c)}{dP}\right|_S \cdot \frac{dP}{dt} \ . \tag{1S.66}$$

Hence the characteristic cross and a shock forms within the fluid layer if the pressure increases sufficiently fast

$$\frac{dP}{dt} > \frac{(\rho c)^2}{\rho_0 \, \Delta x} \cdot \left.\frac{dP}{d(\rho c)}\right|_S \ . \tag{1S.67}$$

We note that after the lead characteristic reaches the right boundary of the fluid layer then the left Riemann invariant is no longer constant and the condition above breaks down. A similar arguments implies that a compressive wave propagating into a uniform fluid will steepen and form a shock in a finite time. Hence, the occurrence of shock waves are a general property of compressible fluid flow.

1.8 The right Riemann invariant is a constant. By Ex 1.5 C

$$c = c_0 - \tfrac{1}{2}(\gamma - 1)\, u \ . \tag{1S.68}$$

From Ex 1.5 A & B,

$$(c/c_0)^2 = (P/P_0)^{\frac{\gamma-1}{\gamma}} \ . \tag{1S.69}$$

Hence, the piston velocity determines its pressure

$$P(U) = \gamma^{-1}\rho_0 c_0^2 \big[1 - \tfrac{1}{2}(\gamma - 1)\, U/c_0\big]^{\frac{2\gamma}{\gamma-1}} \ . \tag{1S.70}$$

Newton's law for the piston is

$$M\frac{dU}{dt} = P(U) \ . \tag{1S.71}$$

Hence

$$t = M\int_0^U \frac{dU}{P(U)} \ . \tag{1S.72}$$

This can be integrated analytically and determines U as a function of time. Note that the asymptotic velocity $U \to 2\, c_0/(\gamma - 1)$ is finite. Thus, the sound speed as well as the total fluid energy can limit the achievable piston velocity.

1.9 **A)** For steady-state flow, the conservation form of the fluid equations reduce to

$$\partial_x \begin{pmatrix} \rho u \\ \rho u^2 + P \\ \rho u \cdot (\frac{1}{2}\, u^2 + E + PV) \end{pmatrix} = 0 \ . \tag{1S.73}$$

The first component implies that the mass flux ρu is constant. Therefore, the third component reduces to

$$\partial_x\big(\tfrac{1}{2}\, u^2 + E + PV\big) = 0 \ .$$

This implies Bernoulli's function, $\frac{1}{2}\, u^2 + E + PV$ is a constant.

B) For an ideal gas, from Eq. (1.17) we can express the enthalpy as

$$\begin{aligned} H = PV + E &= PV\left[1 + 1/(\gamma - 1)\right] \\ &= \gamma PV/(\gamma - 1) \\ &= c^2/(\gamma - 1) \ . \end{aligned} \tag{1S.74}$$

It follows that $\frac{1}{2}\,u^2 + E + PV$ is postive and Eq. (1E.21) can be expressed as Eq. (1E.22). From Eq. (1E.22), the flow is sonic when

$$u = c = c_* \ .$$

Since c decreases as u increases, it follows for supersonic flow that

$$c < c_* < u \ ,$$

and for subsonic flow that

$$u < c_* < c \ .$$

Lecture 2
Wave Structure

The fluid equations have the form of a hyperbolic system of conservation laws

$$\partial_t \vec{w} + \partial_x \vec{F}(\vec{w}) = \vec{0} \ , \tag{1.3}$$

or

$$\partial_t \vec{w} + \mathbf{DF}(\vec{w}) \cdot \partial_x \vec{w} = \vec{0} \ . \tag{1.3a}$$

An important property of hyperbolic PDEs is the wave structure of its solutions. Elementary waves can be used as building blocks to understand and analyze the general solutions. Because the PDEs are scale invariant ($x' = x/\alpha$ and $t' = t/\alpha$), the elementary waves are scale invariant. Moreover, shock waves and their interactions are especially important because they represent the most singular part of a solution. We briefly outline the general theory for the elementary waves and then use the fluid equations as an example to illustrate the non-linear wave structure of quasi-linear hyperbolic PDEs.

For each eigenvalue of **DF**, there is one **wave family**. A wave family can be of two types: **linearly degenerate** if

$$(\vec{R} \cdot \nabla_{\vec{w}})\, \lambda = 0 \ , \tag{2.1}$$

where λ is an eigenvalue and $\vec{R}$ is the corresponding right eigenvector; otherwise **linearly non-degenerate**. For each non-degenerate wave family there are 2 types of elementary waves; (i) a continuous simple wave called a rarefaction and (ii) a discontinuous wave called a shock. For each degenerate wave family there is 1 type of wave called a contact.

For the fluid equations we show that the acoustic wave families ($\lambda = u \pm c$) are non-degenerate, and the wave family corresponding to the particle trajectory ($\lambda = u$) is linearly

degenerate. The density of the conserved quantities (mass, momentum and energy) in the fluid equations (1.1) are

$$\vec{w} = \left(\rho,\ \mathcal{M},\ \mathcal{E}\right)^T \ ,$$

where $\mathcal{M} = \rho u$ and $\mathcal{E} = \rho(E + \frac{1}{2}u^2)$. The flux function

$$\vec{F} = \left(\rho u,\ \rho u^2 + P,\ [\tfrac{1}{2}u^2 + E + PV]\,\rho u\right)^T$$

can be expressed in terms of $\vec{w}$. Rather than perform the straight forward but tedious algebraic computation of $\mathbf{DF} = \nabla_{\vec{w}}\vec{F}$ and its eigenvectors (see Ex. 2.1), we will make use of the characteristic form of the fluid equations (1.13).

It is natural to use the primitive variables

$$\vec{q} = \left(V,\ E,\ u\right)^T \ ,$$

and to consider $\vec{w}$ to be a function of $\vec{q}$. The transformation between $\vec{w}$ and $\vec{q}$ is non-singular, and may be regarded as a change of basis. Using the chain rule, Eq. (1.3a) is transformed to

$$\partial_t \vec{q} + \mathbf{DF}' \cdot \partial_x \vec{q} = \vec{0} \ , \tag{2.2a}$$

where

$$\mathbf{DF}' = (\nabla_{\vec{q}}\vec{w})^{-1} \cdot \mathbf{DF} \cdot (\nabla_{\vec{q}}\vec{w}) \ , \tag{2.2b}$$

and

$$(\nabla_{\vec{q}}\vec{w})_{ij} = \partial_{w_j} q_i \ .$$

It follows that $\mathbf{DF}'$ and $\mathbf{DF}$ have the same eigenvalues, and that the left and right eigenvectors are related by

$$\vec{L}'_i = \vec{L}_i \cdot (\nabla_{\vec{q}}\vec{w}) \ ,$$

and

$$\vec{R}'_i = (\nabla_{\vec{q}}\vec{w})^{-1} \cdot \vec{R}_i \ .$$

Moreover,

$$(R_i \cdot \nabla_{\vec{w}})\, \lambda_i = (R'_i \cdot \nabla_{\vec{q}})\, \lambda_i \ .$$

Therefore, the linear degenerate nature of a wave family is not changed by the transformation. Furthermore, eq. (1.5a) can be rewritten as

$$\vec{L}'_i \cdot (\partial_t + \lambda_i \partial_x)\, \vec{q} = 0 \ . \tag{2.3}$$

The left eigenvectors follow from the characteristic equations. Comparing Eqs. (1.13) and (2.3), and using the thermodynamic relations

$$T\, dS = P\, dV + dE$$

and

$$dP = (\partial_V P) dV + (\partial_E P) dE \ ,$$

where $\partial_V P = \frac{\partial P}{\partial V}|_E$ and $\partial_E P = \frac{\partial P}{\partial E}|_V$, we find that the left eigenvectors are proportional to

$$\begin{aligned}
\vec{L}'_u &= \frac{-2}{\rho c} \begin{pmatrix} P \ , & 1 \ , & 0 \end{pmatrix} , \\
\vec{L}'_{u+c} &= \frac{1}{2\rho c} \begin{pmatrix} \partial_V P, & \partial_E P, & \rho c \end{pmatrix} , \\
\vec{L}'_{u-c} &= \frac{1}{2\rho c} \begin{pmatrix} \partial_V P, & \partial_E P, & -\rho c \end{pmatrix} ,
\end{aligned} \tag{2.4}$$

The normalization has been chosen such that

$$\vec{L}'_{u-c} \cdot \vec{L}'_u \times \vec{L}'_{u+c} = 1 \ .$$

The right eigenvectors are the duals to the left eigenvectors. Therefore,

$$\begin{aligned}
\vec{R}'_{u-c} &= \vec{L}'_u \times \vec{L}'_{u+c} = \frac{1}{\rho c} \begin{pmatrix} -1 \ , & P \ , & -\rho c \end{pmatrix}^T , \\
\vec{R}'_u &= -\vec{L}'_{u-c} \times \vec{L}'_{u+c} = \frac{1}{2\rho c} \begin{pmatrix} -\partial_E P, & \partial_V P, & 0 \end{pmatrix}^T , \\
\vec{R}'_{u+c} &= \vec{L}'_{u-c} \times \vec{L}'_u = \frac{1}{\rho c} \begin{pmatrix} -1 \ , & P \ , & \rho c \end{pmatrix}^T .
\end{aligned} \tag{2.5}$$

We can now use Eq. (2.1) to determine the degeneracy of the wave families. For $\lambda = u$, we have

$$\begin{aligned} \vec{R}'_u \cdot \nabla_{\vec{q}} u &= \frac{1}{2\rho c}\Big[-(\partial_E P)\partial_V + (\partial_V P)\partial_E\Big]u \\ &= 0 \ . \end{aligned} \tag{2.6}$$

Hence, $\lambda = u$ is linearly degenerate. For $\lambda = u + c$, we have

$$\begin{aligned} \vec{R}'_{u+c} \cdot \nabla_{\vec{q}}(u+c) &= \frac{1}{\rho c}\Big[-\partial_V + P\partial_E + \rho c\partial_u\Big]\,(u+c) \\ &= 1 - \frac{1}{\rho c}\,\frac{\partial c}{\partial V}\bigg|_S = \frac{1}{c}\,\frac{\partial(\rho c)}{\partial \rho}\bigg|_S \ . \end{aligned} \tag{2.7a}$$

Similarly,

$$\vec{R}'_{u-c} \cdot \nabla_{\vec{q}}(u-c) = -\Big(\frac{1}{c}\Big)\,\frac{\partial(\rho c)}{\partial \rho}\bigg|_S \ . \tag{2.7b}$$

Because $\rho^2 \partial_\rho (\rho c)^2|_S = \partial_V^2 P|_S$, the right hand side of Eq. (2.7) only vanishes at inflection points of the isentropes in the P–V plane. Therefore, for a convex EOS the acoustic wave families are always non-degenerate. The more general case of a non-convex EOS will be discussed in Lecture 4.

Thus, we have classified the wave families for the fluid equations. Next the elementary waves are described. The two types of elementary waves for the acoustic modes; rarefactions and shocks are analyzed separately.

Remark 2.1: Transformations other than those of the form $\vec{q} = \vec{q}(\vec{w})$ are useful. In particular, the Lagrangian mass coordinate (see Ex. 1.4)

$$dm = \rho dx \quad \text{or} \quad m(x,t) = \int_{x_0(t)}^{x} \rho(x,t)dx$$

is a transformation of the co-ordinate x that depends on the variable $\vec{w}$. For the fluid equations, in Ex. 2.1 it is shown that the wave families are of the same type in either Lagrangian or Eulerian co-ordinates. Transformation that change the wave type can not preserve the isomorphism between solutions.

2.1 Continuous Simple Waves

The scale invariant continuous waves are a type of simple wave known as a centered **rarefaction**. They can be constructed as follows. Let

$$\xi = x/t \quad \text{and} \quad \vec{w}(x,t) = \vec{h}(\xi) \ . \tag{2.8}$$

The scale invariant form for a solution reduces the PDEs (1.3a) to ODEs

$$\begin{aligned} \partial_t \vec{h}(\xi) + \mathbf{DF} \cdot \partial_x \vec{h}(\xi) &= \vec{0} \\ \frac{1}{t} \left(\mathbf{DF} - \xi \, \mathbf{I} \right) \cdot \frac{d\vec{h}}{d\xi} &= \vec{0} \end{aligned} \tag{2.9}$$

where $\mathbf{I}$ is the unit matrix. The only solutions of this equation are of the form

$$\xi = \lambda_i(\vec{h}) \quad \text{and} \quad \frac{d\vec{h}}{d\xi} = n(\vec{h}) \, \vec{R}_i(\vec{h}) \ , \tag{2.10}$$

where n is a normalization factor for the eigenfunction. Hence, **a rarefaction curve is tangent to the right eigenfunction**. For strictly hyperbolic PDEs, by continuity ξ and $\vec{h}$ are well defined; *i.e.*, as $\vec{h}$ varies, there is no ambiguity from the crossing of eigenvalues. The fluid equations are strictly hyperbolic when the sound speed is non-zero.

The eigenvalues are a function of $\vec{h}$. Thus, Eq. (2.10) implies $\xi = \lambda_i(\vec{h}(\xi))$. For the solution to be consistent

$$\begin{aligned} 1 = (d/d\xi)\lambda_i &= \frac{d\vec{h}}{d\xi} \cdot \nabla_h \lambda_i \\ &= n \, \vec{R}_i \cdot \nabla_w \lambda_i \ . \end{aligned}$$

This determines the normalization factor

$$n^{-1} = \vec{R}_i \cdot \nabla_w \lambda_i \ . \tag{2.11}$$

Hence, a rarefaction wave can be constructed only for a linearly non-degenerate wave family. Moreover, the rarefaction curve is only a single valued function of x and t when restricted to the region in which the characteristic velocity varies monotonically.

A wave family that is everywhere linearly non-degenerate is called **genuinely non-linear**. A genuinely non-linear wave family has the property that the characteristic velocity is monotonic along the entire rarefaction curve. For the fluid equations, Eq. (2.7) implies the acoustic wave families are genuinely non-linear when the isentropes in the V–P plane are convex.

The rarefaction waves can also be derived from the characteristic form of the equations. By substituting Eq. (2.8) into the characteristic form of the fluid equations (1.13) we find

$$\begin{aligned} (u-\xi) \quad \cdot \qquad \frac{dS}{d\xi} \qquad &= 0 \ , \\ (u+c-\xi) \cdot \left(\frac{dP}{d\xi} + \rho c \frac{du}{d\xi} \right) &= 0 \ , \\ (u-c-\xi) \cdot \left(\frac{dP}{d\xi} - \rho c \frac{du}{d\xi} \right) &= 0 \ . \end{aligned} \tag{2.12}$$

One factor in each equation must vanish. The non-trivial solutions are given by $\xi = u \pm c$ and a sequence of 2 quadratures: (i) $dS = 0$, which is equivalent to $dE = -PdV$, determines the thermodynamic state on an isentrope; and then (ii) $du = \pm dP/\rho c$ determines the velocity. The second quadrature can be performed after the first because along an isentrope all the thermodynamic quantities (in particular P, ρ and c) are a function of one variable. Thus, for a rarefaction wave, the entropy and one of the Riemann invariants Eq. (1.14) are constant.

Using the variable $\alpha = V$ to parameterize the rarefaction curve, the two quadratures can be expressed as the ODEs

$$\frac{d}{d\alpha} \begin{pmatrix} V \\ E \\ u \end{pmatrix} = \begin{pmatrix} -1 \\ P \\ \pm \rho c \end{pmatrix} = \rho c \, \vec{R}'_{u \pm c} \ . \tag{2.13}$$

Except for the parameterization this is equivalent to Eq. (2.10). Moreover, the variation of the characteristic velocity along the rarefaction curve $d(u \pm c)/d\alpha$ is readily computed. This again shows that the acoustic wave families are genuinely non-linear when the EOS is convex.

Suppose one tries to construct a simple wave solution corresponding to the linearly degenerate eigenvalue; *i.e.*, $\xi = u$. Since $u \pm c - \xi \neq 0$, it follows from Eq. (2.12) that $P_\xi = 0$ and $u_\xi = 0$. Hence $P =$ constant, $u =$ constant and $S_\xi \propto \delta(\xi - \xi_0)$. Therefore, the solution has a discontinuity in S along $x/t = u$. This is called **contact**.

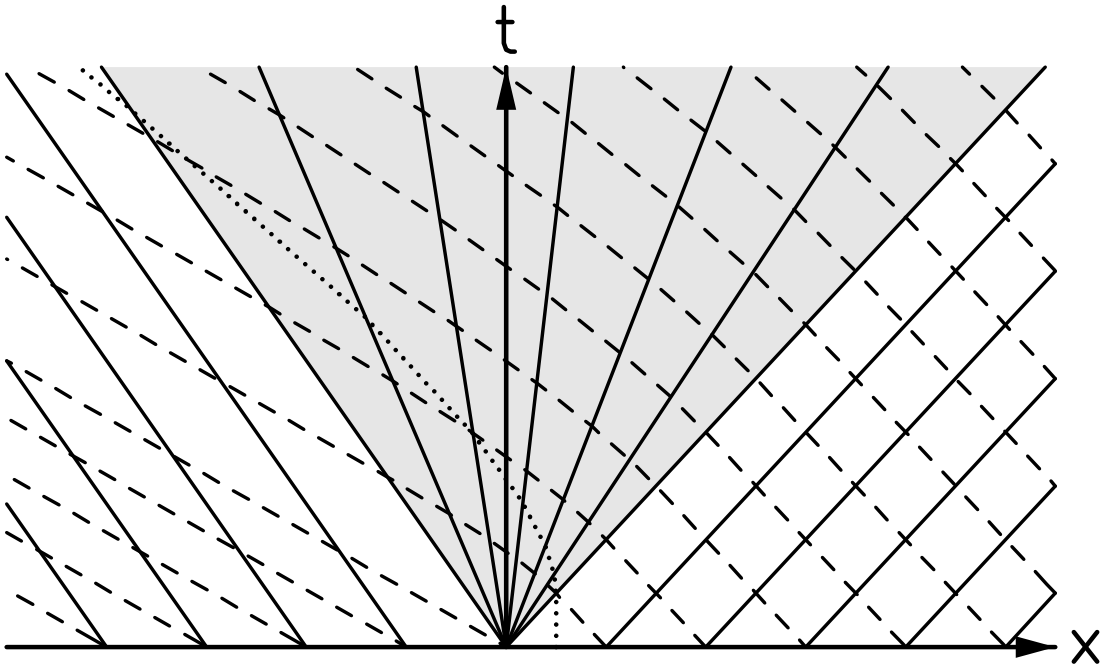

FIGURE 2.1

Characteristics in the x–t plane for a right facing rarefaction wave. The shaded area is the rarefaction fan. The solid lines correspond to characteristics $u + c$ and the dashed lines to characteristics $u - c$. The dotted line is a particle trajectory.

In the x–t plane, for a centered rarefaction all variables (in particular, P, ρ and u) are constant along either the rays $x/t = u + c$ for a **right facing** wave or $x/t = u - c$ for a **left facing** wave. Particle trajectories flow into a right facing wave from the right, and the left Riemann invariant is constant; *i.e.*, R_- in Eq. (1.14). Similarly for a left facing wave particle trajectories flow in from the left and the right Riemann invariant is constant; *i.e.*, R_+ in Eq. (1.14). A rarefaction wave can be parameterized by either the characteristic velocity or the corresponding Riemann invariant; *i.e.*, for a right facing rarefaction either $x/t = u + c$ or R_+, and similarly for a left facing rarefaction.

For the standard case of a convex EOS, discussed later in more detail, when a scale invariant simple wave overtakes a particle its density decreases. Hence, the name rarefaction wave. Rarefaction waves spread out in time. In the x–t plane, both characteristic families for a right facing rarefaction wave are shown in Fig. 2.1. In this case, the forward characteristics $(u+c)$ are straight lines but the backward characteristics $(u-c)$ are curved.

A rarefaction can be joined together with a region of constant state. We note two properties of such a composite solution: (i) The edge (leading or trailing) of the rarefaction travels at the characteristic velocity, and (ii) At the edge of the rarefaction the derivatives of the solution are discontinuous. This is an example of a general property of hyperbolic PDEs, namely, **weak singularities** (discontinuities in derivatives) are possible but can only propagate along a characteristic.

As an illustrative example, for an ideal gas EOS we derive the wave profile of a rarefaction centered about the point $x = 0$, $t = 0$. For a right facing rarefaction, the left Riemann invariant is constant. From Eq. (1.17)

$$u - \frac{2}{\gamma - 1} c = R_L \ .$$

A right facing rarefaction can be parameterized by the variable

$$\xi = x/t = u + c \ .$$

Combining these two equation we obtain

$$u(\xi) = \frac{2}{\gamma + 1} \xi + \frac{\gamma - 1}{\gamma + 1} R_L \ ,$$
$$c(\xi) = \frac{\gamma - 1}{\gamma + 1} \left(\xi - R_L \right) \ .$$

Because the entropy for a rarefaction wave is constant, it follows that the other thermodynamic variables are determined by the sound speed. From Eq. (1.17), we obtain

$$\rho(\xi) = [c(\xi)/c_0]^{\frac{2}{\gamma - 1}} \cdot \rho_0 \ ,$$
$$P(\xi) = [c(\xi)/c_0]^{\frac{2\gamma}{\gamma - 1}} \cdot P_0 \ .$$

For an ideal gas EOS, the profiles at a fixed time ($x = \xi t$) of either u or c are linear in x. Using the relation

$$\frac{dx}{dt} = t \frac{d\xi}{dt} + \xi \ ,$$

the backwards characteristic can be determined analytically by integrating the equation $dx/dt = u - c$. Within the rarefaction fan, the backwards characteristic is given by

$$x/t = R_L + [\xi_0 - R_L] \cdot (t_0/t)^{\frac{2\,(\gamma-1)}{\gamma+1}} \ .$$

Similarly, the particle trajectory is given by

$$x/t = R_L + [\xi_0 - R_L] \cdot (t_0/t)^{\frac{\gamma-1}{\gamma+1}} \ .$$

We note, if the rarefaction extends to a vacuum ($P = 0$) then for all three characteristics $x/t \to R_L$ as $t \to \infty$ and R_L corresponds to the escape velocity.

The fluid equations are time reversal invariant, *i.e.*, invariant under $t \to -t$ and $u \to -u$. Applying time reversal to a rarefaction wave leads to a compressive wave. However, for a compressive wave the characteristics focus and cross in a finite time leading to a singularity; see Exs. 1.6 and 1.7. A shock wave, which we discuss next, is a regularization of the singularity. The regularization (or physical admissible shock waves) breaks the time reversal invariance of the equations.

2.2 Discontinuous Shock Waves

Scale invariant solutions can also be piecewise constant. A discontinuous solution is known as a **shock wave**. Let σ be the wave speed of the discontinuity. The jumps of the variables across the discontinuity are not arbitrary. The conservation form of the fluid equations leads to constraints known as the **Rankine-Hugoniot jump conditions**. These can be derives as follows: (i) Assume a traveling wave solution; *i.e.*, $\rho = \rho(x - \sigma t)$, etc. (ii) Then $\partial/\partial_t = -\sigma\partial/\partial_x$. (iii) Integrating Eq. (1.1) across the wave front, from the ahead state at x_0 to the behind state at x_1 (**relative to the shock front, ahead is upstream and behind is downstream**), we find

$$\Delta[\rho(u - \sigma)] = 0 \ , \tag{2.14a}$$

$$\Delta[\rho u(u - \sigma) + P] = 0 \ , \tag{2.14b}$$

$$\Delta[\rho(\tfrac{1}{2}u^2 + E)(u - \sigma) + Pu] = 0 \ , \tag{2.14c}$$

where $\Delta[f] = f(x_1) - f(x_0)$ is the jump of the quantity f across the shock wave.

Remark 2.2: Shocks waves can be thought of as weak solutions, in the sense of a distribution, to hyperbolic PDEs. Because of the non-linear nature of the flux function, the only sensible distributions are step discontinuities. Constraints on the weak solutions can be derived by integrating the PDEs with a test function and then integrating by parts over the regions between discontinuities. To satisfy the equations for an arbitrary test function, discontinuities in a weak solution must satisfy the Rankine-Hugoniot jump conditions. There is also the notion of a solution in the sense of a measure valued function. This extension of distributions allows for non-linear functions. However, the physical meaning of such solutions is not clear.

The fluid equations are Galilean invariant. Consequently, the jump conditions should be a function of only velocity differences. Linear combinations of Eq. (2.14) lead to

$$\Delta[\rho(u-\sigma)] = 0 \ , \tag{2.15a}$$

$$\Delta[\rho(u-\sigma)(u-\sigma)+P] = 0 \ , \tag{2.15b}$$

$$\Delta[\rho(\tfrac{1}{2}(u-\sigma)^2+E)(u-\sigma)+P(u-\sigma)] = 0 \ . \tag{2.15c}$$

The momentum equation (2.15b) is Eq. (2.14b) $-\ \sigma \times$ Eq. (2.14a), and the energy equation (2.15c) is Eq. (2.14c) $-\ \frac{1}{2}\,\sigma \times$ [Eq. (2.14b) + Eq. (2.15b)].

The **mass flux** through the discontinuity is given by

$$m = \rho \cdot (\sigma - u) \ . \tag{2.16}$$

The mass flux can be thought of as parameterizing the strength of the shock wave. (In Lagrangian mass coordinates, see Ex. 1.4, the mass flux is the wave speed.) When $m > 0$, streamlines enter the discontinuity from the right and the discontinuity is called a **right facing** shock wave; *i.e.*, upstream is on the right side of the front, $x_1- < x_0+$. Right facing waves are associated with the characteristic $\lambda = u + c$. Similar when $m < 0$, the

discontinuity is called a **left facing** shock wave and are associated with the characteristic $\lambda = u - c$. Using m to eliminate u reduces Eq. (2.15) to

$$m = \text{constant} \ , \tag{2.17a}$$

$$\Delta[Vm^2 + P] = 0 \ , \tag{2.17b}$$

$$m \cdot \Delta[\tfrac{1}{2}(mV)^2 + E + PV] = 0 \ . \tag{2.17c}$$

There are two cases to consider:

1. $m = 0$.

   There is no flux through the discontinuity. It follows from Eq. (2.16) that $\sigma = u$ and hence $\Delta[u] = 0$, and from Eq. (2.15b) that $\Delta[P] = 0$. This wave corresponds to the linearly degenerate eigenvalue and is called a **contact**. It has the property that P and u are continuous but S and ρ may be discontinuous. The same contact wave was obtained when we tried to construct a simple wave from the linearly degenerate eigenvalue using the characteristic equations.

   Contacts can also represent **material interfaces**. This allows the fluid equations to be generalized to more than one material. We simply add an index n to the EOS, $P(V, E) \to P_n(V, E)$, and the equation $(d/dt)\, n = 0$ to specify that the index is convected with the material. The continuity of presure and particle velocity across a material interface is a consequence of the conservation laws. It is not an arbitrary assumption, but is an approximation valid when other physical effects such as surface tension can be neglected.

2. $m \neq 0$.

   From the momentum jump condition, Eq. (2.17b), we find

$$m^2 = -\frac{\Delta P}{\Delta V} \ . \tag{2.18}$$

This implies that ΔP and ΔV have the opposite sign; *i.e.*, if P increases then V decreases, and vice versa. For later use we note that Eqs. (2.16) and (2.18) can be combined to give the important relation

$$\Big[\rho_0 \cdot (\sigma - u_0)\Big]^2 = \Big[\rho_1 \cdot (\sigma - u_1)\Big]^2 = -\Delta P/\Delta V \ . \tag{2.19}$$

The energy jump condition can be simplified using the algebraic identity

$$\Delta[AB] = \overline{A}\,\Delta B + \overline{B}\,\Delta A \ , \tag{2.20}$$

where $\overline{f} = \frac{1}{2}\,(f_0 + f_1)$ is the average of the quantity f across the shock. In particular, from Eqs. (2.18) and (2.20)

$$\begin{aligned} \tfrac{1}{2}\,m^2 \Delta[V^2] &= m^2 \overline{V}\,\Delta V \\ &= -\overline{V}\,\Delta P \ . \end{aligned}$$

Substituting this into Eq. (2.17c) we find

$$\Delta H = \overline{V}\,\Delta P \ , \tag{2.21}$$

where $H = E + PV$ is the enthalpy.

Applying the algebraic identity to the left hand side we obtain the **Hugoniot equation**

$$\Delta E = -\overline{P}\,\Delta V \ . \tag{2.22}$$

Finally, from Eqs. (2.14b), (2.16) and (2.18) we find

$$\Delta u = \pm\sqrt{-\Delta P \Delta V} \ , \tag{2.23}$$

where $+$ corresponds to a right facing wave ($m > 0$) and $-$ to a left facing wave ($m < 0$).

It is important to note that from a solution to the Hugoniot equation, the wave speed is determined by Eq. (2.19) and the particle velocity by Eq. (2.23). Hence, a shock wave

is completely determined by the EOS. This is a consequence of the Galilean invariance of the fluid equations.

For a given ahead state (subscript 0), there is a continuous 1-parameter family of shock waves for each linearly non-degenerate eigenvalue ($\lambda = u \pm c$). Because of the symmetry of the fluid equations under $x \to -x$, there is a correspondence between left and right facing shock waves with the same $|m|$; the thermodynamic state is the same but $\Delta u_{\text{left}} = -\Delta u_{\text{right}}$. The possible thermodynamic states behind a shock wave is called the **Hugoniot locus**. The Hugoniot locus is determined by the EOS, from the Hugoniot equation, Eq. (2.22). It depends on the thermodynamic part of the ahead state but is independent of both the ahead velocity and the wave family. Frequently, the Hugoniot locus is projected onto the P–V plane. As an example, the Hugoniot locus for an ideal gas (see Ex. 2.7) is shown in the P–V plane in Fig. 2.2 and in the σ–u plane in Fig. 2.3.

There is striking similarity between the equations for a shock wave and a rarefaction wave when they are written in the form

$$\Delta E/\Delta V = -\overline{P} \quad \longleftrightarrow \quad dE/dV|_S = -P \ , \tag{2.24a}$$

$$\Delta P/\Delta u = \rho(\sigma - u) \quad \longleftrightarrow \quad dP/du|_S = \pm \rho c \ . \tag{2.24b}$$

Equation (2.24a) is important for finite difference algorithms using artificial viscosity and Equation (2.24b) is important for Godunov algorithms using Riemann solvers.

Next we derive two important results for weak shocks, $m \approx 0$. The following lemmas imply that in the limit of weak shock waves the shock relations in Eq. (2.24) for shocks do indeed correspond to the relations for rarefactions.

Lemma 2.3: In a neighborhood of a state 0, the Hugoniot equation has a unique solution that can be parameterized by V. Furthermore, for weak shocks, $\Delta S = O\big((\Delta V)^3\big)$.

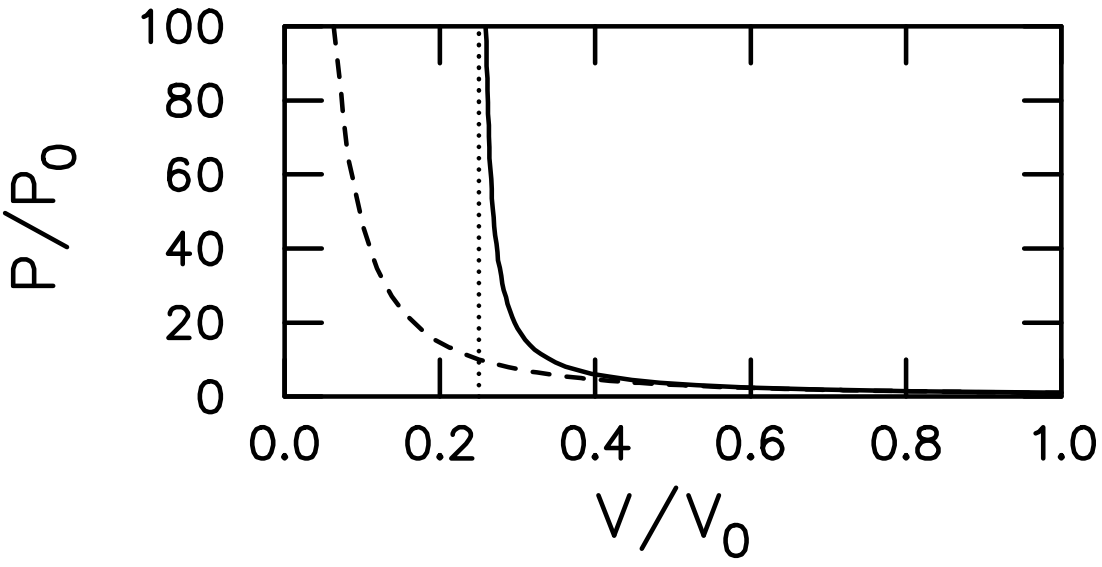

FIGURE 2.2

Loci in the P–V plane for an ideal gas $\gamma = 5/3$. The solid line is shock Hugoniot, the dotted line is the asymptotic strong shock limit, and the dashed line is an isentrope.

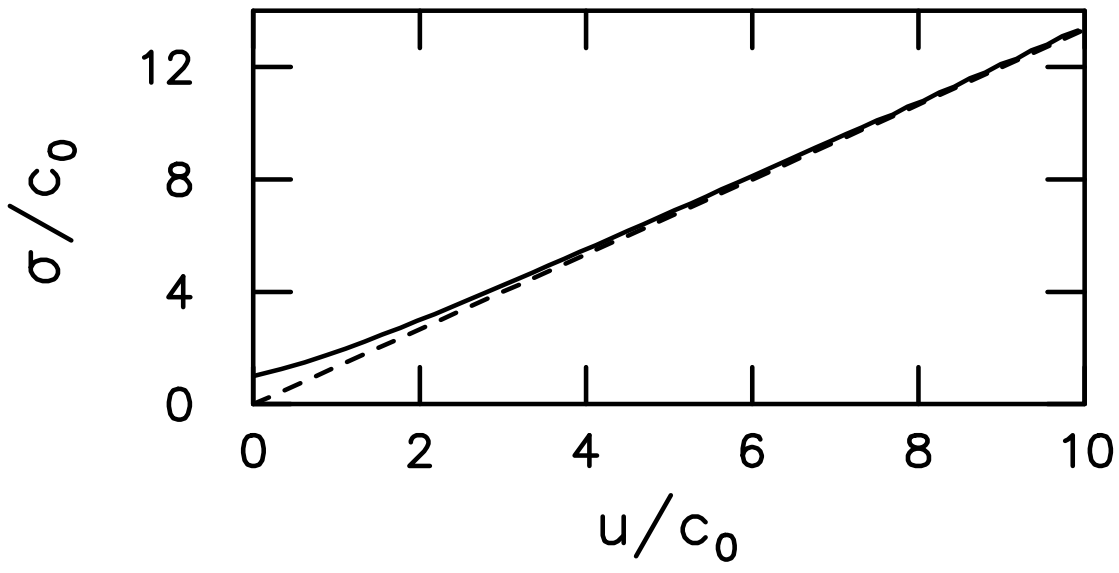

FIGURE 2.3

Loci in (shock velocity)–(particle velocity) plane for an ideal gas with $\gamma = 5/3$. The solid line is shock Hugoniot, and the dashed line is the asymptotic strong shock limit.

Proof: Thermodynamic state space can be parametrized by V and S. From Eq. (2.22), the Hugoniot locus based at state 0, corresponds to the zero level set of the Hugoniot function

$$h(V,S) = E(V,S) - E_0 + \tfrac{1}{2}\Big[P(V,S) + P_0\Big]\cdot(V - V_0)\ . \tag{2.25}$$

Using the thermodynamic identity $dE = -P\,dV + T\,dS$ the differential of h can be expressed as

$$dh = T\,dS + \tfrac{1}{2}\,(V - V_0)\,dP - \tfrac{1}{2}\,(P - P_0)\,dV\ . \tag{2.26}$$

At the initial state, $\partial_S h = T > 0$. By the implicit value theorem, there exists a small neighborhood about $(V_0,\, S_0)$ in which the zero level set of the Hugoniot function is given by a curve $S_h(V)$. We denote the pressure on the Hugoniot locus by $P_h(V) = P(V, S_h(V))$.

The derivatives of S along the Hugoniot locus can be evaluated by taking the derivatives of the equation $h(V, S_h(V)) = 0$. From Eq. (2.26), the first derivative of the Hugoniot function gives

$$2\,T\,\frac{dS_h}{dV} = (P - P_0) + (V_0 - V)\,\frac{dP_h}{dV}\ . \tag{2.27}$$

Evaluating at $V = V_0$, we find that $(d/dV)\,S_h(V_0) = 0$. Taking the second derivative of the Hugoniot function gives

$$2\,T\,\frac{d^2S_h}{dV^2} + 2\,\frac{dT_h}{dV}\cdot\frac{dS_h}{dV} = (V_0 - V)\frac{d^2P_h}{dV^2}\ . \tag{2.28}$$

Evaluating at $V = V_0$, we find that $(d/dV)^2 S_h(V_0) = 0$. Taking the third derivative of the Hugoniot function gives

$$2\,T\,\frac{d^3S_h}{dV^3} + 2\,\frac{dT_h}{dV}\cdot\frac{d^2S_h}{dV^2} + 2\,\frac{d}{dV}\left(\frac{dT_h}{dV}\cdot\frac{dS_h}{dV}\right) = -\frac{d^2P_h}{dV^2} + (V_0 - V)\frac{d^3P_h}{dV^3}\ . \tag{2.29}$$

Evaluating at $V = V_0$, we find that

$$\begin{aligned} 2\,T\,\frac{d^3S_h}{dV^3}(V_0) &= -\frac{d^2P_h}{dV^2}(V_0) \\ &= \left(\frac{\partial}{\partial V}\Big|_S + \frac{dS_h}{dV}\cdot\frac{\partial}{\partial S}\Big|_V\right)^2 P(V_0,S_0) \\ &= -\frac{\partial^2 P}{\partial V^2}\Big|_S (V_0,S_0)\ . \end{aligned} \tag{2.30}$$

The leading order term in the Taylor expansion for $S_h(V)$ then gives

$$\begin{aligned}\Delta S &= \frac{1}{3!}\cdot\frac{d^3S_h}{dV^3}\cdot\big(\Delta V\big)^3 \\ &= -\frac{1}{12T}\cdot\left.\frac{\partial^2 P}{\partial V^2}\right|_S\cdot\big(\Delta V\big)^3 \ .\end{aligned} \tag{2.31}$$

⊠ ⊠

Lemma 2.4: As the mass flux $m \to 0$, the wave speed $\sigma \to u \pm c$.

Proof: From Eqs. (2.19)

$$\big[\rho_0\cdot(\sigma-u_0)\big]^2 = -\frac{\Delta P}{\Delta V}\ .$$

As $V \to V_0$ the right hand side approaches $0/0$. Applying l'Hospital's rule we obtain

$$\big(\rho_0\cdot(\sigma-u_0)\big)^2 \to -\frac{d}{dV}P_h(V_0) \qquad \text{as } V\to V_0\ .$$

From the previous lemma,

$$\begin{aligned}dP_h/dV(V_0) &= (\partial_V + S_h'\partial_S)P(V_0,S_0) \\ &= \partial_V P|_S = -(\rho_0 c_0)^2\ .\end{aligned}$$

Therefore, $\sigma - u_0 \to \pm c_0$. The plus sign is for right facing waves and the minus sign for left facing waves.

⊠ ⊠

From these lemmas it follows that (i) the limit of weak shocks are acoustic waves, and that (ii) mass, momentum, energy and entropy can not simultaneously be conserved across a shock wave. Discontinuous waves with $\Delta S = 0$ are natural from the characteristic form of the fluid equations. However, these would be valid weak solutions only when the entropy equation is used in place of the energy equation. We note, when Riemann introduced the concept of characteristics, he mistakenly assumed entropy rather than energy was conserved across a shock wave.

2.3 Entropy Condition

Even with the restriction that mass, momentum and energy are conserved, there are too many shock waves. A consequence of too many waves is that the initial value problem does not have a unique weak solution. Physically, one need to take into account dissipative effects that smooth out or regularize discontinuities. With viscosity and heat conduction, the fluid equations become (see Ex. 1.1 A)

$$\partial_t \rho + \partial_x(\rho u) = 0 \tag{2.32a}$$

$$\partial_t(\rho u) + \partial_x(\rho u^2 + P) = \partial_x(\mu \partial_x u) \tag{2.32b}$$

$$\partial_t\Big(\rho\,(\tfrac{1}{2}u^2 + E)\Big) + \partial_x\Big(\rho\,(\tfrac{1}{2}u^2 + E + PV)\Big) = \partial_x(\mu u \partial_x u) + \partial_x(\kappa \partial_x T) \tag{2.32c}$$

where $\mu \geq 0$ is the coefficient of dynamic viscosity and $\kappa \geq 0$ is the coefficient of thermal conductivity. It follow that the entropy satisfies (see Ex. 1.1 D)

$$\partial_t(\rho S) + \partial_x\Big(\rho u S - \frac{\kappa \partial_x T}{T}\Big) = \frac{\mu}{T}(\partial_x u)^2 + \kappa\Big(\frac{\partial_x T}{T}\Big)^2 . \tag{2.33}$$

Hence, the total entropy is increasing; *i.e.*, viscosity and heat conduction are each dissipative processes.

Let us consider a steady-state left facing wave in the shock-attached frame. The PDEs then reduce to a system of ODEs for the shock profile. The ODEs have first integrals and can be reduced to the pair of first order equations

$$m\mu \frac{dV}{dx} = J[P + m^2 V] \tag{2.34a}$$

$$\frac{\kappa}{m}\frac{dT}{dx} = J[E - \tfrac{1}{2}\,m^2 V^2 + V(P_0 + m^2 V_0)] \tag{2.34b}$$

where $m = \rho u > 0$ is the mass flux and $J[f] = f(x) - f(-\infty)$ is the change in the quantity f from its initial value ahead of the shock. For a fixed shock strength, mass flux m, these ODEs have two important properties:

(i) The critical points of the ODEs, at which all derivatives vanish, correspond to points on the Hugoniot locus. Furthermore, for the standard case of a convex EOS, it can be

shown from a phase plane analysis that a shock profile exists if and only if the final state has a higher entropy than the initial state; see *e.g.*, [Menikoff & Plohr, 1989, Appendix C].

(ii) If $\mu \to 0$ and $\kappa \to 0$ with a fixed ratio $\mu/\kappa =$ constant, then the shock profile scales and in the limit converges to a discontinuous shock. In particular, when μ and κ are sufficiently small, viscosity and heat conduction are only significant in the shock profile where the spatial derivatives of u and T are large.

For the standard case, this leads to the important conclusion that the initial and final states do not depend on the detailed nature of the dissipation; *i.e.*, the magnitude of the coefficients of either viscosity or heat conduction. Moreover, the physical dissipation for fluid flow can be accounted for by the Hugoniot jump conditions and the choice of admissible shocks, even though there is no explicit source of dissipation (entropy production) in the ideal fluid equations.

The physical width of a shock wave can be very narrow, typically, on the order of a mean free path; *e.g.*, in air at sea level, on the order of 10^{-5} cm. Usually this very short length scale is neither important nor of interest. Hence, for many applications the hyperbolic PDEs of ideal fluid flow are used because the weak solutions with the correct shock waves (conserving mass, momentum and energy, and entropy increasing) are a very good approximation for the underlying physics.

In the standard case of a convex EOS, only compressive shocks are consistent with the thermodynamic condition that entropy increases. In this case, the condition that entropy increases is sufficient to obtain a unique physical solution to the initial value problem. Because shock waves are associated with dissipative processes, the non-uniqueness of weak solutions is resolved by breaking the time reversal invariance of the ideal fluid equations. All other invariances of the fluid equations are maintained for shock waves. In particular, the Hugoniot jump relations are Galilean invariant.

The entropy condition is important for numerical algorithms. Some form of artificial numerical dissipation is the basis for shock capturing algorithms. The physical entropy

increasing shock waves also correspond to the mathematically stable shock waves: If a compressive shock is perturbed, the characteristics refocus into a shock wave. On the other hand, if an expansive shock is smeared out then the characteristics diverge and the discontinuity is unstable. Non-uniqueness of weak solutions for a general EOS will be discussed later in more detail. For a non-convex EOS the entropy condition is necessary but not sufficient for uniqueness.

2.4 Characteristic Condition

Another important property of a shock wave that will be derived in Lecture 4 is the Lax **characteristic condition**

$$(u+c)_{\text{behind}} > \sigma > (u+c)_{\text{ahead}} \ , \quad \text{for right facing wave;} \tag{2.35a}$$

$$(u-c)_{\text{behind}} < \sigma < (u-c)_{\text{ahead}} \ , \quad \text{for left facing wave.} \tag{2.35b}$$

The characteristic condition is needed for 1-D shock stability. It ensures the correct number of degrees of freedom to determine uniquely the interaction of a shock wave with an acoustic wave. This interaction must be accounted for in numerical algorithms in order to obtain the correct time dependence for the propagation of a shock wave. Schematically the characteristics in the x–t plane relative to the shock front are shown in Fig. 2.4.

A shock wave has 7 degrees of freedom; 3 variables for the ahead state, 3 variables for the behind state, and the wave speed. The characteristic condition implies that there are three incoming characteristics ahead of the shock and one incoming characteristic behind the shock. The three ahead characteristic determine the three variables of the ahead state. The conservation laws provide three jump conditions across the shock. Together with the ahead state, the jump conditions determine a one parameter family of possible states behind the shock (Hugoniot locus). An additional condition is needed to determine the shock strength. The incoming characteristic behind the shock provides the remaining information. The two outgoing characteristic are determined from the incoming characteristics

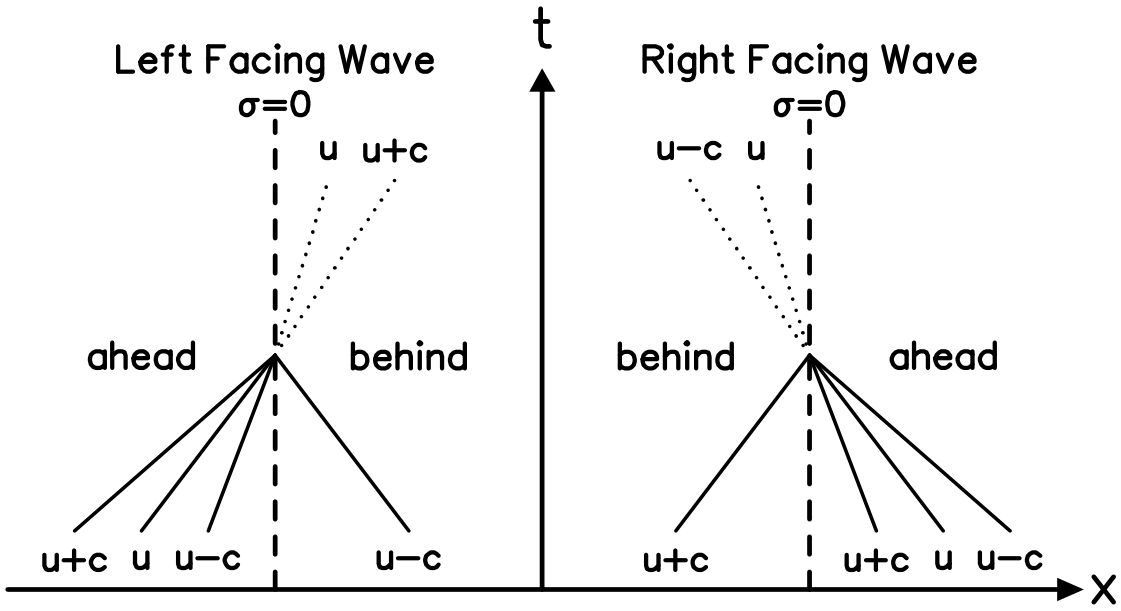

FIGURE 2.4

Characteristics in the x–t plane for left and right facing shock wave relative to the shock front. Dashed line is shock front, solid lines are incoming characteristics and dotted lines are outgoing characteristics.

and provides the boundary information for the region behind the shock. This mechanism is the basis for shock tracking algorithms.

The characteristic condition has the interpretation that relative to the shock front, the flow is **subsonic behind and supersonic ahead**. For either a right or left facing shock wave

$$|\sigma - u|_{\text{behind}} < c_{\text{behind}} \quad \text{and} \quad c_{\text{ahead}} < |\sigma - u|_{\text{ahead}} \,. \tag{2.36}$$

Hence, for two waves of the same family, the second will catch up with and interacts with the first. This provides a non-linear stability for shock waves which is important for shock capturing algorithms. If a shock wave is perturbed or smeared out into a compressive wave, then the focusing of characteristics will steepen the profile forming discontinuities. The initial perturbation or the compressive wave profile determines the order in which

the characteristics will cross. When the characteristic speed varies monotonically within a compressive wave profile, after a transient, the discontinuities will coalesce and reform the initial shock wave. A convex EOS has this property, and in this case all compressive shock waves are stable. For a non-convex EOS, the characteristic speed does not vary monotonically and a shock wave can split into a composite of two shocks separated by a compression wave. Stability of shock waves is the basis for the Oleĭnik-Liu extended entropy condition.

The variation of the characteristic speeds is important for numerical algorithms. For linearly non-degenerate waves, the focusing of characteristics stablizes numerical shock waves. For a linearly degenerate wave, this stabilization is lacking and a numerical contact tends to be diffusive rather than remaining a sharp discontinuity. Artificial compression algorithms modify the linearly degenerate characteristics in order to counteract the numerical diffusion of contacts.

For two shocks of the same family, if the region between the two shocks is not uniform then the characteristic condition does not imply that the trailing shock will alway catch up with the lead shock. This is illustrated by the following examples: (i) N–wave or shock-rarefaction-shock; *e.g.*, sonic boom. Both shocks interact with the rarefaction causing the N-wave to decay. As it decays the N–wave spreads out and the two shocks separate rather than approaching. (ii) Geometric source terms for quasi 1-D flow; *e.g.*, subsonic flow into a converging-diverging nozzle can be transonic. Stable flows exist with two shock waves of the same family; one shock propagating ahead of the nozzle and a second stationary shock in the diverging section of the nozzle.

Finally, we remark that a region of constant state must be bounded by either a simple wave or a shock wave. In applications, the ambient state is usually constant. This simple observation can be quite useful in constructing solutions; see *e.g.*, Exs. 1.6 C&D, 1.7 and 1.8.

General references:

1. [Courant & Friedrichs, 1948]
2. [Lax, 1957, 1972]
3. [Smoller, 1983] chpts. 15–18

Exercises

2.1 For the fluid equations in Lagrangian coordinates (Ex. 1.4):

A) Compute **DF**, and its eigenvalues and eigenfunctions.

B) From the eigenfunction of **DF** determine the state, parametrized by V, along a right facing rarefaction.

Compared to Eulerian coordinates:

C) Are the characteristic velocities the same?

D) Is the linearly degenerate and non-degenerate nature of the wave families the same?

E) Are the Hugoniot jump conditions the same?

F) For smooth solutions show that the equation for conservation of energy can be replaced by the equation for conservation of entropy. Does conservation form of the PDEs uniquely determine weak solutions?

2.2 For the cylindrically or spherically symmetric fluid equations (Ex. 1.2) or the duct flow equations (Ex. 1.3):

A) Are the Hugoniot jump conditions affected by the source terms?

B) Are simple waves affected by the source terms?

2.3 **A)** Prove that the planar fluid equations are Galilean invariant.

B) Are the cylindrically or spherically symmetric fluid equations (Ex. 1.2) Galilean invariant?

C) What other symmetries do the fluid equations satisfy?

2.4 Consider an ideal gas EOS, $P = (\gamma - 1)E/V$.

A) For a right facing rarefaction ($\xi = u + c$), show that the state parameterized by V is given by

$$P/P_0 = (V_0/V)^\gamma \tag{2E.1}$$

$$c/c_0 = (V_0/V)^{\frac{1}{2}(\gamma-1)} \tag{2E.2}$$

$$u = u_0 + \frac{2}{\gamma - 1}\,(c - c_0) \tag{2E.3}$$

B) Show that the limiting or escape velocity is $u_0 - \frac{2}{\gamma-1}c_0$.

C) Do simple waves have to be centered rarefactions? Hint, consider Ex. 1.8.

2.5 For given compression ratio, is the pressure higher for a single shock or multiple shocks or isentropic compression?

2.6 Let σ be the shock velocity, u the particle velocity, and the subscripts 0 and 1 denote the state ahead and behind the shock. From the Hugoniot jump conditions prove:

A)

$$\Delta P = \rho_0 (u_1 - u_0)\,(\sigma - u_0)\ . \tag{2E.4}$$

Moreover, for the 'lab' frame ($u_0 = 0$), show that in the strong shock limit (large σ)

$$P_s \to \rho_0 u_p u_s\ , \tag{2E.5}$$

where u_s is the shock velocity and u_p is the particle velocity behind the shock.

B)

$$\Delta P/\Delta\rho = (\sigma - u_0)\,(\sigma - u_1)\ . \tag{2E.6}$$

C)

$$\Delta E = \tfrac{1}{2}\,(\Delta u)^2 + P_0\,(V_0 - V_1)\ . \tag{2E.7}$$

Moreover, for the 'lab' frame, show that in the strong shock limit

$$E_s \to \tfrac{1}{2}\, u_p^2 \ . \tag{2E.8}$$

D) For a frame co-moving with the shock front ($\sigma = 0$), also known as the 'shock attached frame', show that Bernoulli's function is constant; *i.e.*,

$$\Delta[E + PV + \tfrac{1}{2}\, u^2] = 0 \ . \tag{2E.9}$$

2.7 Let σ be the shock velocity, u the particle velocity, and the subscripts 0 and 1 denote the state ahead and behind the shock. Consider an ideal gas EOS, $P = (\gamma - 1)E/V$, and assume the initial state is at rest, *i.e.*, $u_0 = 0$.

A) Show that the state behind a shock, parameterized by the shock Mach number $M = \sigma/c_0 \geq 1$, is given by

$$\rho_1/\rho_0 = \frac{(\gamma+1)M^2}{(\gamma-1)M^2+2} \ , \tag{2E.10}$$

$$P_1/P_0 = 1 + \frac{2\gamma}{\gamma+1}\cdot\left(M^2-1\right) \ , \tag{2E.11}$$

$$(c_1/c_0)^2 = E_s/E_0 = 1 + \frac{2(\gamma-1)}{(\gamma+1)^2}\cdot\frac{(M^2-1)}{M^2}\cdot(\gamma M^2+1) \ . \tag{2E.12}$$

$$u_1/\sigma = \frac{2}{\gamma+1}\cdot\frac{M^2-1}{M^2} \ , \tag{2E.13}$$

Show that all these quantities vary monotonically with the shock strength.
Comment on the scale invariance of the shock Hugoniot for an ideal gas.

B) Show that the entropy is monotonically increasing with shock strength.

C) Behind the shock show that the flow is subsonic relative to the front.

D) Are the Riemann invariants constant across a shock? What implications does this have for the method of characteristics?

E) In the strong shock limit, $M \gg 1$, show that

$$\rho_1 = \frac{\gamma+1}{\gamma-1}\,\rho_0 \ , \tag{2E.14}$$

$$P_1 = \frac{2}{\gamma+1}\,\rho_0\sigma^2 \ , \tag{2E.15}$$

$$u_1 = \frac{2}{\gamma+1}\,\sigma \ , \tag{2E.16}$$

$$c_1 = \frac{[2\gamma(\gamma-1)]^{\frac{1}{2}}}{\gamma+1}\,\sigma \ , \tag{2E.17}$$

$$E_1 = \tfrac{1}{2}u_1^2 \ . \tag{2E.18}$$

Why is the maximum shock compression ratio finite?

F) Show that

$$\begin{aligned}\Delta P/\Delta u &= \rho_0(\sigma - u_0) \\ &= \left[\gamma P_0\rho_0\left(1+\frac{\gamma+1}{2\gamma}\cdot\frac{\Delta P}{P_0}\right)\right]^{\frac{1}{2}} \ .\end{aligned} \tag{2E.19}$$

In addition, for a weak shock

$$\rho_0\sigma = \tfrac{1}{2}(\rho_1 c_1 + \rho_0 c_0) + O\left((\Delta P)^2\right) \ . \tag{2E.20}$$

These formulae are the basis for some Riemann solvers.

G) Suppose a strong shock reflects from a rigid wall, *i.e.*, $u_{rs} = 0$. Show that the reflected shock corresponds to a Mach number in part (A) of $M_{rs} = \left(\frac{2\gamma}{\gamma-1}\right)^{\frac{1}{2}}$ and that the state behind the reflected shock (with σ_{rs} in the Lab frame) is

$$\rho_{rs}/\rho_1 = \frac{\gamma}{\gamma-1} \ , \tag{2E.21}$$

$$P_{rs}/P_1 = 1 + \frac{2\gamma}{\gamma-1} \ , \tag{2E.22}$$

$$(c_{rs}/c_1)^2 = E_{rs}/E_1 = \frac{3\gamma-1}{\gamma} \ , \tag{2E.23}$$

$$\sigma_{rs}/\sigma_1 = -2\,\frac{\gamma-1}{\gamma+1} \ . \tag{2E.24}$$

Is the reflected shock a strong shock, why not?

Since the reflected shock stagnates the flow, why is $E_{rs} > \frac{1}{2}u_1^2 + E_1 = 2E_1$?

2.8 A point on the shock Hugoniot is specified by the initial state and one additional parameter, either the shock velocity or a single quantity behind the shock. For an arbitrary EOS, devise an algorithm to find a Hugoniot point with a specified shock pressure that is no more complicated than an iterative solution of one algebraic equation in one variable.

2.9 Consider a steady state isentropic flow.

A) Show that Bernoulli's function is constant, *i.e.*,

$$\tfrac{1}{2}u^2 + E + PV = \tfrac{1}{2}u^2 + \int dP/\rho = \text{constant} \; . \tag{2E.25}$$

B) Show that

$$d\rho/\rho = -(u/c)\, du/c \; . \tag{2E.26}$$

Hence, if Δu is comparable to c then compressibility is important. The converse is not necessarily true.

C) For an ideal gas show that

$$u^2 + \frac{2}{\gamma - 1} c^2 = \text{constant} \; . \tag{2E.27}$$

Why is this different from the Riemann invariants for simple waves?

2.10 Consider the shock profile in the steady-state frame for an ideal gas with viscosity but no heat conduction.

A) For a left facing wave show that V is determined by the equation

$$\mu \frac{dV}{dx} = \tfrac{1}{2}\,(\gamma - 1)\, m \frac{(V - V_0) \cdot (V - V_1)}{V} \; , \tag{2E.28}$$

where $m = \rho\sigma$ is the mass flux.

B) Show that the solution is given by

$$\tfrac{1}{2}\,(\gamma - 1) \frac{m}{\mu} x = \frac{V_0 \log(V_0 - V) - V_1 \log(V - V_1)}{V_0 - V_1} \; . \tag{2E.29}$$

C) Show that $V(x)$ defined by Eq. (2E.29) satisfies the appropriate boundary conditions. How are the other variables determined?

D) Show for any reasonable definition of the shock width, such as the distance between 10% and 90% of the value of the profile at the end points or $\Delta V/(dV/dx)_{\max}$, the width approaches 0 in the strong shock limit.

Solutions

2.1 For Lagrangian coordinates the conserved quantities are

$$\vec{w} = (V,\ u,\ \mathcal{E})^{\mathrm{T}}\ , \tag{2S.1}$$

where $\mathcal{E} = \frac{1}{2}u^2 + E$, and the flux functions are

$$\vec{F} = (-u,\ \widetilde{P},\ u\widetilde{P})^{\mathrm{T}}\ , \tag{2S.2}$$

where $\widetilde{P}(\vec{w}) = P(V, \mathcal{E} - \frac{1}{2}u^2)$.

A) By straightforward differentiation

$$\mathbf{DF} = \begin{pmatrix} 0 & -1 & 0 \\ P_V & -uP_E & P_E \\ uP_V & P - u^2 P_E & uP_E \end{pmatrix}\ , \tag{2S.3}$$

where $P_V = \partial_V P|_E$ and $P_E = \partial_E P|_V$. The eigenvalues are determined by the equation

$$\det(\mathbf{DF} - \lambda \mathbf{I}) = \lambda^3 - (-P_V + P \cdot P_E)\lambda = 0\ . \tag{2S.4}$$

By Eq. (1.12), $(\rho c)^2 = -P_V + P\,P_E$, and the characteristic velocities are

$$\lambda = -\rho c,\ 0,\ \rho c\ . \tag{2S.5}$$

The corresponding matrix of eigenvectors is

$$\mathbf{R} = \begin{pmatrix} 1 & P_E & 1 \\ \rho c & 0 & -\rho c \\ -P + \rho c\, u & -P_V & -P - \rho c\, u \end{pmatrix}\ . \tag{2S.6}$$

B) A right facing wave is associated with the characteristic $\lambda = \rho c$. From Eq. (2S.6) the corresponding right eigenfunction of **DF** is

$$\vec{R}_+ = (1,\ -\rho c,\ -P - \rho c u)^{\mathrm{T}}\ . \tag{2S.7}$$

Even though the eigenfunction is not normalized according to Eq. (2.11), it follows from Eq. (2.10) that

$$(d/dV)\,u = R_+^{(2)}/R_+^{(1)} = -\rho c\ , \tag{2S.8a}$$

$$(d/dV)\,(\tfrac{1}{2}u^2 + E) = R_+^{(3)}/R_+^{(1)} = -P - \rho c u\ . \tag{2S.8b}$$

These two equations can be combined to give

$$(d/dV)\,E = -P\ . \tag{2S.8b$'$}$$

These differential equations imply that the left Riemann invariant, Eq. (1.14), and the entropy, Eq. (1.10), are constant.

C) The characteristic velocities in Eulerian coordinates, Eq. (1.13a), are not the same as in Lagrangian coordinates, Eq. (2S.5). Thus, the characteristic velocities depend on the co-ordinates; *i.e.*, (x,t) or (m,t). In fact the characteristic velocities have different dimensions in the two co-ordinate systems.

D) The Lagrangian particle trajectory corresponds to $\lambda = 0$ and is clearly a linearly degenerate mode. For the acoustic modes, $\lambda_\pm = \pm\rho c$, we find

$$\begin{aligned}(\vec{R}_\pm \cdot \nabla_w)\,\lambda_\pm &= \pm\frac{1}{2\rho c}\Big[\partial_V \mp \rho c\partial_u - (P \mp \rho c u)\partial_{\mathcal{E}}\Big]\cdot \partial_V P|_S(V, \mathcal{E} - \tfrac{1}{2}u^2)\\ &= \pm\frac{1}{2\rho c}(\partial_V - P\partial_E)\cdot\partial_V P|_S\\ &= \pm\frac{1}{2\rho c}\partial_V^2 P|_S\ .\end{aligned} \tag{2S.9}$$

Hence, the acoustic modes are linearly non-degenerate except at inflection points of the isentrope in the P–V plane; *i.e.*, $\partial_V^2 P|_S = 0$. We note that

$$\frac{1}{2\rho c}\partial_V^2 P|_S = -\frac{1}{2\rho c}\partial_V(\rho c)^2|_S = \rho^2\partial_\rho(\rho c)|_S\ .$$

Therefore, the degeneracy condition is the same in Lagrangian coordinates, Eq. (2S.9), and in Eulerian coordinates, Eq. (2.7).

E) The Lagrangian wave speed is the mass flux through the shock front, $m = \rho(\sigma - u)$, which is equivalent to Eq. (2.17a). From Eq. (1E.15) the Lagrangian jump conditions are

$$\Delta[mV + u] = 0 \ , \tag{2S.10a}$$

$$\Delta[-mu + P] = 0 \ , \tag{2S.10b}$$

$$\Delta[-m(\tfrac{1}{2}u^2 + E) + Pu] = 0 \ . \tag{2S.10c}$$

Eqs. (2S.10b) and (2S.10c) are equivalent to Eqs. (2.14b) and (2.14c). Eqs. (2S.10b) and (2.17b) imply Eq. (2S.10a). Therefore, the Hugoniot jump conditions in Lagrangian and Eulerian coordinates are equivalent.

F) Fluid flow in Lagrangian coordinates is determined by Eq. (1E.15). Multiplying the momentum equation by u and subtracting from the energy equation gives

$$\partial_t E + P\partial_m u = 0 \ . \tag{2S.11}$$

Substituting for $\partial_m u$ from the mass equation yields

$$0 = \partial_t E + P\partial_t V = T\partial_t S \ . \tag{2S.12}$$

Thus, for smooth solutions the fluid equations can be written in conservation form as

$$\partial_t \begin{pmatrix} V \\ u \\ S \end{pmatrix} + \partial_m \begin{pmatrix} -u \\ P \\ 0 \end{pmatrix} = \vec{0} \ . \tag{2S.13}$$

This would lead to jump conditions for shocks in which conservation of energy, Eq. (2S.10c) is replaced by conservation of entropy

$$\Delta[mS] = 0 \ . \tag{2S.14}$$

Therefore, the conservative form and the corresponding weak solutions of the PDEs are not unique.

2.2 **A)** The Hugoniot jump conditions are derived by integrating the equations from ahead of the shock x_0 to behind the shock x_1. In the limit $x_0 \to x_+$ and $x_1 \to x_-$, the derivative of a discontinuous function contributes but the source functions do not. Hence the jump conditions for planar, cylindrical and spherical geometry are the same. For duct flow, the cross sectional area A is continuous and factors out of the jump conditions. Hence the jump conditions for duct flow are the standard fluid jump conditions.

B) For the planar fluid equations, a simple wave is a function of one Riemann invariant. The other Riemann invariant and the entropy are constants. Source terms in the characteristic equations, compare Eq. (1.13) and Eqs. (1S.23)–(1S.25), affect the Riemann invariants. Therefore, simple waves are affected by source terms. Furthermore, source terms imply additional length or time scales. Consequently, centered rarefactions can not be scale invariant when the equations have source terms.

2.3 **A)** In Euler's equations (1.6) u enters only through $\partial_x u$ or the convective derivative $d/dt = \partial_t + u\partial_x$. These combinations are invariant under a Galilean transformation: $x' = x + u_0 t$, $t' = t$ and $u' = u - u_0$.

B) In cylindrical or spherical geometry, due to the source terms in Eq. (1E.11) the origin is a distinguished point, and the PDEs are not Galilean invariant.

C) The fluid equations are also invariant under: (i) scale transformations $x' = x/\alpha$, $t' = t/\alpha$ and $u' = u$; (ii) parity $x' = -x$, $t' = t$ and $u' = -u$; and (iii) time reversal invariance $x' = x$, $t' = -t$, $u' = u$. However, shock waves and hence weak solutions are not time reversal invariant.

2.4 **A)** Eqs. (2E.1) and (2E.2) follow from Ex. 1.5. For a right facing wave, the left Riemann invariant is constant. From Ex. 1.5 and Eq. (1.14), we obtain

$$R_- = u - \int \frac{dP}{\rho c} = u - \frac{2}{\gamma - 1}\, c\,. \qquad (2S.15)$$

At the initial state $R_- = u_0 - \frac{2}{\gamma-1} c_0$. It follows that Eq. (2E.3) is equivalent to a constant value of R_-.

B) From Eq. (2E.2), when an ideal gas expands isentropically, the sound speed decreases. The minimum sound speed of $c = 0$ corresponds to $V \to \infty$. From Eq. (2E.3) the velocity decreases with c. Hence, the minimum value of u is $u_0 - \frac{2}{\gamma-1} c_0$. The typical case has $u_0 = 0$. Thus, $u < 0$ and its minimum value has the maximum magnitude. This is called the escape velocity. If a piston is withdrawn from a tube faster than the escape speed, then the gas can not keep up and a vacuum forms in front of the piston. This is known as cavitation. It is named after the pits (or cavities) that damage propeller blades on ocean going ships. The pits result from a water jet impacting the propeller blade. The jet is formed when a gas bubble in the water collapses. The gas bubble is due to cavitation.

C) Simple waves have a constant value of S and one Riemann invariant. The characteristics corresponding to the other Riemann invariant are straight lines in the x–t plane, Ex. 1.6 A. Only if all the characteristics in the backwards direction intersect in point is the simple wave a centered rarefaction. Ex. 1.8 is an example of a non-centered rarefaction. In addition, simple waves can correspond to compressive waves, Exs. 1.6 and 1.7. In this case, the characteristics eventually cross and a shock will form in a finite time.

2.5 The limit of multiple weak shocks is an isentropic compression. For most materials in most of phase space, $\partial_S P|_V > 0$. In this case, for a fixed compression ratio, multiple shocks have a lower pressure since the entropy in the final state is lower. Isentropic compression would give the minimum pressure.

2.6 **A)** From Eqs. (2.16), (2.18) and (2.23) it follows that

$$\begin{aligned} \Delta P &= m \Delta u \\ &= \rho_0 \, (\sigma - u_0) \, (u_1 - u_0) \ . \end{aligned}$$

In the 'lab' frame when the ambient fluid is at rest, $u_0 = 0$, this relation can be expressed as

$$P_1 = P_0 + \rho_0 \, u_p \, u_s \ . \tag{2S.16}$$

In the strong shock limit, P_0 is negligible and may be neglected.

B) From Eq. (2.16)

$$m = \rho_0 (\sigma - u_0) = \rho_1 (\sigma - u_1) \ ,$$

and from Eq. (2.18)

$$\begin{aligned} m^2 &= -\frac{\Delta P}{\Delta V} \\ \rho_0 (\sigma - u_0) \cdot \rho_1 (\sigma - u_1) &= \frac{\Delta P}{V_0 - V_1} \\ (\sigma - u_0) \cdot (\sigma - u_1) &= \frac{\Delta P}{\rho_0 \rho_1 (V_0 - V_1)} = \frac{\Delta P}{\Delta \rho} \ . \end{aligned}$$

C) From Eqs. (2.22) and (2.23)

$$\begin{aligned} \Delta E &= -\tfrac{1}{2} \Delta P \, \Delta V + P_0 (V_0 - V_1) \\ &= \tfrac{1}{2} (\Delta u)^2 + P_0 (V_0 - V_1) \ . \end{aligned}$$

In the strong shock limit, E_0 and the term proportional to P_0 are negligible. Consequently, in the 'lab' frame, the energy in the strong shock limit reduces to Eq. (2E.8). Thus, in the strong shock limit, the internal energy and kinetic energy become equal.

D) For smooth steady-state flows, Bernoulli's function $E + PV + \frac{1}{2}u^2$ is a constant, Ex. 1.9 A. Eq. (2E.9) is the statement that Bernoulli's function is also a constant when a shock wave is stationary; *i.e.*, the frame in which the shock front is at rest. This follows from Eqs. (2.16) and (2.17c) with $\sigma = 0$. Eq. (2E.9) is an important relation for steady supersonic flows with shock waves.

2.7 **A)** From Eqs. (2.16) and (2.18) the mass flux is determined by

$$\gamma P_0 M^2 / V_0 = (\rho_0 \sigma)^2 = m^2 = -\frac{\Delta P}{\Delta V} \ . \qquad (2S.17)$$

Thus, M is proportional to the mass flux and parameterizes the shock strength. The strategy for determining the shock state is to substitute the EOS into the Hugoniot equation, Eq. (2.22), and then express P_1 and V_1 in terms of ΔP and ΔV

$$\begin{aligned} (P_1 V_1 - P_0 V_0)/(\gamma - 1) = \Delta E &= \tfrac{1}{2} (P_0 + P_1) (V_0 - V_1) \ , \\ \Delta P \Delta V + P_0 \Delta V + V_0 \Delta P &= -\tfrac{1}{2} (\gamma - 1) \Delta P \Delta V - (\gamma - 1) P_0 \Delta V \ , \\ \tfrac{1}{2}(\gamma + 1) \frac{\Delta P}{P_0} &= -\gamma - \frac{V_0 \Delta P}{P_0 \Delta V} = \gamma (M^2 - 1) \ . \end{aligned} \qquad (2S.18)$$

This is equivalent to Eq. (2E.11).

Having used the EOS to determine one variable, namely P_1, all the other variables are determined from the jump conditions. From (2S.17) we find

$$-\Delta V = \frac{\Delta P}{m^2} = \frac{V_0 \Delta P}{\gamma P_0 M^2} \ , \tag{2S.19}$$

$$1 - \frac{\rho_0}{\rho_1} = \frac{1}{\gamma M^2} \cdot \frac{\Delta P}{P_0} \ , \tag{2S.20}$$

$$\frac{\rho_1}{\rho_0} = \frac{\gamma M^2}{\gamma M^2 - \Delta P/P_0} \ .$$

Substituting $\Delta P/P_0$ from Eq. (2S.18) we obtain Eq. (2E.10).

Having determined P_1 and V_1, the shock energy follows from the Hugoniot equation and Eq. (2S.19)

$$\Delta E = \tfrac{1}{2}\,(P_0 + P_1)\,(V_0 - V_1) = -\tfrac{1}{2}\,\Delta P \Delta V - P_0 \Delta V \ ,$$

$$\frac{\Delta E}{P_0 V_0} = -\tfrac{1}{2}\,\frac{\Delta P}{P_0} \cdot \frac{\Delta V}{V_0} - \frac{\Delta V}{V_0} \ ,$$

$$\frac{\Delta E}{E_0} = \frac{\gamma - 1}{\gamma M^2} \frac{\Delta P}{P_0} \Big(1 + \tfrac{1}{2}\,\frac{\Delta P}{P_0} \Big) \ .$$

Substituting $\Delta P/P_0$ from Eq. (2S.18) we obtain Eq. (2E.12).

The velocity is determined from Eq. (2.16)

$$\rho_1(\sigma - u_1) = m = \rho_0 \sigma$$

$$\frac{u_1}{\sigma} = 1 - \frac{\rho_0}{\rho_1}$$

Substituting ρ_0/ρ_1 from Eqs. (2S.20) and (2S.18) we obtain Eq. (2E.13).

Finally, by inspection, the right hand side of Eqs. (2E.10)–(2E.13) are monotonically increase with M.

One can use the values of P_0 and V_0 to set the scale for pressure and density. Moreover, the sound speed scales; $(c/c_0)^2 = (PV)/(P_0 V_0)$. Because an ideal gas EOS is scale invariant, the scaled shock Hugoniot is the same for any initial state as is indicated by Eqs. (2E.10)–(2E.13).

B) From Eq. (1E.17), the entropy is given by

$$S_1 = \ln\left[\frac{P_1}{P_0}\cdot\left(\frac{V_1}{V_0}\right)^{\gamma}\right] + S_0 \ .$$

Since the shock strength is parametrized by M^2 we examine the derivative

$$\frac{dS_1}{dM^2} = \frac{\frac{d}{dM^2}(P_1/P_0)}{(P_1/P_0)} - \gamma\frac{\frac{d}{dM^2}(\rho_1/\rho_0)}{(\rho_1/\rho_0)} \ .$$

Substituting in Eqs. (2E.10) and (2E.11)

$$\begin{aligned}
&= \frac{1}{M^2 - \frac{\gamma-1}{2\gamma}} - \frac{\gamma}{M^2} + \frac{\gamma}{M^2 + \frac{2}{\gamma-1}} \\
&= \frac{1}{M^2}\cdot\frac{1}{M^2 - \frac{\gamma-1}{2\gamma}}\cdot\frac{1}{M^2 + \frac{2}{\gamma-1}}\cdot\left(M^2-1\right)^2 \\
&> 0 \ , \qquad \text{for } M^2 > 1 \ .
\end{aligned}$$

Hence S is monotonically increasing with shock strength. We also note that the entropy increase for weak shocks, $M^2 \gtrsim 1$, is third order since $\Delta P \propto M^2 - 1$.

C) From Eq. (2E.13) the velocity relative to the front is

$$\frac{\sigma - u_1}{c_0} = \left(\frac{\gamma-1}{\gamma+1} + \frac{2}{\gamma+1}\cdot\frac{1}{M^2}\right)\cdot M \ .$$

From Eq. (2E.12) we find

$$\begin{aligned}
\left(\frac{c_1}{c_0}\right)^2 - \left(\frac{\sigma-u_1}{c_0}\right)^2 &= 1 + \frac{2(\gamma-1)}{(\gamma+1)^2}\cdot\frac{M^2-1}{M^2}\cdot\left(\gamma M^2+1\right) - \left(\frac{(\gamma-1)\,M^2+2}{(\gamma+1)\,M}\right)^2 \\
&= \frac{1}{\gamma+1}\cdot\frac{M^2-1}{M^2}\cdot\left[(\gamma-1)\,M^2+2\right] \\
&> 0 \ , \qquad \text{for } M^2 > 1 \ .
\end{aligned}$$

Hence $u_1 + c_1 > \sigma$, and the flow behind the shock is subsonic relative to the front.

Alternatively, from Eqs. (2.16) and (2E.10) we obtain

$$\begin{aligned}(\sigma - u_0)\cdot(\sigma - u_1) &= (\rho_0/\rho_1)\cdot(\sigma - u_0)^2 \\ &= 2\left(\frac{\gamma-1}{\gamma+1}\right)\cdot\left[\tfrac{1}{2}(\sigma-u_0)^2 + c_0^2/(\gamma-1)\right] \\ &= c_*^2\ . \end{aligned} \qquad (2S.21)$$

This formula is known as **Prandtl's relation**. Since we have taken $u_0 = 0$, the shock Mach number M is equivalent to $M_0 = (\sigma - u_0)/c_0$ and corresponds to the Mach number of the flow ahead relative to the shock front. It then follows from Exs. 1.9 B and 2.6 D that when $M_0 > 1$ the Mach number behind $M_1 = (\sigma - u_1)/c_1 < 1$.

D) For an ideal gas the Riemann invariants are given by (1.17)

$$R_\pm = u \pm \frac{2}{\gamma-1}c\ .$$

The change in the invariants across the shock, normalized to the ahead state, is plotted as a function of the shock pressure in Fig. 2.5 for $\gamma = 5/3$. Suppose the shock is right facing. The change in R_+ is the same as occurs for a compressive simple wave. On the other hand, the change in R_- would cause the method of characteristics to break down. However, some tedious algebra shows that to leading order

$$\frac{\Delta R_-}{c_0} = -\frac{1}{4\,(\gamma+1)}\Big(M^2-1\Big)^3 = \frac{(\gamma+1)^2}{32}\Big(\frac{\Delta V}{V}\Big)^3\ .$$

Consequently, for weak shocks R_- is nearly constant. Even for moderate strength shocks ($\Delta P/P_0 < 10$), Fig. 2.5 shows that the change in the Riemann invariant is relatively small ($\Delta R_-/R_-(0) < 25\%$). This is the basis of a perturbative method for computing flows with weaks shocks; *e.g.*, the interaction in which a rarefaction overtakes a shock (the decay of an N-wave). The Riemann invariants and the method of characteristics are discussed in more detail at the end of Lecture 3.

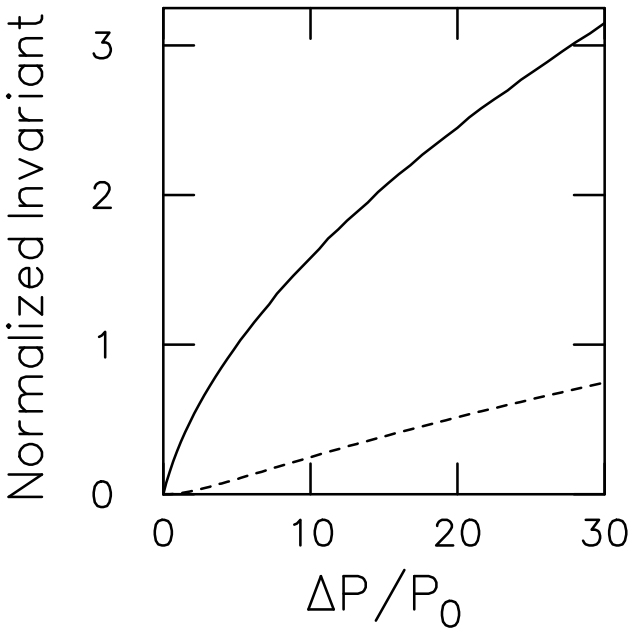

FIGURE 2.5

Normalized Riemann invariant, $\Delta R/R_0$, along shock Hugoniot for $\gamma = 5/3$. Solid line is Riemann invariant corresponding to characteristic family of shock and dashed line is Riemann invariant for the opposite family.

E) As M gets large, it follows from Eqs. (2E.10) and (2E.13) that

$$\rho_1/\rho_0 = (\gamma+1)/(\gamma-1) + O(1/M^2)$$
$$u_1/\sigma = 2/(\gamma+1) + O(1/M^2)$$

In the strong shock limit, $M \to \infty$, this leads to Eqs. (2E.14) and (2E.16). Eq. (2E.15) is a special case of Eq. (2E.5) and Eq. (2E.18) is a special case of Eq. (2E.8). Substituting Eqs. (2E.14) and (2E.15) into the equation for the sound speed $c^2 = \gamma P/\rho$ yield Eq. (2E.17). The compression ratio is finite because the thermal expansion from shock heating is balanced by the shock pressure.

F) Eqs. (2E.11) and (2E.13) determine $\Delta P/\Delta u$ as a function of M^2. Substituting from Eq. (2E.11)

$$M^2 = 1 + \frac{\gamma+1}{2\gamma}\frac{\Delta P}{P_0} \qquad (2S.22)$$

leads to Eq. (2E.19).

The weak shock limit corresponds to $M \to 1$. From Eqs. (2E.10) and (2E.12)

$$\rho_1/\rho_0 = 1 + \frac{2}{\gamma+1}(M^2-1) + O\Big((M^2-1)^2\Big)$$

$$c_1/c_0 = 1 + \frac{\gamma-1}{\gamma+1}(M^2-1) + O\Big((M^2-1)^2\Big)$$

Together with Eq. (2E.11) we find

$$\begin{aligned}\tfrac{1}{2}\left(\rho_0 c_0 + \rho_1 c_1\right) &= \rho_0 c_0\Big[1 + \tfrac{1}{2}\left(M^2-1\right)\Big] + O\Big((M^2-1)^2\Big) \\ &= \rho_0 c_0\Big(1 + \frac{\gamma+1}{4\gamma}\frac{\Delta P}{P_0}\Big) + O\Big((\Delta P/P_0)^2\Big)\end{aligned}$$

Since this is equivalent to the leading order expansion of Eq. (2E.19), we obtain Eq. (2E.20).

G) Let $\widetilde{u}$, $\widetilde{c}$ and $\widetilde{M}$ be the velocity, sound speed and Mach number for the reflected shock in the frame moving with the particle velocity behind the incident shock. The velocity jump across the reflected shock is equal and opposite to that of the incident shock. From Eqs. (2E.16) and (2E.17) we have

$$\widetilde{u}_1/\widetilde{c}_0 = u_1/c_1 = \left[\frac{2}{\gamma(\gamma-1)}\right]^{\frac{1}{2}} .$$

From Eq. (2E.13) we have

$$\widetilde{u}_1/\widetilde{c}_0 = \frac{2}{\gamma+1}\frac{\widetilde{M}^2-1}{\widetilde{M}}$$

Combining these two equation we obtain

$$\widetilde{M}^2 - \left[\frac{(\gamma+1)^2}{2\gamma(\gamma-1)}\right]^{\frac{1}{2}}\widetilde{M} - 1 = 0$$

The solution with $\widetilde{M} > 1$ is

$$\widetilde{M} = \left(\frac{2\gamma}{\gamma-1}\right)^{\frac{1}{2}} .$$

Substituting $\widetilde{M}$ into Eqs. (2E.10)–(2E.12) gives Eqs. (2E.21)–(2E.23). In the lab frame the shock velocity is $\sigma_{rs} = -(\widetilde{c}_0\widetilde{M} - u_1)$. This yields Eq. (2E.24).

For $\gamma = 5/3$ the Mach number of the reflected shock is $M_{rs} = \sqrt{5}$. The reflected Mach number is low (moderate strength shock) because the incident shock raises the sound speed.

The fluid behind the incident shock has a velocity and pressure which does work on the fluid behind the reflected shock. Hence E_{rs} is greater than the stagnation energy behind the incident shock.

2.8 Given the shock pressure and one other state variable, the shock state is completely determined by the jump conditions. By substituting the Hugoniot equation for the energy, Eq. (2.22), into the EOS we obtain an implicit equation for V_s

$$P_s = \widetilde{P}(V_s) = P\Big(V_s, E_0 + \tfrac{1}{2}\,(P_0 + P_s)\,(V_0 - V_s)\Big)\ . \qquad (2S.23)$$

In Lecture 4, physical conditions on the EOS are derived in order for Eq. (2S.23) to have a unique solution. In the standard case with $P_s > P_0$, it can be shown that $V_s < V_0$. A robust means of solving for V_s is to first find a bracket in V for the solution to Eq. (2S.23).

/* find bracket for zero crossing of function $P_s - \widetilde{P}(V)$ */
$V_{\max} = V_0$;
$V_{\min} = 0.5 * V_0$;
while($P_s > \widetilde{P}(V_{\min})$)
{
$V_{\max} = V_{\min}$;
$V_{\min} = 0.5 * V_{\min}$;
}
/* $V_{\min} \le V_s \le V_{\max}$ */

The bracket can then be refined to determine V_s as accurately as desired. Given P_s and V_s the other variables behind the shock are determined from the following jump relations:

$$\Big[\rho_0(\sigma - u_0)\Big]^2 = -\Delta P/\Delta V$$

$$E_s = E_0 + \tfrac{1}{2}\,(P_0 + P_s)\,(V_0 - V_s)$$

$$(u_1 - u_0)^2 = -\Delta P \Delta V$$

2.9 **A)** For steady-state the conservation form of the fluid equations, Eq. (1.1), reduces to

$$\frac{d}{dx}\begin{pmatrix} \rho u \\ \rho u^2 P \\ \rho u(E + PV + \frac{1}{2}\,u^2) \end{pmatrix} = \vec{0}\ .$$

Hence the mass flux ρu is a constant. Then energy conservation equation implies that the Bernoulli function $E+PV+\frac{1}{2}\,u^2$ is constant. From the thermodynamic relation, Eq. (1.8), we find

$$d(E+PV) = V\,dP + T\,dS\ .$$

Hence, for isentropic flow the Bernoulli function is

$$E + PV + \tfrac{1}{2}\,u^2 = \tfrac{1}{2}\,u^2 + \int dP/\rho\ .$$

B) The differential of the Bernoulli function gives

$$\begin{aligned} 0 &= d(E + PV + \tfrac{1}{2}\,u^2) \\ &= u\,du + dP/\rho \\ &= u\,du + \partial_\rho P|_S\,d\rho/\rho \\ d\rho/\rho &= -(u/c)\,du/c \end{aligned}$$

Clearly, when $\Delta u/c = O(1)$ the change in density is also $\Delta\rho/\rho = O(1)$ and the fluid can not be treated as incompressible; *i.e.*, $\nabla\cdot\vec{u} = 0$ is not a good approximation.

C) Using the expression for the sound speed along an isentrope, Eq. (1.17), we find

$$\begin{aligned} \int dP/\rho &= \int \frac{c^2}{\rho}\,d\rho \\ &= \int (\rho/\rho_0)^{\gamma-2}\,c_0^2\,d(\rho/\rho_0) \\ &= (\rho/\rho_0)^{\gamma-1}\,c_0^2/(\gamma-1) = c^2/(\gamma-1) \end{aligned}$$

Hence by part (A)

$$u^2 + \frac{2}{\gamma-1}c^2 = \text{constant}$$

for isentropic steady flow. Since a simple wave is not steady, for steady flow neither Riemann invariant is constant and the velocity does not have the same form as a rarefaction, Eq. (2E.3).

2.10 The shock profile is determined by Eq. (2.34). With zero heat conduction

$$J[E - \tfrac{1}{2}\, m^2 V^2 + V(P_0 + m^2 V_0)] = 0$$

and for an ideal gas EOS

$$P(V) = \frac{\gamma - 1}{V}\left[\tfrac{1}{2}\, m^2 V^2 - (P_0 + m^2 V_0)\, V + \left(\tfrac{1}{2} m^2 V_0^2 + \frac{\gamma}{\gamma - 1} V_0 P_0\right)\right] . \qquad (2S.24)$$

Substituting $P(V)$ into Eq. (2.34a) and noting that the numerator is quadratic and vanishes when the Hugoniot equation is satisfied we obtain Eq. (2E.28).

B) Eq. (2E.28) can be transformed as follows

$$\begin{aligned} \tfrac{1}{2}\,(\gamma - 1)\, m\, x/\mu &= \int dV \Big(\frac{V_0}{V - V_0} - \frac{V_1}{V - V_1}\Big)/(V_0 - V_1) \\ &= \frac{V_0 \log(V_0 - V) - V_1 \log(V - V_1)}{V_0 - V_1} \end{aligned}$$

C) As $V \nearrow V_0$, the right hand side and hence $x \to -\infty$. Similarly, as $V \searrow V_1$, the right hand side and hence $x \to +\infty$. Therefore, the appropriate boundary conditions are satisfied and $V_1 \le V(x) \le V_0$. Eq. (2S.24) determines the pressure profile and mass conservation the velocity profile. The specific energy profile is determined from the EOS. Thus, we obtain the shock profile for all the hydrodynamic variables. These are shown in Fig. 2.6 for $\gamma = 5/3$.

D) From Ex. 2.7 C, in the strong shock limit $V_1 \to [(\gamma - 1)/(\gamma + 1)]V_0$. From part (B), the profile depends on the combination $m\, x/\mu$. Therefore, for fixed V_1 (strong shock limit) the shock profile gets steeper and the width shrinks with either increasing m or decreasing μ. The profile is not physically meaningful when the width is less than the mean free path of particles in a gas or a fluid.

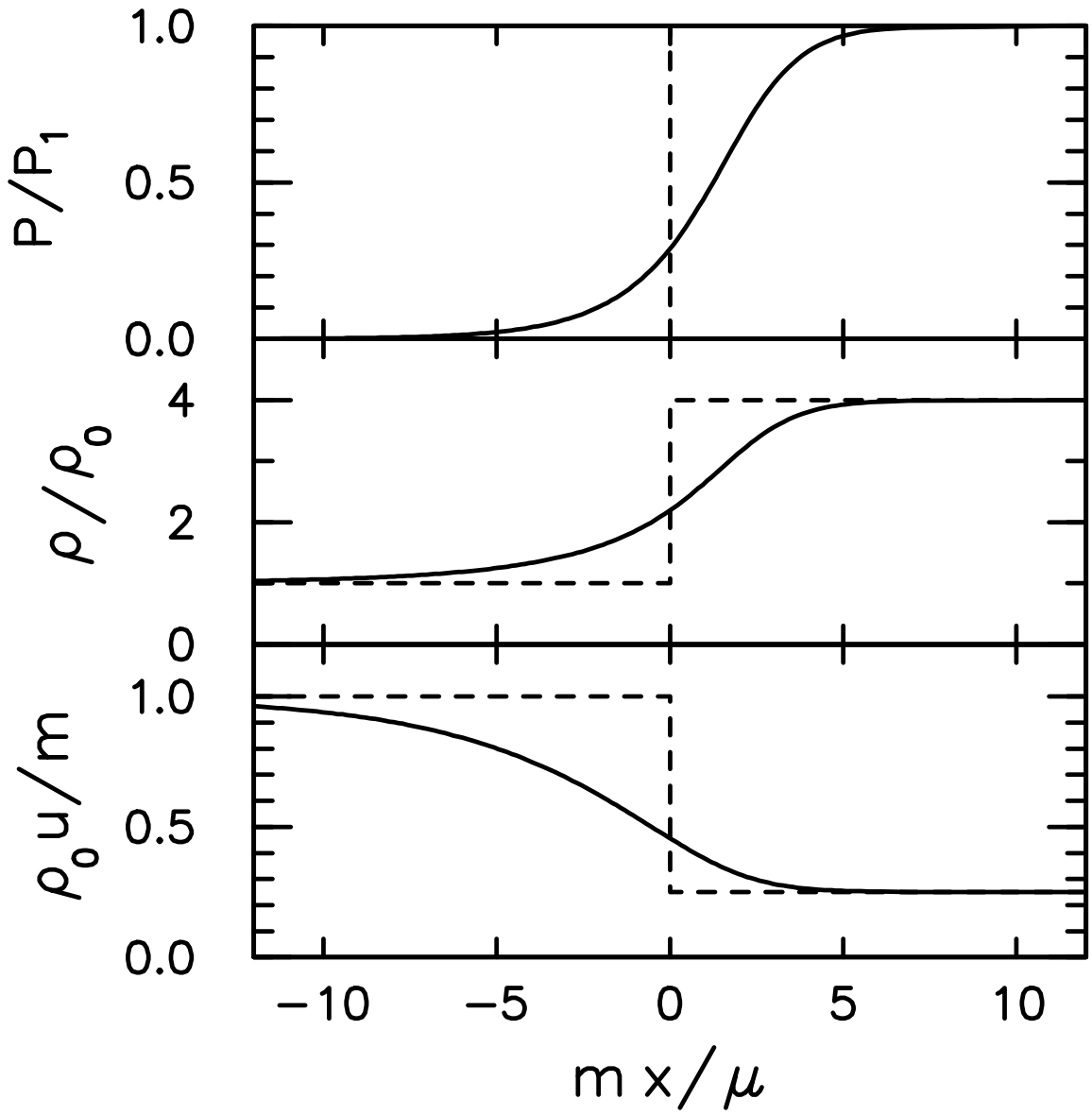

FIGURE 2.6

Viscous profile for strong shock and $\gamma = 5/3$ ideal gas.

Lecture 3
Equation of State and Riemann Problem

The fluid flow equations must be supplemented with an EOS to specify the material properties of a particular fluid. For a numerical simulation, the EOS should be regarded as input data. As with any calculation, bad input leads to bad output. Because an EOS is a function of 2 variables, the question arises as to what is a good EOS. We consider the qualitative properties a general EOS must satisfy.

3.1 Thermodynamic Constraints on an EOS

One requirement is that the equilibrium EOS be compatible with thermodynamics. An isentrope is defined for an incomplete EOS, $P(V,E)$, by $dE = -PdV$. This is sufficient to specify one important constraint on an EOS. Namely, the adiabatic compressibility is positive or $c^2 = -V^2 dP/dV|_S > 0$. This condition implies that the fluid equations are hyperbolic.

Even though the ideal fluid flow equations only require an incomplete EOS, in order to specify other thermodynamic constraints a complete EOS is needed. In addition to the pressure, a complete EOS requires specifying both the temperature and entropy such that the thermodynamic identity

$$dE = -PdV + TdS \tag{3.1}$$

is satisfied.

An incomplete EOS can be extended to a complete EOS by finding an integrating factor T such that $dS = dE/T + PdV/T$ is a perfect differential [Cowperthwaite, 1969]. The equality of the cross derivatives leads to a scalar hyperbolic PDE for T in 2 variables, V and E:

$$\partial_V (1/T) = \partial_E (P/T)$$

$$\partial_V T - P\partial_E T = -(\partial_E P)_V \cdot T$$

$$dT/dV = -(\partial_E P)_V \cdot T \ , \quad \text{along} \quad dE/dV = -P \ . \tag{3.2}$$

The characteristics for the scalar equation corresponds to the isentropes. Therefore, a complete EOS can be constructed from an incomplete EOS as follows: (i) Compute the isentropes in the V–E plane. (ii) Choose a curve that intersects every isentrope exactly once. (iii) Define T arbitrarily along this curve. (iv) Define the value of S for each isentrope by integrating along the chosen curve $dS = dE/T + PdV/T$. (v) Define T by integrating the compatibility condition along each isentrope, Eq. (3.2).

In effect, an incomplete EOS defines the isentropes while a complete EOS, in addition, labels each isentrope with a value of entropy. We note that the transformation $\widetilde{S} = f(S)$ and $\widetilde{T} = T/f'(S)$, for an arbitrary function f, satisfies $\widetilde{T}d\widetilde{S} = TdS$. Consequently, the construction of a complete EOS from an incomplete EOS can not be unique. The non-uniqueness corresponds to the arbitrary function in step (iii) of the above construction.

Alternatively, a complete EOS can be specified by the specific internal energy, $E(V, S)$. The temperature and pressure are then given by $P = -\partial_V E|_S$ and $T = \partial_S E|_V$. The additional thermodynamic constraints for a complete EOS are: (i) the entropy $S(V, E)$ is jointly concave, (ii) $T \geq 0$, and (iii) the isentrope with $S = 0$ coincides with the isotherm with $T = 0$. Each of these conditions has a simple physical meaning.

The first condition implies that when two masses in different thermodynamic states are mixed together and allowed to equilibrate their combined entropy increases. This condition is necessary for thermodynamic stability. It also has two consequences for numerical computations: (i) Implementing advection in an Eulerian algorithm as a remap of a Lagrangian step is a dissipative process; and, (ii) The entropy of mixing is an additional dissipative process for Godunov algorithms that use Riemann solvers to determine the flux at cell interfaces. Both these effects are important for shock capturing algorithms that rely

on the entropy condition to select out the admissible shock waves. After we have defined the relevant EOS parameters, a necessary and sufficient condition for the concavity of the entropy will be given, Eq. (3.11).

The second condition implies that non-equilibrium processes are required for population inversions. Whether local thermodynamic equilibrium is an appropriate assumption for fluid dynamics depends on the relevant time scales for a given application. Non-equilibrium effects are essential for some applications, such as a gas dynamic laser, and can be detrimental for other applications, such as the thrust of a jet engine.

The third condition implies that the specific heat goes to 0 as $T \to 0$. Consequently, a temperature of absolute zero is not achievable. Physically, this guarantees that the flow stays within the domain of state space. However, all materials solidify at low temperature (with the exception of helium which also requires sufficient pressure). Thus, extremely low temperatures, are not relevant to fluid flow. The concept of an absolute zero for temperature is important to define a temperature scale; *e.g.*, as used in an ideal gas equation of state, $PV = RT$. We note that $0^\circ\,\mathrm{K} = -273.16^\circ\,\mathrm{C}$.

It is difficult to verify whether an incomplete EOS is thermodynamically consistent because of the nonuniqueness in constructing a complete EOS from an incomplete EOS. Furthermore, though thermodynamic constraints are necessary, they are not sufficient for a physically reasonable fluid flow. An EOS must be such that the initial value problem for fluid flow is well posed. By this we mean that the solution to the fluid equations exists, is unique and is stable in the sense of varying continuously with the initial data. Additional constraints on the EOS that follow from analyzing interactions of elementary waves (the Riemann problem) will be derived in the next lecture.

In the following we assume an EOS is thermodynamically consistent. A simplified phase diagram in the P–T plane is shown in Fig. 3.1. Phase space is the quadrant $P > 0$, $T > 0$. With material strength, phase space can include a region of tension $P < 0$. Phase boundaries are curves in the P–T plane.

In the P–V plane the corresponding phase diagram is shown in Fig. 3.2. We note that there is an unphysical region below the cold curve, $T = 0$ isotherm. Moreover, the phase boundaries in the P–T plane expand into mixed phase regions in the P–V plane.

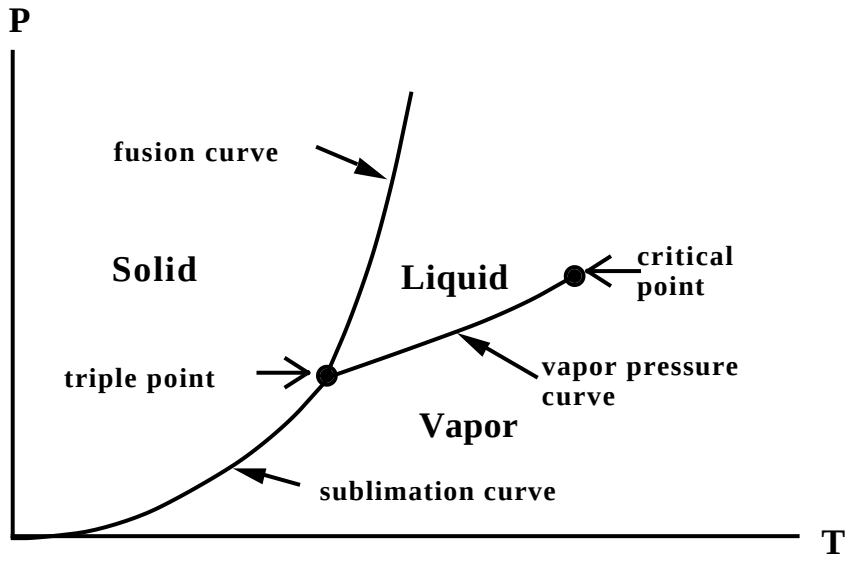

FIGURE 3.1

Simplified phase diagram in P–T plane.

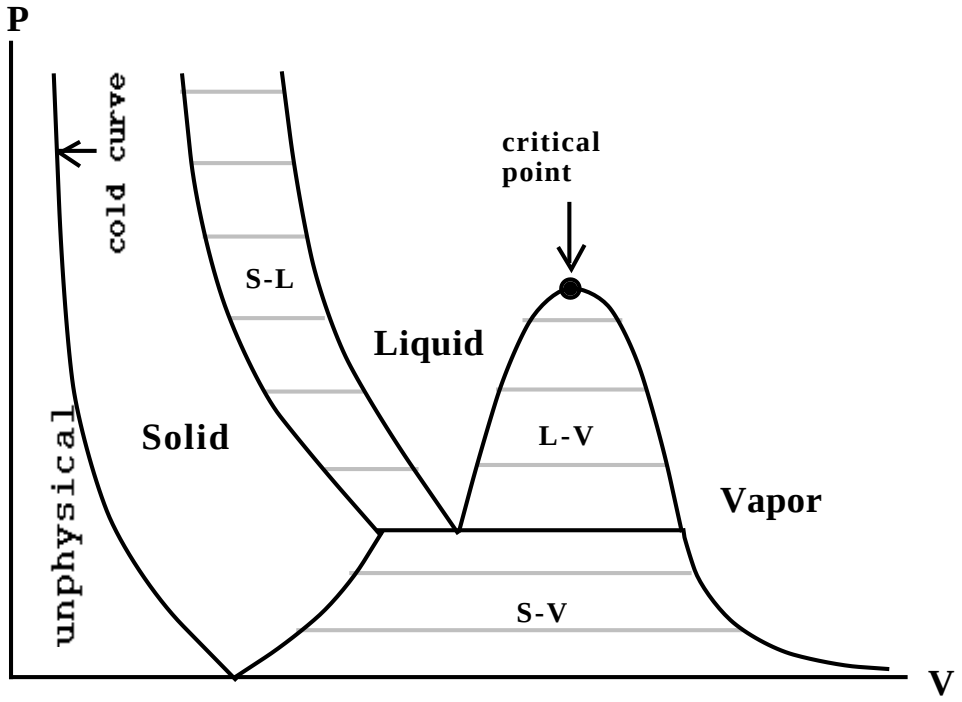

FIGURE 3.2

Simplified phase diagram in P–V plane. Horizontal lines in the mixed-phase regions correspond to points on the coexistence curves in the P–T plane.

It is important to recognize the range of validity for the physical assumption on which the fluid equations are based. The fluid equations assume that the stress tensor is isotropic (rotationally invariant), and consequently a multiple of the identity matrix, $\boldsymbol{\sigma} = -P\mathbf{I}$. Hence material strength is neglected and the solid region in the phase diagram should be excluded.

For the continuum model to apply the length scale of the flow must be much greater than the mean free path of a constituent particle. For air the mean free path at sea level is $\sim 10^{-5}\,\mathrm{cm}$, and the particle number density is $\sim 10^{19}/\mathrm{cm}^3$. Hence, the continuum model is a very good approximation. However, the mean free path can be quite large for a rarefied gas. When this occurs, such as spacecraft reentry through the upper atmosphere, the continuum model breaks down and one must resort to the Boltzmann equation. An extreme example with a very large mean free path is the solar wind.

Finally, we note that there is a continuous path in phase space from the liquid to the vapor regime. Fluids and gases differ in material properties; EOS and transport coefficients. But the equations of fluid dynamics and gas dynamics are the same and these terms sometimes are used interchangeably.

3.2 Dimensionless Parameters Characterizing an EOS

Next we define the important dimensionless parameters that characterize an EOS and give their geometric interpretation:

1. **The adiabatic exponent**

$$\gamma = -\frac{V}{P}\left.\frac{\partial P}{\partial V}\right|_S = -\left.\frac{\partial \log P}{\partial \log V}\right|_S \tag{3.3}$$

is the negative slope of the isentrope as drawn in the $\log P$–$\log V$ plane. For V near V_0, the isentrope through (V_0, P_0) is given approximately by

$$P \approx P_0 \left(\frac{V}{V_0}\right)^{-\gamma} , \tag{3.4}$$

where γ is evaluated at (V_0, P_0); whence the name adiabatic exponent. Moreover, γ is the dimensionless form of the sound speed

$$c^2 = \gamma PV \ . \tag{3.5}$$

As previously noted, thermodynamics requires $\gamma > 0$, and implies that the fluid equations are hyperbolic.

2. **The Grüneisen coefficient**

$$\Gamma = -\frac{V}{T}\left.\frac{\partial T}{\partial V}\right|_S = -\left.\frac{\partial \log T}{\partial \log V}\right|_S \tag{3.6}$$

is the negative slope of the isentrope in the $\log T$–$\log V$ plane. For V near V_0, the isentrope through (V_0, T_0) is given approximately by

$$T \approx T_0 \left(\frac{V}{V_0}\right)^{-\Gamma} \ , \tag{3.7}$$

where Γ is evaluated at (V_0, T_0). Thermodynamic identities imply that the Grüneisen coefficient also measures the spacing of the isentropes:

$$\Gamma = V\left.\frac{\partial P}{\partial E}\right|_V = \frac{V}{T}\left.\frac{\partial P}{\partial S}\right|_V \ . \tag{3.8}$$

We note that Γ is the variable in the compatibility relation, Eq. (3.2), that determines the temperature along an isentrope for an incomplete EOS. Moreover, Γ enters into the differential thermodynamic relations for the pressure

$$V\,dP = \qquad -\gamma\,P\,dV + \Gamma\,T\,dS \ , \tag{3.9a}$$

$$V\,dP = -\,(\gamma - \Gamma)\,P\,dV + \Gamma\,dE \ . \tag{3.9b}$$

When $\Gamma > 0$, the temperature varies monotonically along an isentrope, and thermodynamic phase space may be parametrized by (P, V); *i.e.*, for V fixed, $P(V, E)$ is a single valued function of E and hence has a unique inverse $E(V, P)$.

3. **Inverse specific heat**

$$g = \frac{PV}{C_v T} \ , \tag{3.10}$$

where $C_v = \partial_T E|_V$ is the specific heat at constant volume. Using thermodynamic identities, see *e.g.*, [Menikoff & Plohr, 1989, Appendix A], it can be shown that concavity of the entropy $S(V, E)$ is equivalent to the conditions

$$\gamma \geq 0, \qquad g \geq 0, \quad \text{and} \quad \gamma g \geq \Gamma^2 \ . \tag{3.11}$$

Moreover, g enters into thermodynamic relations in differential form when V and T are chosen as the independent thermodynamic variables;

$$\begin{aligned} g\,T\,dS &= \Gamma\,P\,dV + PV\,dT/T \ , \\ g\,dE &= (\Gamma - g)\,P\,dV + PV\,dT/T \ , \\ g\,V\,dP &= -(\gamma g - \Gamma^2)\,P\,dV + \Gamma\,PV\,dT/T \ . \end{aligned} \tag{3.12}$$

From Eqs. (3.9) and (3.12) it follows that the partial derivative of any combination among the thermodynamic variables V, E, P, T and S can be determined in terms of the parameters γ, Γ and g. We note that the specific heat is not defined for an incomplete EOS, nor is it needed for the fluid equations when heat conduction and radiation are neglected.

4. **The fundamental derivative**

$$\mathcal{G} = -\tfrac{1}{2} V \frac{\partial^2 P/\partial V^2|_S}{\partial P/\partial V|_S} = \tfrac{1}{2}\frac{V^2}{\gamma P}\left.\frac{\partial^2 P}{\partial V^2}\right|_S \tag{3.13}$$

measures the convexity of the isentropes in the P–V plane. In particular, if $\mathcal{G} > 0$ then the isentropes are convex. Moreover,

$$\mathcal{G} = \frac{1}{c}\left.\frac{\partial(\rho c)}{\partial \rho}\right|_S \tag{3.14}$$

and the Lagrangian sound speed is monotonic when $\mathcal{G} > 0$. The name fundamental derivative is due to [Thompson, 1971]. Though this quantity had previously been identified, Thompson emphasised its great importance for fluid flow.

The fundamental derivative determines the structure of weak waves. The important properties of simple waves and weak shock waves are derived below:

(i) Simple waves

For a simple wave, the entropy and one Riemann invariant are constant. Along a simple wave the variation of the characteristic velocity is given by

$$d(u \pm c) = \pm \mathcal{G} dP/\rho c \; . \tag{3.15}$$

When $\mathcal{G} > 0$ everywhere, the characteristic velocities are monotonic and simple waves, in particular centered rarefactions, are always well defined. This is the condition that the acoustic wave families are genuinely non-linear; see Eqs. (2.1) and (2.7).

(ii) Weak shock waves

For a weak shock wave, it follows from Lemma 2.3, Eq. (2.31), that to leading order the change in entropy is given by

$$\Delta S = -\tfrac{1}{6}\, \mathcal{G} \frac{c^2}{T} (\Delta V/V)^3 \cdot [1 + O(\Delta V/V)] \; . \tag{3.16}$$

Hence, for entropy to be increasing, $\mathcal{G} \cdot (V_0 - V)$ must be positive.

In the standard case when all isentropes are convex, $\mathcal{G} > 0$ everywhere, shock waves are compressive and centered rarefactions are expansive. The wave structure for a non-convex EOS is described later in more detail. In addition, it is shown in the next lecture that important properties of shock waves and rarefactions are determined by the parameters γ, Γ and $\mathcal{G}$.

The fact that the change in entropy is third order in $\Delta V/V$ has additional important consequences.

Lemma 3.1: For weak shocks, to leading order the wave speed is given by

$$\sigma = \tfrac{1}{2}\,(\lambda_0 + \lambda_1) + O\Big((\Delta V/V)^2\Big) \; , \tag{3.17a}$$

and

$$\rho_0 \cdot (\sigma - u_0) = \tfrac{1}{2}\,(\rho_0 c_0 + \rho_1 c_1) + O\Big((\Delta V/V)^2\Big)\ . \tag{3.17b}$$

Proof: In the P–V plane, the Hugoniot locus and the isentrope through the initial state correspond to second order. Therefore, to second order the Hugoniot locus is given by

$$P_h(V) = P_0 - (\rho_0 c_0)^2 \cdot (V - V_0) + \mathcal{G}_0 \cdot (\rho_0 c_0)^2 \rho_0 \cdot (V - V_0)^2 + O\Big((\Delta V/V_0)^3\Big)\ . \tag{3.18}$$

For definiteness, we assume the shock is right facing, and hence the characteristic velocity is $\lambda = u + c$. From the Hugoniot jump conditions, Eq. (2.19), we find

$$\begin{aligned}\rho_0^2 \cdot (\sigma - u_0)^2 &= -\Delta P/\Delta V \\ &= (\rho_0 c_0)^2 + \mathcal{G}_0 \cdot (\rho_0 c_0)^2 \cdot (V_0 - V_1)/V_0 + O\Big((\Delta V/V_0)^2\Big)\ .\end{aligned}$$

Hence,

$$\begin{aligned}\sigma &= u_0 + c_0 \cdot \Big(1 + \tfrac{1}{2}\,\mathcal{G}_0 \cdot (V_0 - V_1)/V_0\Big) + O\Big((\Delta V/V_0)^2\Big) \\ &= \lambda_0 + \tfrac{1}{2}\,\mathcal{G}_0 \rho_0 c_0 \cdot (V_0 - V_1) + O\Big((\Delta V/V_0)^2\Big)\ .\end{aligned} \tag{3.19}$$

From Eq. (2.23), we find

$$\begin{aligned}(u_1 - u_0)^2 &= -\Delta P \cdot \Delta V = -\frac{\Delta P}{\Delta V} \cdot (\Delta V)^2 \\ &= (\rho_0 c_0)^2 \cdot (\Delta V)^2 \cdot \Big[1 - G_0 \cdot (\Delta V/V_0) + O\Big((\Delta V/V_0)^2\Big)\Big]\ .\end{aligned}$$

Hence,

$$u_1 = u_0 + \rho_0 c_0 \cdot (V_0 - V_1) \cdot \Big[1 - \tfrac{1}{2}\,G_0 \cdot (\Delta V/V_0) + O\Big((\Delta V/V_0)^2\Big)\Big]\ . \tag{3.20}$$

From Eq. (3.14) we have

$$\rho_1 c_1 = \rho_0 c_0 + \mathcal{G}_0 \rho_0 c_0 \cdot (V_0 - V_1)/V_0 + O\Big((\Delta V/V_0)^2\Big)\ , \tag{3.21a}$$

and using $V_1 = V_0 - (V_0 - V_1)$ we find

$$c_1 = c_0 + (\mathcal{G}_0 - 1) \cdot \rho_0 c_0 \cdot (V_0 - V_1) + O\Big((\Delta V/V_0)^2\Big)\ . \tag{3.21b}$$

Combining Eqs. (3.20) and (3.21b), the characteristic velocity is given by

$$\lambda_1 = \lambda_0 + \mathcal{G}_0\, \rho_0 c_0 \cdot (V_0 - V_1) + O\Big((\Delta V/V_0)^2\Big)\ . \tag{3.22}$$

We note that the leading order change in ρc and in the characteristic velocity are the same for both a weak shock and a simple wave, Eqs. (3.14) and (3.15). Combining Eqs. (3.19) and (3.22) yields Eq. (3.17a), and combining Eqs. (3.19) and (3.21a) yields Eq. (3.17b).

⊠ ⊠

The lemma is a special case of a general theorem on hyperbolic PDEs due to [Lax, 1957]. The theorem states that to leading order the wave speed is the average of the characteristic velocities ahead and behind the shock front; see *e.g.*, [Smoller, 1983], Thm. 17.16(a). Equations (3.17a) and (3.17b) are an application of Lax's theorem in Eulerian and Lagrangian coordinates respectively. An important consequence of these relations is that the Godunov algorithm for smooth flow coincides with the method of characteristics to second order in time; see Ex. 3.6 D. Hence, Riemann solvers can be used to generate the numerical dissipation needed for shock waves without affecting the smooth flow.

The structure of weak shocks can be further characterized.

Corollary 3.2: For weak shocks, to leading order

$$\frac{\sigma - \lambda_0}{c_0} = -\tfrac{1}{2}\,\mathcal{G}_0 \rho_0 \Delta V = \tfrac{1}{2}\,\mathcal{G}_0 \frac{\Delta P}{\rho_0 c_0^2} = \tfrac{1}{2}\,\mathcal{G}_0 \frac{\Delta u}{c_0}\ . \tag{3.23a}$$

Moreover, when the fluid ahead of the shock is at rest

$$u_s/c_0 = 1 + \tfrac{1}{2}\,\mathcal{G}_0 \cdot (u_p/c_0) + O\Big((u_p/c_0)^2\Big)\ , \tag{3.23b}$$

where u_s is the shock velocity and u_p is the particle velocity behind the shock front.

Proof: From Eq. (3.17a)

$$\sigma - \lambda_0 = \tfrac{1}{2}\,(\lambda_1 - \lambda_0) + O\Big((\Delta V/V)^2\Big)\ .$$

Equation (3.23a) follows from Eq. (3.22) and the derivatives at the initial state; $dP/dV|_h = -(\rho_0 c_0)^2$ and $dP/du|_h = \rho_0 c_0$. Equation (3.23b) follows from identifying u_s with σ, λ_0 with c_0, and u_p with u_1. The error estimate follows from the relation $\Delta V/V_0 = u_p/u_s$ which to leading order is u_p/c_0.

⊠ ⊠

Corollary 3.2 has the following interpretation. On the Hugoniot locus, from Lemma 2.4 the limiting shock speed is the characteristic velocity; *i.e.*, $\sigma_0 = \lambda_0$. Then from Eq. (3.23a), the first order correction is $d\sigma/du|_0 = \pm\frac{1}{2}G$, where the + and − signs are for right and left facting waves respectively. For a rarefaction wave, from Eqs. (1.16) and (3.15) $d\lambda/du|_0 = \pm\mathcal{G}$. Thus, at the initial state the slope of the wave speed as a function of particle velocity for a shock wave is half the value of the slope for a rarefaction wave. Corollary 3.2 also will be important for the discussion in Lecture 5 of realistic equations of state for metals at high pressure.

As an example, for an ideal gas EOS, Ex. 1.5,

$$\begin{aligned} PV &= (\gamma - 1)E \ , \\ T &= E/C_V, \quad \text{with } C_V \text{ constant}, \\ S &= C_v \ln\Big(\frac{PV^\gamma}{P_0 V_0^\gamma}\Big) + S_0 \ , \end{aligned}$$

the value of the key dimensionless parameters are:

1. $\gamma = C_\mathrm{p}/C_\mathrm{v} > 1$.

   In general, the adiabatic exponent is not equal to the ratio of the specific heats and may be less than 1. Larger γ corresponds to a stiffer material.

2. $\Gamma = \gamma - 1 > 0$.

   In general, Γ has the same sign as the coefficient of thermal expansion and may be negative, *e.g.*, water near freezing.

3. $g = \gamma - 1 > 0$.

   It follow that Eq. (3.11) is satisfied and hence the entropy as a function of V and E is jointly concave.

4. $\mathcal{G} = \frac{1}{2}(\gamma + 1) > 1$.

   In general, $\mathcal{G}$ may be less than 1 or negative. In particular, $\mathcal{G} < 0$ near the critical point for fluids with large specific heats, see *e.g.*, [Cramer, 1989].

We note that an ideal gas equation of state is physically reasonable in all of phase space, $V > 0$ and $E > 0$. However, it is only a good approximation for some gases in a limited range of phase space. Similarly, model equations of state used to describe realistic materials are only quantitatively accurate in a limited domain of phase space. Unlike an ideal gas EOS, when a realistic EOS is extended outside its domain, in addition to losing accuracy it may also become qualitatively wrong and lead to an unphysical wave structure for fluid flow. This is discussed in more detail in lecture 5. The dimensionless parameters introduced to characterize an EOS will play a key role in analyzing the wave structure.

Though an ideal gas EOS is quite useful for developing an intuition for the non-linear wave properties of compressible fluid flow, some of the qualitative properties associated with an ideal gas are not always valid. Typically an ideal gas EOS is used with $5/3 \geq \gamma > 1$. In this case, for rarefaction waves the sound speed increases with density, and for shock waves $\sigma - u_0 > c_1$. These properties depend on the value of $\mathcal{G}$. From Eq. (3.14) we obtain

$$\mathcal{G} - 1 = (\rho/c)\partial_\rho c|_S \ .$$

Hence, if $\mathcal{G} < 1$ then along an isentrope (hence for rarefactions and weak shocks) the sound speed decreases with density. Furthermore, if $\mathcal{G} > 2$ (corresponding for ideal gas to $\gamma > 3$) then from Eqs. (3.19) and (3.21b) for weak shocks $c_1 > \sigma - u_0$.

For a given material, statistical mechanics can be used to determine a complete EOS in terms of the Helmholtz free energy, $F(V,T) = E - TS$; $P = -\partial F/\partial V$ and $S = -\partial F/\partial T$. An important example, is a thermally perfect gas for which $PV = RT$ where $R = \frac{\mathcal{R}}{\text{Mol-Wt}}$, $\mathcal{R}$ is the gas constant, $8.317 \frac{\text{J}}{\text{deg}\cdot\text{mole}}$, and Mol–Wt is the molecular weight. Moreover, $dE = C_v dT$ and the specific heat C_v is a function of temperature only. Physically this model accounts for the internal degrees of freedom of an atom or molecule, such as vibration and rotation, but neglects interactions between them. Using thermodynamic identities, it can be shown for this case that the sound speed is given by $c^2 = (C_p/C_v)RT$ and $C_p = C_v + R$. Hence $\gamma = C_p/C_v > 1$, and c is a function of only T. An ideal gas is a

special case of a thermally perfect gas in which $C_v = R/(\gamma - 1)$ is constant. Furthermore, for a monatomic gas $\gamma = 5/3$, for a diatomic gas $\gamma = 7/5$, and for a polyatomic gas $\gamma = 4/3$. A thermally perfect gas is a good description of air in the lower atmosphere and is widely used in aerodynamics.

3.3 Domain of EOS and Asymptotic Conditions

Thermodynamic phase space can be parameterized by two variables, such as (P, T), (V, T), (P, S), or (V, S). Physically, in any pair of these variables, phase space should consist of the positive quadrant; *e.g.*, $0 < V$ and $0 \leq S$. The freedom to chose independent variables for phase space results from the thermodynamic requirement that some partial derivatives never vanish. For example, $-\partial P/\partial V|_S = (\rho c)^2 > 0$. Hence, an isentrope can be parameterized by either V or P.

For the domains of the different parameterizations to be consistent, asymptotic properties are needed on an EOS. Physically, an EOS is expected to satisfy the following asymptotic properties:

(EOS–1) For S fixed, $P(V, S) \to \infty$, $E(V, S) \to \infty$ and $T(V, S) \to \infty$ as $V \to 0$. Moreover, for S fixed, $E/P \to 0$ as $V \to 0$. This is because $P = -\partial E/\partial V|_S$ and at a singularity the derivative blows up faster than the function. Alternatively, the adiabatic index has the property

$$\lim_{V \to 0} \gamma(V, S) = \gamma_0(S) > 1 \ ,$$

and the Grüneisen coefficient has the property

$$\lim_{V \to 0} \Gamma(V, S) = \Gamma_0(S) > 0 \ .$$

This asymptotic condition is a consequence of the strong repulsion between atoms at short distances.

(EOS–2) For S fixed, $P(V,S) \to 0$, $E(V,S) \to E_\infty$ and $T(V,S) \to 0$ as $V \to \infty$. Alternatively, the adiabatic index has the property

$$\lim_{V\to\infty} \gamma(V,S) = \gamma_\infty(S) > 1 \ ,$$

and the Grüneisen coefficient has the property

$$\lim_{V\to\infty} \Gamma(V,S) = \Gamma_\infty(S) > 0 \ .$$

This asymptotic condition is a consequence of the negligible force between atoms at large distances.

Since we are interested in fluids, we are neglecting material strength or regions of tension, and the associated binding energy of a solid. As a consequence the global minimum of the specific energy occurs at $V = \infty$; *i.e.*, $E(V,S) > E_\infty$ for all V and S. Henceforth, we denote the minimum by $E_{\min}$ rather than E_∞. A global minimum of the specific energy is necessary for the stability of matter and to rule out perpetual motion machines.

For applications in which ionization is unimportant, the binding energy of the electrons in an atom may be neglected. Then for a monotonic gas we may take $E_{\min} = 0$, while for molecules $E_{\min}$ is related to the binding energy of its constituent atoms; *i.e.*, the heat of formation. The difference in $E_{\min}$ among different molecules is important when considering chemical reactions; *i.e.*, reactive hydrodynamics.

As $V \to 0$ or ∞ along an isentrope, it follows from the asymptotic conditions (EOS–1) and (EOS–2) that if $\mathcal{G}$ has a limit then the limit must be positive and non-zero; *i.e.*, isentropes are asymptotically convex.

(EOS–3) For V fixed, $P(V,S) \to \infty$, $E(V,S) \to \infty$ and $T(V,S) \to \infty$ as $S \to \infty$. Moreover, the specific heat approaches a constant and in the limit $\tilde{\Gamma}_\infty = \tilde{g}_\infty = PV/E = \tilde{\gamma}_\infty - 1$. Hence, in the limit the EOS reduces to an ideal gas. This asymptotic condition is a consequence of the thermal energy at high temperatures dominating the potential energy between atoms at fixed volume.

(EOS–4) For P fixed, $V(P,S) \to \infty$, $E(P,S) \to \infty$ and $T(P,S) \to \infty$ as $S \to \infty$. Moreover, the specific heat approaches a constant and in the limit $\Gamma = g = PV/E = \gamma - 1$. Again, in the limit the EOS reduces to an ideal gas. This asymptotic condition is a consequence of the thermal energy at high temperatures dominating the potential energy between atoms as the atoms get far apart.

We note that "non-interacting" particles behave like an ideal gas. However, some interaction between particles is necessary for thermodynamic equilibrium to be established. The weaker the interaction, the larger the time constant for a system to approach equilibrium. Assuming thermodynamic equilibrium, for large V (rarefied gas) or large T (high temperatures) the EOS of a material approaches an ideal gas EOS. However, at sufficiently high temperatures molecules dissociate and atoms ionize resulting in a plasma. Magnetohydrodynamics is the extension of hydrodynamics that accounts for the electro-magnetic effects in a plasma.

(EOS–5) In the V–P plane, the $T = 0$ isotherm is convex and a lower bound; *i.e.*, $V(P,0) < V(P,T)$ for any P and $P(V,0) < P(V,T)$ for any V. Physically, the $T = 0$ isotherm corresponds to the $S = 0$ isentrope. From the thermodynamic identities

$$\partial \log P / \partial \log V|_S = -\gamma \ ,$$

$$\partial \log P / \partial \log V|_T = -\gamma + \Gamma^2/g \ ,$$

it follows that along the zero isotherm $g = \infty$.

However, for an ideal gas the zero isotherm corresponds to $S = -\infty$ rather than $S = 0$; *i.e.*, an ideal gas violates the thermodynamic condition that the specific heat vanishes at $T = 0$. In this case, the $T = 0$ isotherm corresponds to the limit of $S \to -\infty$ and consist of the union of the curves $P = 0$ and $V = 0$. Our analysis of the Hugoniot locus in the next lecture can still be applied with the additional condition that $E = E_{\min}$ everywhere on the $T = 0$ isotherm.

We call an EOS satisfying conditions (EOS–1) to (EOS–4) **asymptotically regular**. Though it is convenient to impose these asymptotic conditions in order for the fluid equations to have well posed mathematical solutions, the physical applicability of the fluid dynamic model breaks down as the asymptotic limits are approached.

In general, a point in the V–P plane can correspond to several points in thermodynamic state space; *i.e.*, isentropes can cross. The V–P plane provides a unique parameterization only if $\Gamma > 0$. Furthermore, phase space consist of the portion of the V–P plane above the zero isotherm (often refered to as the cold curve) and may not be the entire quadrant $V > 0$, $P > 0$. Because dissipation is important for a shock wave, it is convenient to use S and either V or P when analyzing the Hugoniot locus.

3.4 Riemann Problem

The **Riemann problem** (RP) is the initial value problem with scale invariant initial data. In 1-D the initial data consists of two constant states and describes a shock tube experiment or an impedance match experiment. A shock tube experiment consists of two gases separated by a membrane. At an instance in time the membrane is broken and the subsequent motion of the gases is measured. In an impedance match experiment, an incident shock wave impinges on the interface between two materials, and the transmitted and reflected waves are measured.

The solution to the RP characterizes the elementary interactions of shock and contact waves: (i) Shocks of the opposite family colliding; (ii) A shock overtaking a shock of the same family; and (iii) A shock colliding with a contact. In addition, for an initial value problem in which the initial data is constant outside a bounded region, the asymptotic solution for large time consists of the outgoing waves in the solution to the RP [Liu, 1979]. Riemann problems play a key role for hyperbolic PDEs in both the mathematical analysis of solutions and the construction of numerical algorithms for solutions. Important applications of RPs are: (i) Glimm's theorem on global existence of the initial value problem with small initial data [Glimm, 1965]; (ii) The Random Choice Method (Glimm's scheme), see *e.g.*, [Colella, 1982]; (iii) Godunov type (upwind) algorithms; and (iv) The Front Tracking algorithm.

Since the PDEs are scale invariant, the solution to the RP is scale invariant. The most general scale invariant solution of the fluid equations consists of 3 outgoing waves: a left and right facing wave separated by a contact. Because of the characteristic condition, Eq. (2.36), if a solution had more than one wave of any family then the waves would interact and the solution would not be scale invariant for all time.

The Riemann problem can be solved by introducing the concept of a **wave curve**. For each wave family, a (forward) wave curve based on an initial state is defined as the locus of final states of stable scale invariant waves of the given wave family connected to the given initial state. Relative to the wave propagation, the initial and final states correspond to the ahead (upstream) and behind (downstream) states respectively. For the fluid equations, the contact is linearly degenerate and its wave curve has two global invariance; u and P. As a consequence, we need only consider the wave curves for the two non-degenerate wave families; *i.e.*, the right and left wave familes associated with the characteristic velocities $u \pm c$.

Using wave curves the Riemann problem is solved as follows: In the u–P plane, plot the projection of the right wave curve based on the right state and the left wave curve based on the left state. The intersection of the wave curves defines the left and right outgoing waves in the solution. Behind these waves, the jump in the thermodynamic variables determines the contact. The same solution algorithm applies if the left and right state correspond to different materials characterized by different equations of state. In this case the contact is the material interface.

In the standard case of a convex EOS, $\mathcal{G} > 0$ everywhere, we show in the next lecture that the wave curve consists of shock waves in compression and rarefaction waves in expansion. Depending on the initial data, there are five possibilities for the outgoing waves in the solution to a Riemann problem, as are shown in Fig. 3.3:

A. shock, contact, shock;

B. rarefaction, contact, shock;

C. shock, contact, rarefaction;

D. rarefaction, contact, rarefaction;

E. rarefaction, vacuum, rarefaction; *i.e.*, cavitation.

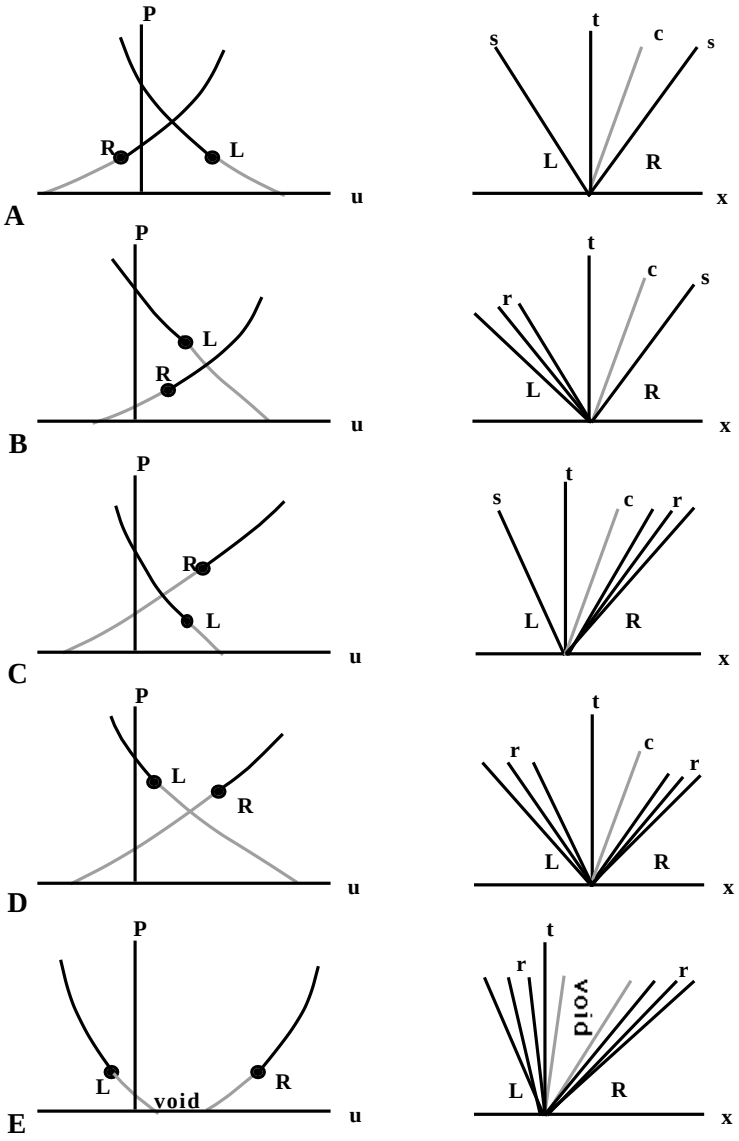

FIGURE 3.3

Types of solutions to 1-D Riemann problem.

The first four cases are quite intuitive. We postpone discussing the fifth case until after we have analyzed the existence of a solution to the RP.

The graphical construction is both necessary and sufficient for a solution to the RP. Consequently, uniqueness and existence of solutions to the RP can be related to properties of the wave curves. Two important properties of the wave curves follow from the symmetry of the fluid equations:

(WC–1) The wave curve of each family simply translates with the velocity of the initial state. This is a consequence of Galilean invariance of the fluid equations.

(WC–2) The right wave curve based on velocity u_0 is the reflection about the line $u = u_0$ of the left wave curve based on u_0. This is a consequence of the reflection invariance, $x \to -x$ and $u \to -u$, of the fluid equations.

From these two properties it follows that the only way the Riemann problem for any initial data can have a unique solution is to require that the wave curves are monotonic in both P and u. In particular, dP/du must be positive for the right wave curve and negative for the left wave curve. Because dP/du has the opposite sign for the right and left wave curves, at most one intersection can occur for the two wave curves that enter into the graphical solution to the RP. On the other hand, if a wave curve is not monotonic then from the reflection symmetry of right and left wave curves, the Riemann problem with initial data corresponding to a symmetric impact, $u_{\rm L} = -u_{\rm R} > 0$, will not have a unique solution for a range of initial velocities, see Fig. 3.4.

In the next lecture, as a consequence of the asymptotic properties of an EOS, it is shown that the wave curves have the following asymptotic property.

(WC–3) The wave curve is semi-infinite, extending from $P = 0$ and $u =$ finite (escape velocity) to $P = \infty$ and $u = \pm\infty$ ($+$ for a right wave curve and $-$ for a left wave curve).

It then follows that the wave curves used in the graphical construction of the solution to the RP either intersect at a finite $P > 0$ or else the minimum Δu is at $P = 0$. The latter

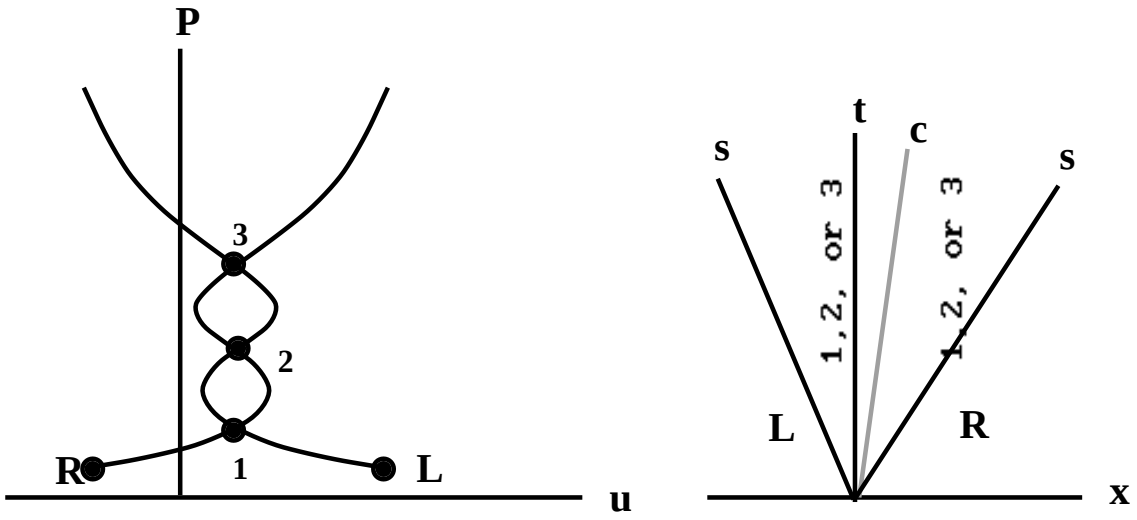

FIGURE 3.4

Nonuniqueness of solution to Riemann problem when the wave curve is not monotonic in u–P plane.

case corresponds to cavitation; instead of a contact, the left and right rarefactions waves are separated by a vacuum. We note that $P = 0$ corresponds to $\rho = 0$, and hence the mass, momentum or energy fluxes all vanish in a vacuum. Consistency of a solution with a vacuum places a further constraint on the EOS. Normally, a particle trajectory traverses through the rarefaction fan. For a rarefaction to end in a vacuum, the characteristic velocity and the particle velocity must coincide. Therefore, the sound speed must vanish at the 'contact' between a rarefaction and a vacuum. When $c = 0$, all three characteristic velocities are the same and the PDEs are not strictly hyperbolic.

Remark 3.3: The characteristic equations are unaffected if the pressure is shifted by a constant. Furthermore, a shift in pressure can be implemented by a simple transformation of the EOS; $V' = V$, $E' = E + P_0 V$, $P' = P - P_0$, $T' = T$ and $S' = S$. The transformed EOS satisfies the thermodynamic identity, Eq. (3.1). The dimensionless parameters that characterize the transformed EOS are given by $\gamma' = \frac{P}{P-P_0}\gamma$, $\Gamma' = \Gamma$, and $g' = \frac{P-P_0}{P}g$. Consequently, provided $P > P_0$ and $P > 0$, Eq. (3.11) remains valid and the transformed EOS is thermodynamically consistent. However, a vacuum requires that

the wave curve end with $dP/du = 0$. Hence the existence of a vacuum gives meaning to a pressure origin. One can not arbitrarily cut-off the pressure and expect the Riemann problem to have a solution for any initial data; *i.e.*, case E in Fig. 3.3 would not be a valid solution. In nature, expansion to low pressures for a gas leads to low densities and a large mean free path. Hence, the continuum approximation breaks down. For a liquid, rather than a vacuum, expansion to low pressures leads to a phase transition to a vapor region. For a solid, material strength can support tension. Large tension leads to spall. This is the analog of the formation of a vacuum region.

Our results on the Riemann problem can be summarized as follows.

Theorem 3.4: If every wave curves satisfies the asymptotic condition (WC–3), then a solution exists to any Riemann problem. Furthermore, monotonicity of the wave curves is both necessary and sufficient for uniqueness to all Riemann problems, *i.e.*, for any initial data.

The requirement that the RP has a unique solution naturally leads to the question: How are the monotonicity properties of the wave curve related to conditions on the EOS? For the rarefaction branch, from Eq. (1.16), (3.14) and (3.15) we find that

$$dP/du = \pm \rho c \ , \tag{3.24a}$$

$$d^2P/du^2 = \rho\, \mathcal{G} \ . \tag{3.24b}$$

Hence, in the u–P plane a rarefaction curve is monotonic and convex when $\mathcal{G} > 0$. Therefore, in the standard case of a convex EOS we only need to examine the monotonicity of the shock branch of the wave curve. In the next lecture the shock locus is analyzed in detail for an arbitrary EOS.

Here we note some further properties of weak shocks. It follows from Eqs. (2E.4) and (3.23b) that the first two derivatives in the u–P plane at the initial state are also given by Eq. (3.24). Hence, at the initial state where the shock and the rarefaction branch

of the wave curve meet, both dP/du and d^2P/du^2 are continuous. Thus, the fundamental derivative measures the convexity at the initial state of the projection of the wave curve in the u–P plane. This will be shown to have important consequences for numerical algorithms. In fact it is a general property of hyperbolic systems that the Hugoniot locus and the rarefaction locus for a genuinely non-linear wave family can be parameterized such that the first two derivatives are continuous at the initial state; see *e.g.*, [Smoller, 1983], Thm. 17.15.

On the rarefaction branch of the wave curve, R_- is constant for right facing waves and R_+ is constant for left facing waves; see Eq. (1.14). We can generalize the Riemann invariants to allow for variable S as follows

$$R_\pm(u,V,S) = u - u_0 \pm \int_V^{V_0} \rho c \, dV \Bigg|_{\substack{\text{isentrope} \\ \text{thru } V_0,S}} + R_{\pm,V_0}(S) \ .$$

The last term gives a degree of freedom which can be used, for example, to define for an ideal gas global Riemann invariants, $R_\pm = u - u_0 \pm 2\,(c-c_0)/(\gamma-1)$. From Eqs. (3.16), (3.20) and (3.21a), to leading order for a right facing shock $\Delta R_- = O\Big((\Delta V/V_0)^3\Big)$, and for a left facting shock $\Delta R_+ = O\Big((\Delta V/V_0)^3\Big)$. Thus, for weak shocks the entropy and one of the Riemann invariants are constant to second order. This is also a general property of hyperbolic systems; see *e.g.*, [Smoller, 1983], Thm. 17.16(b).

Consider the method of characteristics for homentropic flow (constant entropy). The characteristic curves, $dx/dt = u \pm c$, provide a local co-ordinate system for the x–t plane. The co-ordinates can be chosen as the right and left Riemann invariants, $R_\pm$. The fluid variables can be obtained from the Riemann invariants using a variant of the wave curves which determine the solution to the Riemann problem. Suppose one modifies the wave curve by extending Eq. (1.16) from the rarefaction branch to compressive simple wave, *i.e.*, entropy and one Riemann invariant are constant. Then in the u–P plane, the intersection of the modified right wave curve associated with the left facing characteristic and the modified left wave curve associated with the right facing characteristic uniquely

determines the (u, P) state with given left and right Riemann invariants. Consequently, the interaction of simple waves with boundaries (rigid wall, constant pressure or contact) can be determined with the same graphical construction based on wave curves that is used to analyze the interaction of shock waves; see *e.g.*, Ex. 3.4 and 3.5.

The Taylor expansion of $P(u)$ for the wave curve and the modified wave curve are the same to second order. Consequently, the solution to the Riemann problem and the characteristic equations agree to second order. As a result, the Godunov algorithm is the natural extension of the method of characteristics. The Riemann problems used in the Godunov algorithm account for the upwind flow of information and add the dissipation necessary for shock waves without affecting smooth flow. This is possible because the entropy change in weak shocks is third order.

As an example of the theory developed up to this point, consider an ideal gas EOS. From the explicit formulae for the shock Hugoniot (Ex. 2.7 A) all variables, P, u, E and V, vary monotonically with shock strength. In particular, for a right facing shock

$$dP/du = \frac{dP/dM}{du/dM} = 2\rho_0 c_0 \cdot \frac{M^3}{M^2+1} > 0 \ , \qquad (3.25a)$$

$$d^2P/du^2 = \frac{1}{du/dM} \cdot \frac{d}{dM}\Big(dP/du\Big) = (\gamma+1)\,\rho_0 \cdot \frac{1+3/M^2}{(1+1/M^2)^3} > 0 \ , \qquad (3.25b)$$

where M is the shock Mach number. Hence, for both shocks and rarefactions, the projection of the wave curve in the u–P plane is monotonic and convex. From the monotonicity, there is a unique solution to the Riemann problem with an ideal gas EOS and any initial data. Moreover, from the convexity of the wave curve, a Newton's iteration method will converge to the solution for the intersection of the left and right wave curves; see Ex. 3.7. In addition, the escape velocity $u \pm 2c/(\gamma-1)$ is finite, and the rarefaction curve ends with $c = 0$. Hence, one can construct initial data for a RP corresponding to each of the 5 cases shown in Fig. 3.3 .

General references:

1. [Davis, 1985]
2. [Menikoff & Plohr, 1989]
3. [Smoller, 1983], chpts. 17 and 18

Exercises

3.1 Wave interactions are a special case of a Riemann problem and can be solved with the use of wave curves. As an example, consider an ideal gas EOS with $\gamma = 5/3$. Furthermore, suppose the ambient state is given by $V_0 = 1$, $P_0 = 1$, and $u_0 = 0$.

A) Plot the wave curve in the u–P plane for the collision of two shocks of the opposite family. Assume the shock pressure for the left facing shock is 15 and for the right facing shock is 5. Show the outgoing waves are both shocks.

B) Plot the wave curve in the u–P plane for the overtake of two shocks of the same family. Assume both shocks are right facing and the shock pressure for the lead shock is 5 and for the second shock is 30. Show the outgoing waves are a right facing shock and a left facing rarefaction.

3.2 Consider an ideal gas EOS with $\gamma = 4$. Suppose H_0 is the shock Hugoniot based at the initial state $P_0 = 1$, $V_0 = 1$ and $u_0 = 0$. Let the subscript '1' denote the state on H_0 with $P_1 = 10$.

A) Verify the shock Hugoniot H_0 and H_1 in the u–P plane are as shown in Fig. 3.5.

B) Can one conclude from the intersection of the Hugoniot loci in the u–P that the shock 0–i can split into two shocks; 0–1 and 1–i.

C) Conclude that the overtake of two shocks of the same family, depending on shock strengths, can result in an outgoing shock of the same family and either a shock or rarefaction of the opposite family.

D) For any $\gamma > 1$, when the second shock is sufficiently strong (large P), show that in the u–P plane H_1 lies to the left of H_0. What can you conclude about the overtake of a shock by a strong shock of the same family.

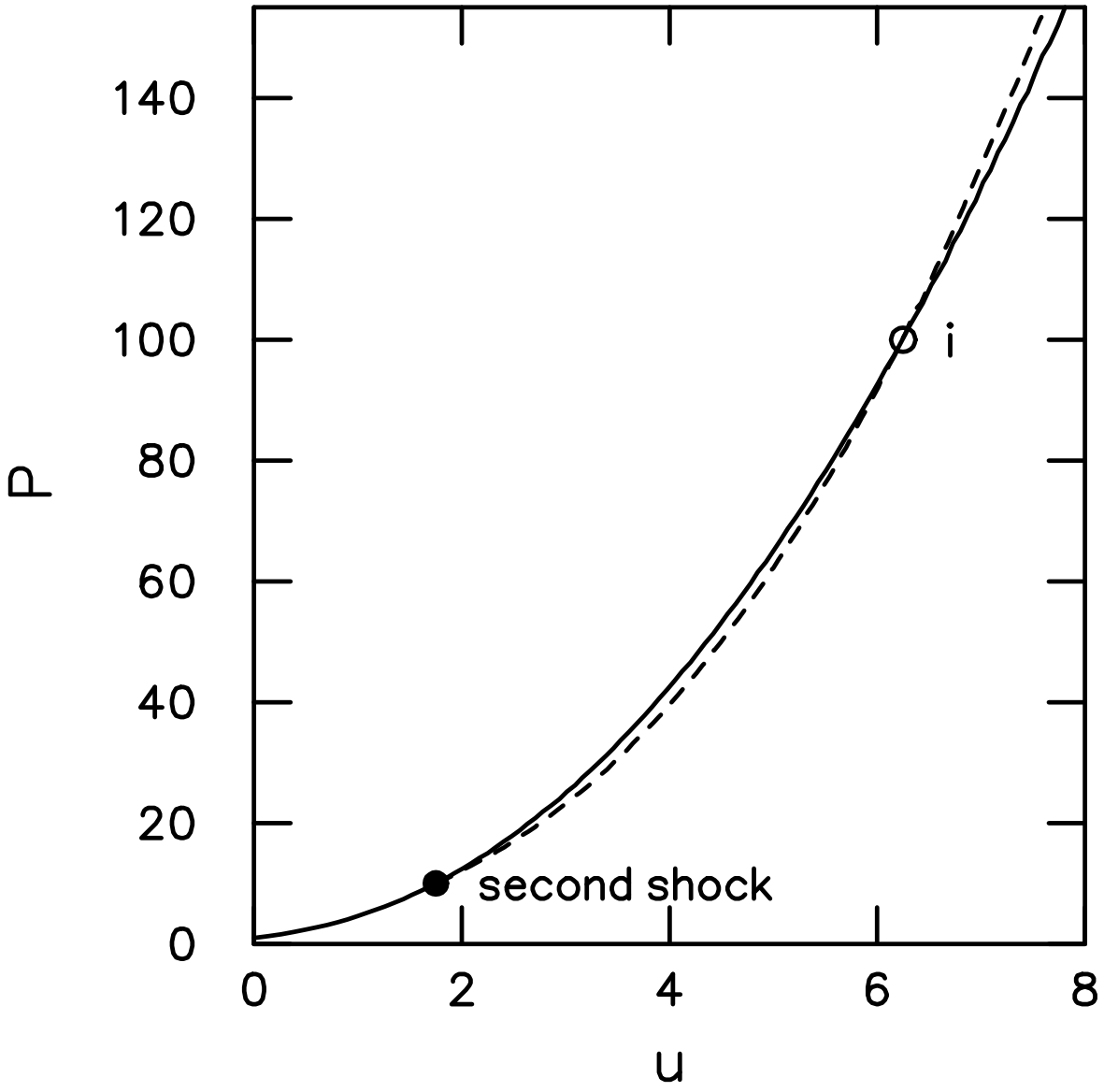

FIGURE 3.5

Shock loci in u–P plane for ideal gas with $\gamma = 4$. Initial shock is solid line. Second shock from state $P_1/P_0 = 10$ is shown as dashed line emanating from solid circle. Intersection of the two loci is labeled 'i'.

3.3 Suppose an EOS has the properties that (i) $0 < \Gamma < \gamma$, (ii) $\mathcal{G} > 0$, and (iii) on any Hugoniot locus both the entropy and the mass flux through the shock front are monotonically increasing. From Ex. 2.7, an ideal gas EOS satisfies these conditions. In the next lecture it will be shown that the second property implies the third. Let H_0 be the shock Hugoniot based at the initial state denoted by the subscript '0'. In addition, let the subscript '1' denote any state on H_0, and H_1 the shock Hugoniot based at the state 1. Consider any state 2 on H_0 and corresponding state $2'$ on H_1 with $P_2 = P_{2'}$.

A) In the V–P show that H_1 lies to the left of H_0; *i.e.*, $V_{2'} < V_2$.

B) Show that the entropy increase from a sequence of two shocks is lower than that of a single strong shock to the same final pressure; *i.e.*, $S_{2'} < S_2$. Moreover, $E_{2'} < E_2$.

C) Let the velocity difference across a shock from state i to state j be denoted $u_{i,j} = u_i - u_j$. Show that $u_{1,2'} < u_{0,2}$.

D) Show that the collision of two shocks of the opposite family always results in two outgoing shocks.

3.4 **A)** Sketch the wave curves for a shock reflecting from a rigid wall.

B) Generalize to the case when the wall is moving with velocity U_p, *i.e.*, a piston.

3.5 A shock impedance match refers to the interaction that occurs when an incident shock impinges on a contact or an interface between two materials. The result is a transmitted shock and a reflected wave.

A) How do you determine whether the reflected wave is a shock or a rarefaction? Show that when the pressure increases the particle velocity decreases and vice versa.

The shock Hugoniot of many metals at high pressures (exceeding the yield strength) have been determined experimentally from a sequence of impedance match experiments in which a flyer plate (*e.g.*, driven by a gas gun) strikes a target. The flyer plate velocity before impact u_f and the shock velocity in the target σ are measured.

B) One starts by calibrating a standard material. When the flyer plate and the target are the same material, how is a point on the Hugoniot locus P_s and V_s determined from u_f and σ? Repeated experiments varying u_f are needed to determine the principal Hugoniot locus of the standard.

C) Suppose the Hugoniot locus of the flyer plate is known. How is a point on the Hugoniot locus of the target determined from u_f and σ ? Again repeated experiments varying u_f are needed to determine the principal Hugoniot locus of the target.

D) Can the sound speed be determined from the Hugoniot locus, or if not, can a lower or upper bound be placed on the sound speed?

3.6 For weak waves, the projection of the wave curve in the u–P plane can be linearized and approximated by a straight line. The slope dP/du at the initial state is called the **acoustic impedance**.

A) Show that the acoustic impedance is equal to ρc.

B) For a weak shock incident on a contact (previous problem) show that the reflected wave is a shock if and only if the acoustic impedance is larger for the transmitted material than for the incident material.

C) Show that weak shock waves of the opposite family pass through each other, *i.e.*, to first order the outgoing waves have the same strength as the incoming waves, and $\Delta P = \Delta P_L + \Delta P_R$.

D) Show that to second order a finite difference approximation of the characteristic equations is equivalent to calculating the contact state of the solution to a Riemann problem from the intersection of the left and right wave curves. Hint, consider Eqs. (1.16), (2E.4) and (3.17b).

3.7 Consider the Riemann problem when the left and right state obey ideal gas equations of state. The solution to the Riemann problem is determined by the equation

$$u(P) \equiv u_\ell(P) - u_r(P) = 0 \ , \tag{3E.1}$$

where u_ℓ and u_r are the left and right wave curves. A common technique for solving a non-linear equation is a Newton iteration:

$$P_{n+1} = P_n - \left. \frac{u}{du/dP} \right|_{P_n} \ , \tag{3E.2}$$

starting with some initial guess P_0.

A) Show that $u(P)$ is a convex function.

B) In the u–P plane, there is a simple geometric construction which corresponds to a Newton iteration. Illustrate the construction when the initial guess is both above and below the solution. When P_0 lies below the solution, conclude from the geometric picture that (i) the sequence P_n is monotonically increasing, (ii) P_n converges to the solution, and (iii) the convergence rate is second order. Also show that the acoustic approximation, the intersection of the tangents of the left and right wave curves, gives a lower bound for P.

C) Determine $u_{\ell,r}(P)$ for the shock branch and for the rarefaction branch of the wave curve.

D) If the solution to the Riemann problem consists of two rarefactions show that P at the contact is bounded by

$$A^{1/n_{\rm min}} \le \frac{P}{P_{\rm min}} \le A^{1/n_{\rm max}} \ , \tag{3E.3}$$

where

$$\begin{aligned}
n_\ell &= \frac{\gamma_\ell - 1}{2\gamma_\ell} \ , \\
n_r &= \frac{\gamma_r - 1}{2\gamma_r} \ , \\
n_{\rm min} &= \min(n_\ell, n_r) \ , \\
n_{\rm max} &= \max(n_\ell, n_r) \ , \\
P_{\rm min} &= \min(P_{\ell 0}, P_{r0}) \ , \\
A &= \frac{u_{\ell 0} - u_{r0} + \frac{2c_{\ell 0}}{\gamma_\ell - 1} + \frac{2c_{r0}}{\gamma_r - 1}}{\frac{2c_{\ell 0}}{\gamma_\ell - 1}\left(\frac{P_{\rm min}}{P_{\ell 0}}\right)^{n_\ell} + \frac{2c_{r0}}{\gamma_r - 1}\left(\frac{P_{\rm min}}{P_{r0}}\right)^{n_r}} \ .
\end{aligned}$$

Note, if $\gamma_\ell = \gamma_r$ then Eq. (3E.3) gives the exact solution for case of two rarefactions.

E) On the shock branch show that the wave curve is bounded by

$$\rho_0 \Delta u \cdot \left(c_0 + \tfrac{\gamma+1}{4} \Delta u \right) \leq P - P_0 \leq \rho_0 \Delta u \cdot \left(c_0 + \tfrac{\gamma+1}{2} \Delta u \right) , \qquad (3E.4)$$

where $\Delta u = u_1 - u_0$. When the solution to the Riemann problems consists of two shocks, how can analytic bounds on P at the contact be determined.

F) Write a subroutine to solve Eq. (3E.1).

Solutions

3.1 For an ideal gas EOS the shock locus can be computed using the formulae derived in Ex. 2.7 A, and the rarefaction locus from the formulae derived in Ex. 2.4 A. The wave curves for the two cases are shown below.

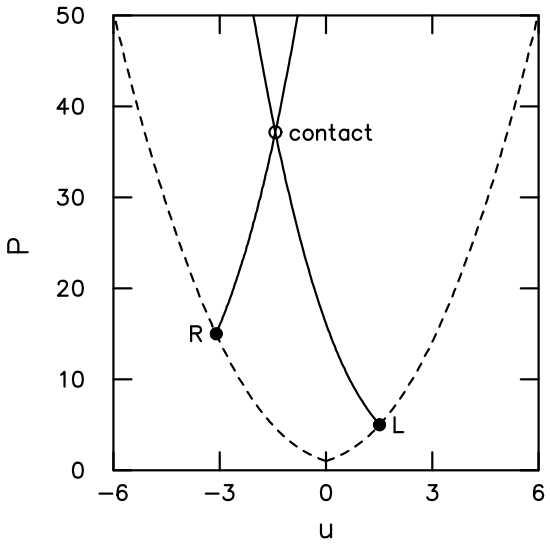

Fig. 3.6 A: The collision of two shocks of the opposite family.

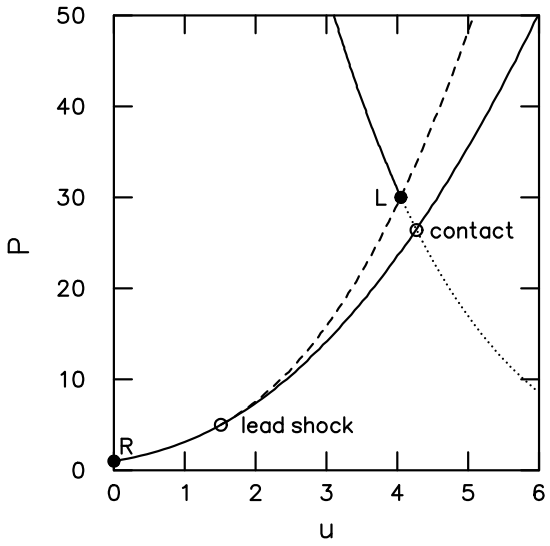

Fig. 3.6 B: The collision of two shocks of the same family.

A) In Fig. A, the dashed curves are the right and left shock loci from the ambient state. The state behind the left and right facing incoming shocks are the indicated right and left initial states for a Riemann problem. The solid lines are the wave curves based at the initial states for the Riemann problem. Their intersection represents the contact state for the outgoing waves. It follows from the figure that both outgoing waves are shocks.

B) In Fig. B, the shock loci for the ambient state and the lead shock (dashed line) are shown. The ambient state and the state behind the second shock are the right and left states for a Riemann problem. The left facing wave curve from the state behind the second shock is shown; solid line for the shock locus and dotted line for the rarefaction locus. The intersection with the shock locus for the ambient state represents the contact state for the outgoing waves. It follows from the figure that the outgoing right facing wave is a shock and the outgoing left facing wave is a rarefaction.

3.2 **A)** For an ideal gas EOS the shock locus can be computed using the formulae derived in Ex. 2.7 A.

B) The conclusion is false. The shock loci H_0 and H_1 are of the same family. Because of the characteristic condition, Eq. (2.35) (verified in Ex. 2.7 C), two shocks of the same family will interact. For the graphical solution of the Riemann problem, it is essential that the wave curves from the right and left state be of the opposite family.

C) If the first shock is on H_0 at state 1, and the second shock is on H_1 between states 1 and i, then the Riemann problem corresponding to the overtake of the two shocks will have a solution with two outgoing waves consisting of two shocks. On the other hand, if the second shock is above state i then the outgoing waves will be a shock of the same family and a rarefaction of the opposite family.

D) Consider the state 2 on H_0 and the state $2'$ on H_1. From Ex. 2.7 E, in the strong shock limit

$$P_2 = \frac{\gamma+1}{2}\rho_0 u_2^2$$
$$P_{2'} = \frac{\gamma+1}{2}\rho_1 u_{2'}^2$$

Since $\rho_0 < \rho_1$, when $P_2 = P_{2'}$, it follows that $u_{2'} < u_2$. Hence asymptotically, H_1 lies to the left of H_0 in the u–P plane. When the second shock is strong the geometry of the wave curves is the same as in Fig. 3.6 B. Therefore, the solution to the Riemann problem corresponding to the overtake by a strong second shock will have a reflected rarefaction.

3.3 **A)** By Lemma 2.3, for weak shocks the entropy change is third order in shock strength, and $\Delta V < 0$ since $\mathcal{G} > 0$. It follows from Eq. (3.9a) when $\Gamma > 0$ that for every point on the shock Hugoniot $-\partial_V P|_S \leq -dP/dV|_H$, with equality only at the initial state. Therefore, at the state 1, $-dP/dV|_{H_1} = -\partial_V P|_S < -dP/dV|_{H_0}$. Hence, in the V–P plane H_1 starts out to the left of H_0. To show that H_1 remains to the left of H_0, it is sufficient

to proof in the V–P plane that H_0 and H_1 intersect only at the state 1. The proof is by contradiction. Suppose H_0 intersects H_1 at a state 2 different from state 1. At the intersection, the energy E must be the same since P and V parameterize phase space when $\Gamma > 0$. From the Hugoniot equation, (2.22), we have

$$E_2 - E_0 = (E_2 - E_1) + (E_1 - E_0)$$
$$\tfrac{1}{2}(P_2 + P_0)\cdot(V_0 - V_2) = \tfrac{1}{2}(P_2 + P_1)\cdot(V_1 - V_2) + \tfrac{1}{2}(P_1 + P_0)\cdot(V_0 - V_1)\ . \qquad (3S.1)$$

Geometrically, each term is the area of a trapezoid in the V–P plane. Hence, Eq. (3S.1) implies that the points (V_0, P_0), (V_1, P_1) and (V_2, P_2) lie on a straight line. In particular,

$$\frac{P_2 - P_0}{V_0 - V_2} = \frac{P_1 - P_0}{V_0 - V_1}\ .$$

By Eq. (2.18) this implies the mass flux through the two shocks on H_0 to state 1 and state 2 are the same. This contradicts the assumption that the mass flux is monotonically increasing. Therefore, H_1 must lie to the left of H_0 in the V–P plane; *i.e.*, $V_{2'} < V_2$ whenever $P_{2'} = P_2 > P_1$.

B) Since $P_{2'} = P_2$, from Eq. (3.9a),

$$S_2 - S_{2'} = \int_{V_{2'}}^{V_2} \frac{\gamma P}{\Gamma T}\, dV\ .$$

By the previous part, $V_{2'} < V_2$. Since the integrand is positive, $S_{2'} < S_2$. This has the interpretation that a sequence of two shocks generates less entropy than a single shock to the same final pressure. Similarly from Eq. (3.9b) and the assumption (i), it follows that $V_{2'} < V_2$ implies $E_{2'} < E_2$.

C) From Eq. (2E.7) we have

$$\tfrac{1}{2}\,u_{0,2}^2 = E_2 - E_0 - P_0\cdot(V_0 - V_2)\ ,$$
$$\tfrac{1}{2}\,u_{1,2'}^2 = E_{2'} - E_1 - P_1\cdot(V_1 - V_{2'})\ .$$

Since state 1 is on H_0

$$E_1 - E_0 = \tfrac{1}{2}\,(P_1 + P_0)\cdot(V_0 - V_1)\ .$$

Combining these three equation we obtain,

$$\tfrac{1}{2}\left(u_{0,2}^2 - u_{1,2'}^2\right) = (E_2 - E_{2'}) + (P_1 - P_0)\cdot\left[\tfrac{1}{2}\,(V_0 + V_1) - V_{2'}\right] + P_0\cdot(V_2 - V_{2'})\ .$$

Since $E_{2'} < E_2$, $P_1 > P_0$, $V_{2'} < V_2$ and $V_{2'} < V_1 < V_0$, each term on the right hand side is positive. Therefore, $u_{1,2'} < u_{0,2}$.

D) For the collision of two shocks of the opposite family, the qualitative structure of the wave curves is shown in Fig. 3.6 A. The previous part implies that the wave curves from states R and L never intersect the initial wave curves; *i.e.*, the solid lines do not intersect the dotted lines. Consequently, for the Riemann problem the shock branches of the wave curves must intersect. Therefore, the outgoing waves are both shocks.

3.4 **A)** The reflection of a shock from a rigid wall is equivalent to the symmetric collision of two shocks shown in Fig. 3.7. The wall pressure after the reflection is the same as the pressure at the contact.

B) A Galilean transformation to the frame moving with the piston reduces the problem to the reflection from a rigid wall.

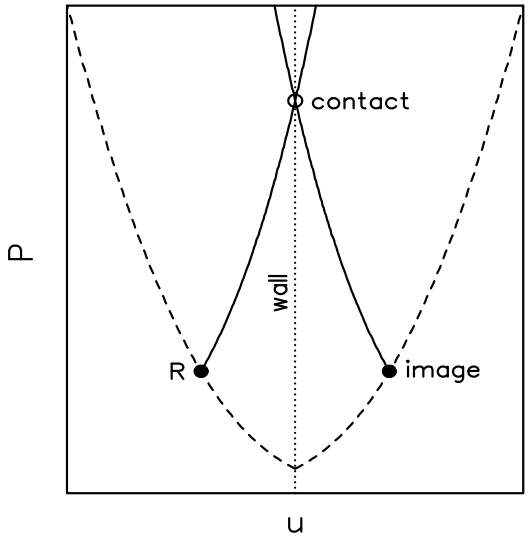

FIGURE 3.7

Wave curves for the reflection of left facing shock from rigid wall.

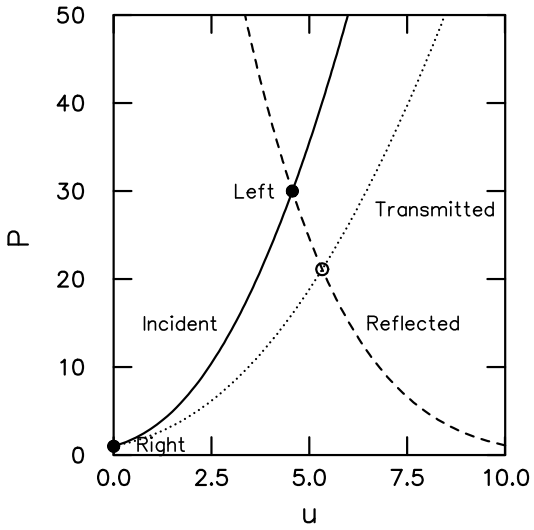

Fig. 3.8 A: Impedance match with reflected rarefaction.

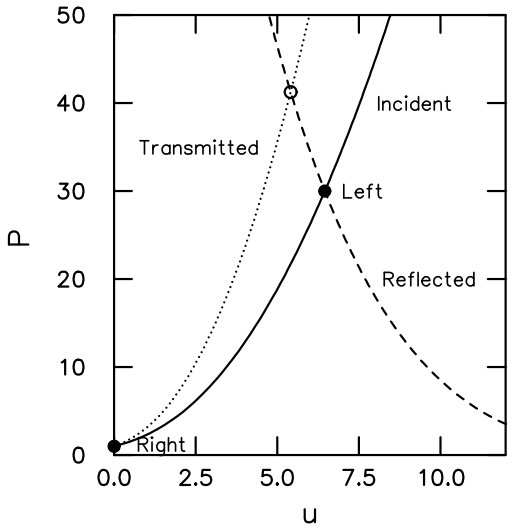

Fig. 3.8 B: Impedance match with reflected shock.

3.5 **A)** At the moment the incident shock impacts the interface, the state of the fluid flow defines the initial conditions for a Riemann problem. For simplicity we assume that the ambient material is at rest, and that the incident material is on the left and the transmitted material is on the right. Hence the incident shock and the transmitted shock are right facing waves, and the reflected wave is left facing. Let P_L be the pressure behind the incident shock, and P_R be the ambient pressure. These correspond to the pressure of the left and right states for the Riemann problem. The wave curves in the u–P plane for an impedance match are shown in Fig. 3.8. The incident, transmitted and reflected wave curves are represented by solid, dotted and dashed lines respectively. The left and right states for the Riemann problem are shown as solid circles and the solution state as an open circle. There are two cases; $u_I(P_L) < u_T(P_L)$ and $u_T(P_L) < u_I(P_L)$. In the first case, shown in Fig. 3.8 A, the reflected wave is a rarefaction. In the second case, shown in Fig. 3.8 B, the reflected wave is a shock.

For a left facing wave curve the pressure decreases as the velocity increases. Consequently, when the reflected wave is a rarefaction the pressure decreases and the velocity increases. On the other hand when the reflected wave is a shock the pressure increases and the velocity decreases. For the special case when $u_I(P_L) = u_T(P_L)$, the reflected wave has zero strength and is degenerate; *i.e.*, there is no reflected wave.

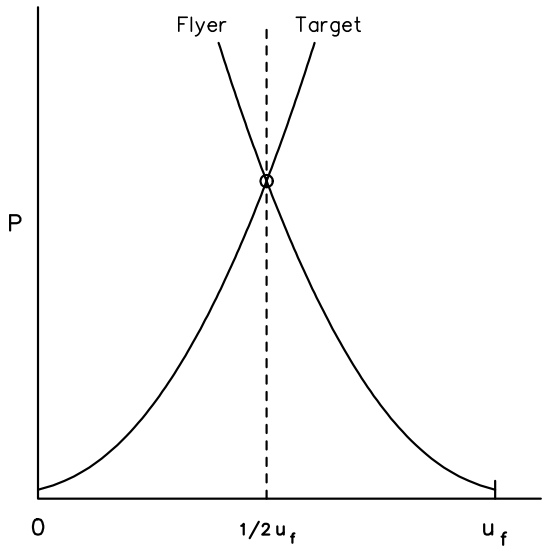

Fig. 3.9 A: Impedance match for calibrating standard.

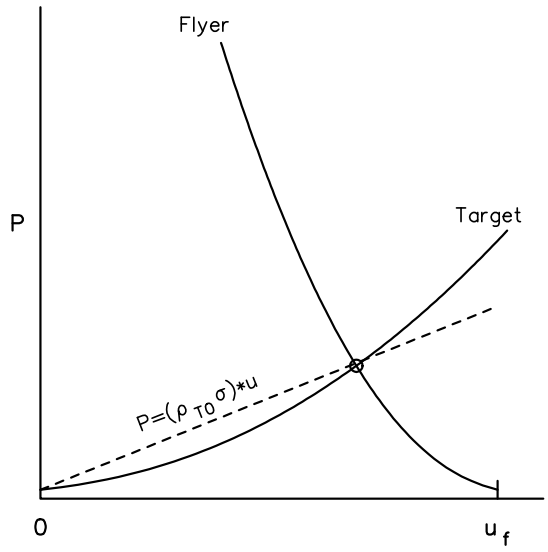

Fig. 3.9 B: Impedance match for target EOS.

B) Consider the Riemann problem corresponding to the instant when the flyer plate impacts the target. When the flyer plate and target are in the same thermodynamic state, the reflected wave curve and the transmitted wave curve are related by $P_R(u) = P_T(u_f - u)$. By symmetry the solution is $u = \frac{1}{2}\, u_f$. This is illustrated in Fig. 3.9 A. From the Hugoniot relations

$$P_h = \tfrac{1}{2}\, \rho_0 u_f \sigma \ ,$$
$$\rho_h = \frac{\sigma}{\sigma - \frac{1}{2}\, u_f} \rho_0 \ .$$

There are two main experimental difficulties: (i) To avoid shock heating the flyer plate from rapid acceleration to velocity u_f. For gas guns and explosively driven flyer plates, the maximum velocity typically is limited to $u_f < 10\,\mathrm{km/s}$. This in turn limits the peak Hugoniot pressure to a few Mbars. (ii) The flyer plate and target must be aligned such that the impact is normal to the interface. Otherwise, 2-D effects complicate the interpretation and increase the error bar of the equation of state data point from the experiment.

C) Let the wave curve of the standard be denoted by P_{std}. The reflected wave curve for the flyer is given by

$$P = P_{\mathrm{std}}(u_f - u) \ .$$

From the Hugoniot relations, the shock in the target satisfies

$$P = (\rho_{T0}\sigma)u \ .$$

Because u and P match at the interface between the flyer and the target, the solution of the Riemann problem is the intersection of the two curves; (u_c, P_c). This is illustrated in Fig. 3.9 B. From the Hugoniot relations, the density in the target behind the shock is $\rho_{Ts} = \frac{\sigma}{\sigma - u_c}\,\rho_{T0}$.

Determining the principal Hugoniot for a material is a time consuming and expensive process. High pressure Hugoniot data for a large number of materials is given in [Marsh, 1980].

D) Because the entropy changes with shock strength, the sound speed can not be determined from the shock Hugoniot alone. However, the characteristic condition, Eq. (2.36), gives a lower bound on the sound speed, $\sigma - u_c < c$.

3.6 **A)** For simplicity we can assume that $u_0 = 0$. From Eq. (2E.4), $P = P_0 + \rho_0 u\sigma$. Therefore, at the initial state $(d/du)P = \rho_0\sigma = \rho_0 c_0$.

B) When the wave curves are linearized, a larger acoustic impedance in the incident material corresponds to Figs. 3.8 A and a reflected rarefaction. Similarly, a larger acoustic impedance in the transmitted material corresponds to Figs. 3.8 B and a reflected shock.

C) The wave curves in the u–P plane for the collision of two shocks of the opposite family are shown in Fig. 3.6 A. In the acoustic approximation the wave curves form a parallelogram. Hence, the change in pressure across the two waves add linearly.

D) The following notation is convenient. Let

$$P = P(x,\, t + \Delta t) \ , \qquad u \ = u(x,\, t + \Delta t) \ ,$$

$$P_\ell = P(x - c\,\Delta t,\, t) \ , \quad u_\ell = u(x - c\,\Delta t,\, t) \ ,$$

$$P_r = P(x + c\,\Delta t,\, t) \ , \quad u_r = u(x + c\,\Delta t,\, t) \ .$$

From Eq. (1.16), the finite difference form of the characteristic equations are

$$P - P_\ell = -(\overline{\rho c})_\ell \cdot (u - u_\ell)$$
$$P - P_r = \quad (\overline{\rho c})_r \cdot (u - u_r) \ .$$

Suppose $\overline{\rho c}$ is approximated by

$$(\overline{\rho c})_\ell = \tfrac{1}{2} (\rho_\ell c_\ell + \rho c)$$
$$(\overline{\rho c})_r = \tfrac{1}{2} (\rho_r c_r + \rho c) \ .$$

This corresponds to the trapezoidal rule for $\int \rho c \, du$. Hence the difference equations are accurate to second order.

Now consider the Riemann problem with initial data (u_ℓ, P_ℓ) for the left state and (u_r, P_r) for the right state. The solution of the Riemann problem is determined by the intersection of the wave curves in the u–P plane. From Eq. (2E.4), for a shock wave

$$\Delta P = \rho_0 \cdot (\sigma - u_0) \cdot \Delta u \ .$$

Equation (3.17b) gives the wave speed to order $(\Delta V/V)^2$

$$\rho_0 \cdot (\sigma - u_0) = \pm \tfrac{1}{2} (\rho_0 c_0 + \rho_1 c_1) \ .$$

With this approximation,

$$\Delta P = \pm \tfrac{1}{2} (\rho_0 c_0 + \rho_1 c_1) \cdot \Delta u \ .$$

This equation is also valid to the same order for a rarefaction wave because the first and second derivatives of $P(u)$ are continuous, Eq. (3.25). Moreover, the intersection of the wave curves is accurate to second order. To this order, the equations for the projection of the wave curves in the u–P plane are identical to the finite difference form of the characteristic equations. Hence, to second order the solution of the Riemann problem is equivalent to the solution of the finite difference characteristic equations. Note, this analysis has neglected the variation in entropy over the spatial interval $(x - c\Delta t, x + c\Delta t)$ and the time interval $(t, t + \Delta t)$.

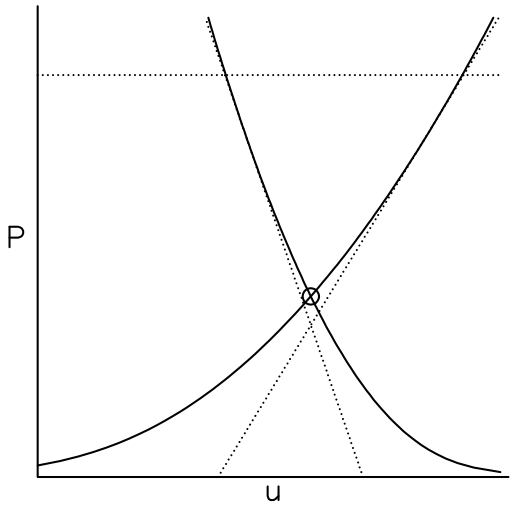

Fig. 3.10 A: Geometric construction of Newton iteration when P is above the solution.

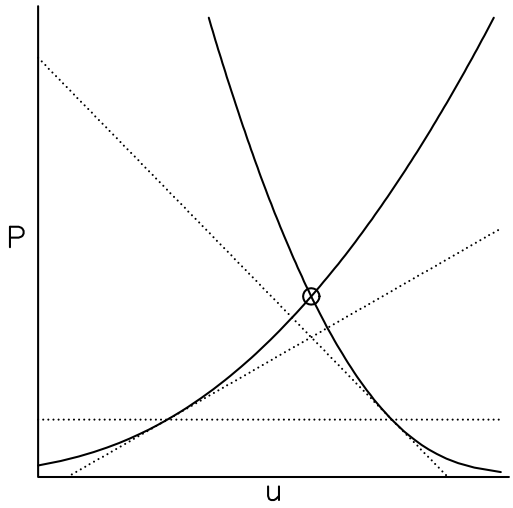

Fig. 3.10 B: Geometric construction of Newton iteration when P is below the solution.

3.7 **A)** From Eq. (3.25), $P(u)$ is convex for both the left and right facing wave curve. Inverting the function we find

$$\frac{du}{dP} = \frac{1}{dP/du} \ ,$$
$$\frac{d^2u}{dP^2} = -\frac{d^2P/du^2}{(dP/du)^3} \ .$$

For the right wave curve $dP/du > 0$ and for the left wave curve $dP/du < 0$. Therefore, $u_\ell(P)$ is convex and $u_r(P)$ is concave. The negative of a concave function is convex. Hence, $u_\ell(P) - u_r(P)$ is convex.

B) A Newton iteration applied to the function $u(P)$ is equivalent to finding the intersection of the tangents of the left and right wave curve. The geometric construction is shown in Fig. 3.10. From the convexity of $P(u)$, the intersection of the slopes always lies below the solution. Furthermore, when P lies below the solution the iteration increases P. Therefore, if P_0 is below the solution then P_n is monotonically increasing. For smooth functions, its well known that the convergence rate of Newton method is second order. However, the first iteration may be out of range if P_0 lies above the solution; *i.e.*, $P_1 < 0$ is possible.

Therefore, it is important to determine a lower bound that can be used as the initial guess to start the iteration.

It also follows from the geometric picture (convexity of the wave curves) that the value of P from the intersection of any tangent to the left wave curve with any tangent to the right wave curve lies below the solution. In particular, the acoustic approximation which uses the tangents at the left and right states gives a lower bound for P.

C) For a shock wave, from Ex. 2.7 A

$$u_1 = u_0 \pm \frac{2}{\gamma+1}\Big(M - \frac{1}{M}\Big)c_0 \ ,$$
$$M^2 = \frac{\gamma+1}{2\gamma}\cdot\frac{P-P_0}{P_0} \ ,$$

where the + and − signs are for right and left facing waves respectively.

For a rarefaction wave, from Eq. (1.17)

$$\begin{aligned} u_1 &= u_0 \pm \frac{2}{\gamma-1}c_0\Big(\frac{c}{c_0} - 1\Big) \\ &= u_0 \pm \frac{2}{\gamma-1}c_0\left[\Big(\frac{P}{P_0}\Big)^{\frac{\gamma-1}{2\gamma}} - 1\right] . \end{aligned}$$

D) From part (C) when both waves are rarefactions, Eq. (3E.1) can be written

$$\frac{2c_{\ell 0}}{\gamma_\ell - 1}\Big(\frac{P_{\min}}{P_{\ell 0}}\Big)^{n_\ell}\cdot\Big(\frac{P}{P_{\min}}\Big)^{n_\ell} + \frac{2c_{r0}}{\gamma_r - 1}\Big(\frac{P_{\min}}{P_{r0}}\Big)^{n_r}\cdot\Big(\frac{P}{P_{\min}}\Big)^{n_r} = u_{\ell 0} - u_{r0} + \frac{2c_{\ell 0}}{\gamma_\ell - 1} + \frac{2c_{r0}}{\gamma_r - 1} \ .$$

We note that if $x, n \in (0,1)$ then for fixed x the value of x^n increases as n decreases. Since $P < P_{\min}$ and $n_\ell, n_r < \frac{1}{2}$, we can apply the inequality and factor out the term $(P/P_{\min})^n$. This leads to the bounds given in Eq. (3E.3). When $\gamma_\ell = \gamma_r$, the inequality is not needed.

E) It follows from Eq. (2E.13) that

$$\Big(u_s/c_0\Big)^2 - \frac{\gamma+1}{2}\Big(\Delta u/c_0\Big)\cdot\Big(u_s/c_0\Big) - 1 = 0 \ ,$$

where $u_s = \sigma - u_0$. It is easy to verify that for fixed Δu the left hand side flips sign and hence a solution u_s lies in the interval

$$c_0 + \tfrac{\gamma+1}{4}\Delta u \le u_s \le c_0 + \tfrac{\gamma+1}{2}\Delta u \ .$$

The other solution of the quadratic is extraneous because $u_s < 0$. The bounds on the wave curve, Eq. (3E.4), follows from the bound on the wave speed and Eq. (2E.4), $\Delta P = \rho_0 \, \Delta u \cdot u_s$.

The solution to the Riemann problem can be determined from the equation

$$P_\ell(u) = P_r(u) \ ,$$

where P_ℓ and P_r are the left and right wave curves. From the convexity of $P(u)$, a lower bound on both wave curves gives a lower bound for the solution P, and conversely an upper bound on both wave curves gives an upper bound for P. The bounds in Eq. (3E.4) give rise to a quadratic equation in u which can be solved analytically and used to determine bounds on P.

F) Based on the previous parts, the algorithm shown in Fig. 3.11 is a robust means for finding the solution to a Riemann problem. The convergence rate of the iteration is second order. Improving the initial guess would result in fewer iterations and speed up the algorithm. This can be done by first determining the type of outgoing waves; *i.e.*, the solution type in Fig. 3.3. When the outgoing waves are both rarefactions or both shocks the initial guess can be based on parts (D) or (E). For a survey of other algorithms see [Gottlieb & Groth, 1988].

/* **Riemann solver for ideal gas equation of state** */
/* (u_{l0}, P_{l0}) is left state and (u_{r0}, P_{r0}) is right state */
/* $u(P)$ and $dudP(P)$ on wave curve to be evaluated from formulae in part (C) */
$P_{\min} = \min(P_{l0}, P_{r0})$;
/* **Acoustic approximation for initial guess** */
$dudP_r = 1/(\rho_{r0} * c_{r0})$;
$dudP_l = 1/(\rho_{l0} * c_{l0})$;
$P = (P_{r0} * dudP_r - P_{l0} * dudP_l - (u_{r0} - u_{l0})) \ / \ (dudP_r - dudP_l)$;
$P = \max(P, P_{\min})$;
for(N_{iter} = **MaxIterations**; N_{iter}--;) /* **MaxIterations** = 5 */
{ /* **Newton iteration** */
Evaluate $u_l(P)$, $dudP_l(P)$, and $u_r(P)$, $dudP_r(P)$
$dP = (u_r - u_l) \ / \ (dudP_r - dudP_l)$;
P -= dP;
if(abs(dP) < **RelativeError** $* P$) /* **RelativeError** = 10^{-4} */
{ /* **Found solution** */
Compute full left & right state at P
return;
}
if($dP < 0$ AND $P < 0.1 * P_{\min}$)
{ /* **This can only occur on first iteration** */
$u_l = u_{l0} + 2/(\gamma_l - 1) * c_{l0}$
$u_r = u_{r0} - 2/(\gamma_r - 1) * c_{r0}$
if($u_l < u_r$)
{ /* **vacuum solution** /*
$P = 0$;
Compute full left & right state at P
return;
}
P = lower bound from Eq. (3E.3)
}
}
/* **Error**, failed to converge. However, P is lower bound. */

FIGURE 3.11: Algorithm for Riemann solver with ideal gas equation of state.

Lecture 4
Constraints on Equation of State

For the fluid flow equations to be predictive and hence useful for applications, a solution to the PDEs must exist for all physically realizable initial conditions. Moreover, the solution must be unique and stable to small perturbations in the initial data. A necessary condition for all initial value problems to have a unique solution is that any Riemann problem has a unique solution. In the previous lecture, theorem 3.4, we found that solutions to the Riemann problem were related to asymptotic and monotonicity properties of the wave curves. We further require that all shock waves are stable to perturbations in both one and two dimensions.

In this lecture, we relate properties of the wave curves to conditions on the EOS. In particular, we analyze the Hugoniot locus. This leads to constraints on an EOS that are necessary for a reasonable fluid flow. It is convenient to distinguish two classes of equations of state. An EOS is called convex if every isentrope is convex; *i.e.*, $\mathcal{G} > 0$ everywhere. For a convex EOS, the wave curve is simple. We will show it consists only of compressive shock waves and expansive rarefaction waves. The non-convex case is more difficult because the wave curve requires additional composite wave types. This will be discused later in more detail.

We assume an equations of state is thermodynamically consistent and asymptotically regular. This is the expected behavior of an EOS corresponding to a real material. Based on the analysis of the wave curve, additional constraints on an EOS are introduced as required.

4.1 Parameterization of Hugoniot Locus

The projection of the Hugoniot locus in thermodynamic state space is determined by either Eq. (2.22) or by Eq. (2.21). This leads us to introduce the Hugoniot function in V–S plane

$$h(V,S) = E(V,S) - E(V_0,S_0) + \tfrac{1}{2}\left[P(V,S) + P_0\right]\cdot(V - V_0)\ , \quad (4.1a)$$

or equivalently in the P–S plane

$$\tilde{h}(P,S) = h\big(V(P,S),S\big) = H(P,S) - H(P_0,S_0) - \tfrac{1}{2}\left[V(P,S) + V_0\right]\cdot(P - P_0)\ . \quad (4.1b)$$

The Hugoniot locus based on the initial state (V_0, S_0) or (P_0, S_0) is the zero level set of its associated Hugoniot function.

Our analysis will heavily utilize the differential of the Hugoniot function. Taking the differential of $h(V,S)$ and substituting the thermodynamic relation $dE = -P\,dV + T\,dS$ we obtain

$$dh = T\,dS - \tfrac{1}{2}\,\Delta P\,dV + \tfrac{1}{2}\,\Delta V\,dP\ . \quad (4.2)$$

Substituting the thermodynamic relation $V\,dP = -\gamma P dV + \Gamma T dS$ then leads to

$$dh = \left(1 + \tfrac{1}{2}\,\Gamma\frac{\Delta V}{V}\right)T\,dS - \tfrac{1}{2}\left(\gamma\frac{\Delta V}{V} + \frac{\Delta P}{P}\right)P\,dV\ , \quad (4.3a)$$

or

$$d\tilde{h} = \left(1 - \frac{\Gamma}{2\gamma}\cdot\frac{\Delta P}{P}\right)T\,dS + \frac{1}{2\gamma}\left(\gamma\frac{\Delta V}{V} + \frac{\Delta P}{P}\right)V\,dP\ . \quad (4.3b)$$

A zero of the Hugoniot function specifies the thermodynamic variables for a shock. The shock velocity is determined by Eq. (2.19) and the particle velocity by (2.23), provided that ΔP and ΔV have the opposite sign. We first show that every zero of the Hugoniot function corresponds to a shock state.

Lemma 4.1: The Hugoniot function associated with the state (V_0, S_0) or (P_0, S_0) has no zeros in the quadrants $\Delta P > 0$, $\Delta V > 0$ or $\Delta P < 0$, $\Delta V < 0$.

Proof: Let (V, P) be a point in the quadrant $\Delta P > 0$, $\Delta V > 0$. If $S < S_0$ then

$$h(V,S) = h(V_0,S_0) + \int_{S_0}^{S} \partial_S h \, dS\Big|_{V_0} + \int_{V_0}^{V} \partial_V h \, dV\Big|_S .$$

We note that (i) $h(V_0, S_0) = 0$, (ii) $\partial_S h|_{V_0} = T > 0$, and (iii) $\partial_V h|_S = -\frac{1}{2}(\gamma \Delta V/V + \Delta P/P)P < 0$ when $\Delta V > 0$ and $\Delta P > 0$. Consequently, $h(V, S) < 0$.

On the other hand, if $S > S_0$ then

$$\tilde{h}(P,S) = \tilde{h}(P_0,S_0) + \int_{S_0}^{S} \partial_S \tilde{h} \, dS\Big|_{P_0} + \int_{P_0}^{P} \partial_P \tilde{h} \, dP\Big|_S .$$

Now we note that (i) $\tilde{h}(P_0, S_0) = 0$, (ii) $\partial_S \tilde{h}|_{P_0} = T > 0$, and (iii) $\partial_P \tilde{h}|_S = (2\gamma)^{-1}(\gamma \Delta V/V + \Delta P/P)V > 0$ when $\Delta V > 0$ and $\Delta P > 0$. Consequently, $\tilde{h}(P, S) > 0$.

When $\Delta P < 0$, $\Delta V < 0$, similar arguments can be applied. Alternatively, interchanging the initial and final shock states reduces the problem to the case we have already proved.

⊠ ⊠

The Hugoniot function reduces the problem of determining the Hugoniot locus to finding the solutions of a single equation in two variables V and S, or P and S, rather than solving the three jump conditions in four variable V, E, u and σ. Lemma 4.1 implies that the reduction does not introduce any extraneous solutions.

We next determine conditions on the EOS in order for the Hugoniot locus to be a single curve connected to the initial state. The following result plays a key role.

Theorem 4.2 (Bethe-Weyl)**:** For an asymptotically regular EOS, the Hugoniot locus based on any state (V_0, S_0) intersects each isentrope at least once. Moreover, if $\mathcal{G} > 0$ along an isentrope, then for $S > S_0$ there is a unique compressive shock and for $S < S_0$ there is a unique expansive shock. Furthermore, for an entropy increasing compressive shock $|u - \sigma| < c$, and for an entropy decreasing expansive shock $|u - \sigma| > c$. In addition, if either condition $-2 \le \Gamma$ or $\Gamma \le 2\gamma$ is satisfied everywhere, then there are no entropy increasing expansive shocks and no entropy decreasing compressive shocks; *i.e.*, the Hugoniot locus intersects every isentrope exactly once.

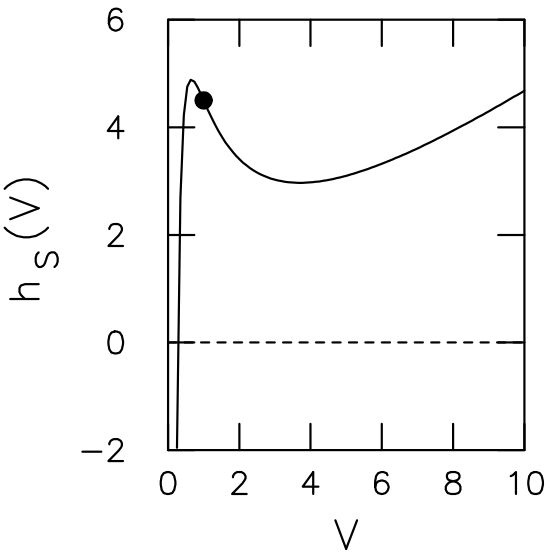

Fig. 4.1 A: Hugoniot function along isentrope with $S > S_0$. Solid circle corresponds to $V = V_0$.

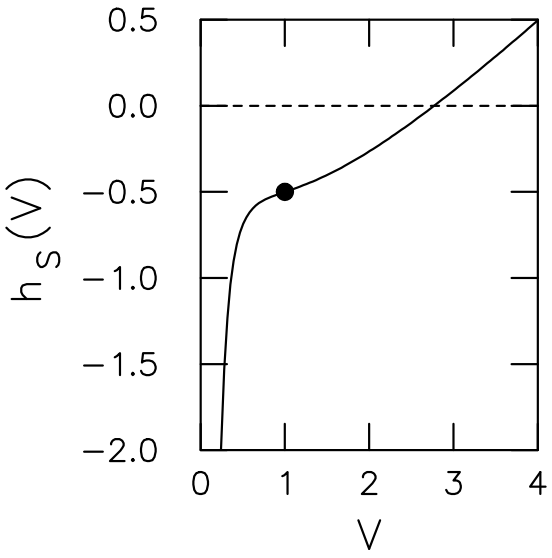

Fig. 4.1 B: Hugoniot function along isentrope with $S < S_0$. Solid circle corresponds to $V = V_0$.

Proof: The original proof by Bethe used entropy as the basis for the analysis, and the proof by Weyl used a convexity argument in the V–P plane. The two methods can be combined by applying the convexity argument to an isentrope. The proof here follows that given by [Menikoff & Plohr, 1989].

A point on the Hugoniot locus based at the state (V_0, S_0) and with a given value of S corresponds to a zero of the Hugoniot function restricted to the isentrope

$$h_S(V) = E(V,S) - E(V_0,S_0) + \tfrac{1}{2}\left[P(V,S) + P_0\right] \cdot (V - V_0) \ , \tag{4.4}$$

where $P_0 = P(V_0, S_0)$. For an ideal gas EOS with $\gamma = 5/3$ and initial state $(V_0, P_0) = (1, 1)$, the restricted Hugoniot function is plotted in Fig. 4.1. The form of $h_S(V)$ is similar to that of a cubic function. Fig. 4.1 A shows for $S > S_0$ that $h_S(V)$ has a local maximum for $V < V_0$ and a local minimum for $V > V_0$, while Fig. 4.1 B shows for $S < S_0$ that $h_S(V)$ has an inflection point but no local extremum. The crossover occurs at $S = S_0$ when h_S, h'_S and h''_S all vanish at $V = V_0$. Figure 4.1 illustrates the canonical behavior that occurs when the sign of $P(V_0, S) - P_0$ is the same as the sign of $S - S_0$. The anomalous case has

property	$S > S_0$	$S < S_0$	comment
(i)	$h_S(V) \to -\infty$ as $V \to 0$		asymptotics of EOS
(ii)	$h_S(V) \to \infty$ as $V \to \infty$		asymptotics of EOS
(iii)	$h_S(V_0) > 0$	$h_S(V_0) < 0$	$T > 0$
(iv)	$h'_S(V_0) < 0$	$h'_S(V_0) > 0$	canonical case
	$h'_S(V_0) > 0$	$h'_S(V_0) < 0$	anomalous case
(v)	$h''_S(V) < 0$ for $V < V_0$		$\mathcal{G} > 0$
	$h''_S(V) > 0$ for $V > V_0$		
(vi)	additional constraint when isentropes cross		$-2 \le \Gamma$ or $\Gamma \le 2\gamma$
	$\min_{V>V_0} h_S(V) > 0$	$---$	canonical case
	$---$	$\max_{V<V_0} h_S(V) < 0$	anomalous case

Table 4.1: Properties of the restricted Hugoniot function.

the opposite behavior; $h_S(V)$ is monotonic when $S > S_0$ and has two local extremum when $S < S_0$. The strategy of the proof is to show that the qualitative features of the restricted Hugoniot function are independent of the equation of state provided that $\mathcal{G} > 0$. The important properties of the Hugoniot function shown in Fig. 4.1 are listed in Table 4.1.

Before proving the general properties, we first show how they imply the result of the theorem.

1. Existence of solution.

   From the asymptotic behavior, properties (i) and (ii), the range of $h_S(V)$ is $(-\infty, \infty)$. It follows from continuity that the Hugoniot function has at least one zero.

2. $S > S_0$, entropy increasing shocks.

   From property (iii) the Hugoniot function is positive at $V = V_0$. For $V < V_0$, from property (v) the Hugoniot function is concave. Therefore, there is a unique entropy increasing compressive shock. For $V > V_0$, from property (v) the Hugoniot function is convex. In the canonical case, the slope is initially negative. But by property (vi) the Hugoniot function is always positive. In the anomalous case, the slope is initially positive and the Hugoniot function is monotonic. Hence, it is always positive. Therefore, in either case, there are no entropy increasing expansive shocks.

3. $S < S_0$, entropy decreasing shocks.

   The case $V > V_0$ and $S < S_0$ is analogous to the case $V < V_0$ and $S > S_0$. Consequently, there is a unique entropy decreasing expansive shock. The case $V < V_0$ and $S < S_0$ is analogous to the case $V > V_0$ and $S > S_0$. Consequently, there are no entropy decreasing compressive shocks.

4. Subsonic/supersonic state behind shock.

   We will show that the subsonic/supersonic nature of the state behind the shock depends on the sign of the slope of the Hugoniot function at its zero crossing. For now we note that $h'_S(V) > 0$ at the zero crossing when either $S > S_0$ and $V < V_0$ or $S < S_0$ and $V > V_0$.

We now prove the general properties of the restricted Hugoniot function.

(i) By the asymptotic condition (EOS–1), for S fixed, $P \to \infty$, $E \to \infty$ and $E/P \to 0$ as $V \to 0$. It then follows from Eq. (4.4) that $h_S(V) \to P \cdot [E/P - \frac{1}{2}(V_0 - V)] \to -\infty$ as $V \to 0$.

(ii) By the asymptotic condition (EOS–2), for S fixed, $P \to 0$ and $E \to E_\infty$ as $V \to \infty$. Therefore, $h_S(V) \to E_\infty - E_0 + \frac{1}{2} P_0 \cdot (V - V_0) \to \infty$ as $V \to \infty$.

(iii) At the initial state the restricted Hugoniot function is given by

$$\begin{aligned} h_S(V_0) &= E(V_0, S) - E(V_0, S_0) \\ &= \int_{S_0}^{S} T\, dS \Big|_{V_0} . \end{aligned}$$

The second line follows from the thermodynamic relation $dE = -P\, dV + T\, dS$. Because $T > 0$, the sign of the $h_S(V_0)$ is the same as the sign of $S - S_0$.

(iv) The derivative of the restricted Hugoniot function is

$$h'_S(V) = -\tfrac{1}{2}\Big(P(V, S) - P_0 - \frac{\partial P}{\partial V}\Big|_S (V - V_0)\Big) . \tag{4.5}$$

At the initial state

$$h'_S(V_0) = -\tfrac{1}{2}\Big(P(V_0,S) - P(V_0,S_0)\Big) \ .$$

Therefore, the sign of $h'_S(V_0)$ is the same as the sign of $P(V_0,S_0) - P(V_0,S)$.

We note from the thermodynamic relation $V\,dP = -\gamma P\,dV + \Gamma T\,dS$ that

$$P(V_0,S) - P(V_0,S_0) = V_0^{-1} \int_{S_0}^{S} \Gamma\, T\, dS\Big|_{V_0} \ .$$

Therefore, if $\Gamma > 0$ then the sign of $P(V_0,S) - P(V_0,S_0)$ is the same as the sign of $S - S_0$. This is an important example of the canonical case.

(v) The second derivative of the restricted Hugoniot function is

$$h''_S(V) = \tfrac{1}{2}\,(V - V_0)\,\frac{\partial^2 P}{\partial V^2}\Big|_S \ . \tag{4.6}$$

Since we are assuming $\mathcal{G} > 0$, the sign of $h''_S(V)$ is the same as the sign of $V - V_0$.

For $S = S_0$, we note that h, h' and h'' all vanish at $V = V_0$.

(vi) We first consider the canonical case when $S > S_0$ and $V > V_0$. By the thermodynamic relation $dE = -P\,dV + T\,dS$, the energy difference can be written as the path integral

$$E(V,S) - E(V_0,S_0) = \int_{S_0}^{S} T\,dS'\Big|_V - \int_{V_0}^{V} P\,dV'\Big|_{S_0} \ .$$

When $G > 0$, the isentrope is convex and the integral of $P\,dV$ is less than the area of the trapezoid formed by the end points,

$$\int_{V_0}^{V} P\,dV'\Big|_{S_0} < \tfrac{1}{2}\Big[P(V_0,S_0) + P(V,S_0)\Big]\cdot(V - V_0) \ .$$

Therefore, we have the bound on the energy difference

$$E(V,S) - E(V_0,S_0) > \int_{S_0}^{S} T\,dS'\Big|_V - \tfrac{1}{2}\Big[P(V_0,S_0) + P(V,S_0)\Big]\cdot(V - V_0) \ .$$

Substituting into Eq. (4.4) we obtain the bound on the Hugoniot function

$$h_S(V) > \int_{S_0}^{S} T\,dS'\Big|_V + \tfrac{1}{2}\Big[P(V,S) - P(V,S_0)\Big]\cdot(V - V_0) \ . \tag{4.7}$$

For the canonical case with $S > S_0$, we note that $\int T\,dS > 0$ and $P(V_0, S) > P(V_0, S_0)$. If the isentropes don't cross then $P(V, S) > P(V, S_0)$. It follows from Eq. (4.7) that $h_S(V) > 0$ for $V > V_0$. Therefore, condition (vi) is satisfied if the isentropes don't cross.

When $\Gamma < 0$, the isentropes can cross and we need a more refined estimate for $h_S(V)$. Substituting the thermodynamic relation $V\,dP = -\gamma P\,dV + \Gamma T\,dS$ into Eq. (4.7) gives

$$h_S(V) > \int_{S_0}^{S} \Big(1 + \tfrac{1}{2}\,\Gamma \frac{V - V_0}{V}\Big) T\,dS\Big|_V \ .$$

For $V > V_0$, we note that $0 < (V - V_0)/V < 1$. It follows that the integrand is positive when $\Gamma \geq -2$. Therefore, $\Gamma \geq -2$ is a sufficient condition for $h_S(V) > 0$ and condition (vi) to be satisfied whether or not the isentropes cross. For later use we note that we have proved the following.

Lemma 4.2.1: If the isentrope S_0 is convex and $\Gamma \geq -2$ everywhere then there are no specific volume increasing, entropy increasing shocks relative to any state along the isentrope S_0.

Alternatively, an isentrope can be parameterized by P. The restricted Hugoniot function can be written as

$$\tilde{h}_S(P) = h_S\big(V(P,S)\big) = H(P,S) - H(P_0,S_0) - \tfrac{1}{2}\left[V(P,S) + V_0\right] \cdot (P - P_0) \ .$$

In terms of the enthalpy, the fundamental thermodynamic identity can be expressed as $dH = V\,dP + T\,dS$. We now consider the canonical case with $S > S_0$ and $P < P_0$. A bound on $\tilde{h}_S(P)$ can be obtained using the same arguments we previously applied to $h_S(V)$. Using both the fundamental thermodynamic identity and the thermodynamic relation $V\,dP = -\gamma\,P\,dV + \Gamma\,T\,dS$, we obtain

$$\begin{aligned} \tilde{h}_S(P) &> \int_{S_0}^{S} T\,dS\Big|_{P_0} - \tfrac{1}{2}\Big[V(P_0,S) - V(P_0,S_0)\Big] \cdot (P_0 - P) \\ &> \int_{S_0}^{S} \Big(1 - \frac{\Gamma}{2\gamma} \cdot \frac{P_0 - P}{P_0}\Big) T\,dS\Big|_{P_0} \ . \end{aligned}$$

For $P < P_0$, we note that $0 < (P_0 - P)/P_0 < 1$. It follows that the integrand is positive when $\Gamma < 2\gamma$. Hence, $\Gamma < 2\gamma$ is also a sufficient condition for condition (vi) to be satisfied. For later use we note that we have proved the following.

Lemma 4.2.2: If the isentrope S is convex and $\Gamma < 2\gamma$ everywhere then there are no pressure increasing, entropy decreasing shocks relative to any state along the isentrope S.

The anomalous case with $S < S_0$ and $V < V_0$ is proved in a similar manner. In effect, an expansive entropy increasing shock and a compressive entropy decreasing shock are related by interchanging the end states. Consequently, either lemma 4.1.1 or 4.1.2 is sufficient to exclude these non-standard shocks for a convex EOS. However, we later show that for a non-convex EOS and some initial states, expansive entropy increasing shocks are needed in order to construct a wave curve.

Finally, we relate the Mach number of the flow behind the shock to the sign of the Hugoniot function at the zero crossing. From Eq. (2.19) and (1.12), we find

$$\begin{aligned} -\frac{\Delta P}{\Delta V} + \left.\frac{\partial P}{\partial V}\right|_S &= -\frac{\Delta P}{\Delta V} - \gamma \frac{P}{V} \\ &= \rho^2 \cdot \left[(\sigma - u)^2 - c^2\right] \\ &= \rho^2 \cdot (\sigma - \lambda_+) \cdot (\sigma - \lambda_-) \ . \end{aligned} \tag{4.8}$$

Then from Eqs. (4.5) we obtain

$$2\,\frac{h_S'}{V - V_0} = \rho^2 \cdot \left[(\sigma - u)^2 - c^2\right] \ .$$

Therefore, the flow is supersonic when $h_S'/(V - V_0) > 0$, and subsonic when $h_S'/(V - V_0) < 0$. Since $h_S' > 0$ at the zero crossing, it follows that the flow is subsonic for entropy increasing compressive shocks and supersonic for entropy decreasing expansive shocks. We note that if the isentrope is not convex then there could be more than one compressive shock, and these would alternate between subsonic and supersonic.

⊠ ⊠

One important consequence of the Bethe-Weyl theorem follows from the continuity of the Hugoniot function.

Corollary 4.3: Suppose an EOS is convex. Then the connected branch of the Hugoniot locus based on any state can be parameterized by S. Denoting the base state by the subscript 0, $P_h(S) > P_0$ and $V_h(S) < V_0$ for $S > S_0$ while $P_h(S) < P_0$ and $V_h(S) > V_0$ for $S < S_0$. In addition, if either condition $-2 \leq \Gamma$ or $\Gamma \leq 2\gamma$ is satisfied everywhere then the connected branch contains all possible shock waves.

The Bethe-Weyl theorem has another important consequence.

Corollary 4.4: For a convex EOS, an entropy increasing compressive shock satisfies the characteristic criterion.

Proof: The Hugoniot equation (2.22) is symmetric in the end states. Hence the state behind an entropy increasing compressive shock corresponds to the state ahead of an entropy decreasing expansive shock. Moreover, the velocities are given by Eq. (2.19), $-\Delta P/\Delta V = [\rho\cdot(\sigma - u)]^2 = [\rho_0\cdot(\sigma - u_0)]^2$, and are not affected by how the states are labeled. Therefore, by the Bethe-Weyl theorem, for an entropy increasing compressive shock the behind state is subsonic and the ahead state is supersonic. This is the characteristic criterion, Eq. (2.36).

⊠ ⊠

Remark 4.5: For an explosive material, a chemical reaction releases energy. This energy can be accounted for by shifting the energy in the Hugoniot equation (2.22)

$$E - E_0 = \tfrac{1}{2}\,(P + P_0)\cdot(V_0 - V) + Q\ ,$$

where $Q > 0$ is the chemical energy released per unit mass. Consequently, the Hugoniot locus for an explosive is determined by the level set Q of the Hugoniot function with the EOS of the reaction products and a meta-stable initial state (V_0, E_0, P_0) satisfying the EOS of the reactants. It follows from the non-monotonicity of the restricted Hugoniot function shown in Fig. 4.1 A and the proof of the Bethe-Weyl theorem that the Hugoniot locus for an explosive can intersect an isentrope with $S > S_0$ three times; either twice with $V < V_0$ and once with $V > V_0$ or vice versa. Moreover, the flow behind the solution with the minimum V is subsonic, the maximum V is supersonic, and the middle V is supersonic if $V < V_0$ and subsonic if $V > V_0$. The multiple solutions gives rise to a non-uniqueness in the choice of detonation and deflagration waves; see Ex. 4.5.

For a convex EOS, we next consider which shocks on the connected branch of the Hugoniot locus should be admissible. From the Bethe-Weyl theorem, the expansive branch of the Hugoniot locus is entropy decreasing and unphysical. In addition, an entropy decreasing shock is unstable. To see this, consider a perturbation in which an expansive shock wave is given a smooth profile. Because the characteristics along the profile diverge, the profile spreads out and evolves into a rarefaction wave. In contrast, a compressive shock is entropy increasing and stable. If a perturbation gave a compressive shock a smooth profile then the convergence of the characteristics would cause the profile to steepen and the shock to reform. Moreover, by corollary 4.4, entropy increasing shocks satisfy the characteristic criterion and are 1-D stable. Similarly, an expansive rarefaction is stable and a compressive rarefaction evolves into a shock wave. Therefore, for a convex EOS, the locus of stable scale invariant waves connected to a given initial state consists of shock waves in compression and rarefaction waves in expansion. Consequently, the expansive entropy decreasing shocks and the compressive simple waves must be excluded from the wave curve.

Asymptotic properties of the wave curve are required for the existence of a solution to the Riemann problem. By the Bethe-Weyl theorem, for a convex EOS, the Hugoniot locus can be parameterized by S. As a consequence, strong shock waves have the necessary asymptotic properties.

Lemma 4.6: Consider an asymptotically regular EOS. Suppose the connected branch of a Hugoniot locus extends to $S \to \infty$. Then for sufficiently large S, the projection of the Hugoniot locus in the u–P plane extends to $P = \infty$ and $u = \pm\infty$; $+$ for right facing wave and $-$ for left facing.

Proof: Let the Hugoniot locus be based on the state (V_0, S_0). From the proof of the Bethe-Weyl theorem, for $S > S_0$ there is at least one compressive shock. Let us denote by $P_h(S)$ the minimum P of a compressive shock with entropy S. Since the shock is compressive, $P_h(S) > P(V_0, S)$. For an asymptotically regular EOS, $P(V_0, S) \to \infty$ as $S \to \infty$. Hence $P_h(S) \to \infty$ as $S \to \infty$.

Similarly, $E_h(S) > E(V_0, S) \to \infty$ as $S \to \infty$. From Ex. 2.6 C, the equation

$$\Delta E = \tfrac{1}{2} (\Delta u)^2 + P_0 (V_0 - V_1) \ . \tag{2E.7}$$

can be derived from the Hugoniot jump conditions. Therefore, $|u_h(S)| \to \infty$ as $S \to \infty$.

⊠ ⊠

The results up to this point completely determine the wave curve for a convex EOS. They can be summarized as follows.

Theorem 4.7: For an asymptotically regular convex EOS satisfying either condition $-2 \leq \Gamma$ or $\Gamma \leq 2\gamma$ everywhere, the wave curve based on any state consists of compressive shock waves and expansive rarefaction waves. Moreover, the wave curve satisfies the asymptotic properties that ensure the existence of a solution to any Riemann problem.

The monotonicity conditions on the wave curve needed for uniqueness of a solution to the Riemann problem are analyzed in the next subsection.

The first step in generalizing to a non-convex EOS is to find conditions such that any Hugoniot locus consists of a single connected branch. It is instructive to view the convex case from an alternative perspective. The Bethe-Weyl theorem implies that the initial state is the only sonic point on the Hugoniot locus. From Eq. (4.3), if a point on the Hugoniot locus is not sonic then $\partial_V h|_S \neq 0$. It follows from the implicit value theorem that the Hugoniot locus can locally be parameterized by S. Because there is a unique point on the Hugoniot locus for each S, the Hugoniot locus can globally be parameterized by S. The key to generalizing this line of reasoning is to analyze the bifurcation points of the Hugoniot locus.

The Hugoniot locus is the zero level set of the Hugoniot function. By the implicit value theorem, the Hugoniot locus is locally a curve in phase space, except at bifurcation points where the coefficients of both differentials of the Hugoniot function vanish. Hence, from Eq. (4.3), the Hugoniot locus bifurcates if and only if

$$-\frac{V}{P} \cdot \frac{\Delta P}{\Delta V} = \gamma = \tfrac{1}{2} \Gamma \frac{\Delta P}{P} \ . \tag{4.9}$$

In particular, from Eq. (4.8), at a bifurcation point the flow behind the shock must be sonic. We note that the connected branch of the Hugoniot locus is sonic at the initial state but that the initial state is not a bifurcation point because $\partial_S h(V_0, S_0) = \partial_S \tilde{h}(P_0, S_0) = T > 0$.

Two conditions on an EOS can be used to exclude any bifurcation point from the Hugoniot locus. From Eq. (4.3b), if $\Gamma \leq 2\gamma$ then for pressure increasing shock waves $0 < \Delta P/P < 1$ and

$$\left.\frac{\partial \tilde{h}}{\partial S}\right|_P = \left(1 - \frac{\Gamma}{2\gamma} \cdot \frac{\Delta P}{P}\right) T > 0 \ .$$

Hence the condition $\Gamma \leq 2\gamma$ excludes bifurcation points with $P > P_0$. Moreover, the implicit value theorem implies the Hugoniot locus can locally be parameterized by P and hence there can be no local pressure extremum on the Hugoniot locus with $P > P_0$.

Similarly, from Eq. (4.3a), if $-2 \leq \Gamma$ then for expansive shock waves $0 < \Delta V/V < 1$ and

$$\left.\frac{\partial h}{\partial S}\right|_V = \left(1 + \tfrac{1}{2}\,\Gamma \frac{\Delta V}{V}\right) T > 0 \ .$$

Hence the condition $-2 \leq \Gamma$ excludes bifurcation points with $V > V_0$. Moreover, the implicit value theorem implies the Hugoniot locus can locally be parameterized by V and hence there can be no local specific volume extremum on the Hugoniot locus with $V > V_0$.

The zero isotherm provides the following boundary condition.

Lemma 4.8: Suppose an EOS is asymptotically regular. For any state (V_0, S_0) with $T_0 > 0$, there is a unique shock on the zero isotherm. The shock on the zero isotherm has specific volume $V_* > V_0$. Moreover, the Hugoniot function restricted to the zero isotherm is negative for $V < V_*$ and positive for $V > V_*$.

Proof: There are two cases to consider. Suppose the zero isotherm corresponds to the zero isentrope. Then the zero isentrope is convex. The restricted Hugoniot function along $S = 0$ corresponds to the case of the Bethe-Weyl theorem shown in Fig. 4.1 B. Hence there is unique expansive shock. The other possibility allowed by (EOS–5) is that the zero

isotherm corresponds to the union of the lines $V = 0$ and $P = 0$, and that $E = E_{\min}$ along the zero isotherm. Along $V = 0$, the Hugoniot function is

$$h = E_{\min} - E_0 - \tfrac{1}{2}\,(P + P_0) \cdot V_0 < 0 \ .$$

Hence there can be no shock with $V = 0$. Along $P = 0$, the Hugoniot function is

$$h = E_{\min} - E_0 - \tfrac{1}{2}\,P_0 \cdot (V_0 - V) \ .$$

Hence, there is a unique shock and its specific volume is given by $V_* = 2\,(E_0 - E_{\min})/P_0$. Since the Hugoniot function restricted to the zero isotherm has only one zero, to be compatible with the asymptotics as $P \to \infty$ it must be negative for $V < V_*$, and as $P \to 0$ it must be positive for $V > V_*$.

⊠ ⊠

Excluding bifurcation points on the Hugoniot locus leads to the following result.

Theorem 4.9: Suppose an EOS is asymptotically regular and $-2 \le \Gamma \le 2\gamma$ is satisfied everywhere. Then the Hugoniot locus based on any state consists of a single curve connected to the initial base state. Moreover, the compressive branch can be parameterized by P and extends upto $P = \infty$, while the expansive branch can be parameterized by V and extends down to the zero isotherm.

Proof: Let the subscript 0 denote the base state of the Hugoniot locus. We first consider the quadrant $\Delta P > 0$, $\Delta V < 0$ and show that the Hugoniot locus can be parameterized by P. It follows from the condition $\Gamma \le 2\gamma$ that $\partial_S \tilde{h}|_P > 0$ for $P \ge P_0$. Since (P, S) parameterizes thermodynamic phase space, there can be at most one point on the Hugoniot locus for any $P_1 \ge P_0$. By lemma 4.8, $h_{T=0}(P_1) < 0$ for $P_1 > P_0$. By (EOS–2), for any $P_1 > P_0$ there is a $S_1 > S_0$ such that $P_1 = P(V_0, S_1)$. Therefore,

$$\tilde{h}(P_1, S_1) = h(V_0, S_1) = \int_{S_0}^{S_1} T dS > 0 \ .$$

By continuity there must be an S' such that $\tilde{h}(P_1, S') = 0$. Hence there is a unique shock for every $P_1 > P_0$. Since $\partial_S \tilde{h}|_P > 0$, the implicit value theorem implies that any portion

of the Hugoniot locus can locally be parameterized by P. Because there is a unique shock for each $P > P_0$, the connected branch of the shock Hugoniot extends upto $P = \infty$.

We next consider the quadrant $\Delta P < 0$, $\Delta V > 0$ and show that the Hugoniot locus can be parameterized by V. It follows from the condition $-2 \leq \Gamma$ that $\partial_S h|_V > 0$ for $V > V_0$. Since (V, S) parameterizes thermodynamic phase space, there can be at most one point on the Hugoniot locus for any $V \geq V_0$. By lemma 4.8, there is a $V_* > V_0$ on the zero isotherm such that the restriction of the Hugoniot function to the zero isotherm is positive for $V > V_*$ and negative for $V < V_*$. Since the Hugoniot function increases above the zero isotherm, there are no shocks with $V > V_*$. By (EOS–4), for any $V_1 > V_0$ there is a S_1 such that $V_1 = V(P_0, S_1)$. Therefore,

$$h(V_1, S_1) = \tilde{h}(P_0, S_1) = \int_{S_0}^{S_1} T dS > 0 \ .$$

Hence there is a unique shock for any $V_0 < V \leq V_*$. Since $\partial_S h|_V > 0$, the implicit value theorem implies that any portion of the Hugoniot locus can locally be parameterized by V. Because there is a unique shock for each $V_0 < V \leq V_*$, the connected branch of the shock Hugoniot extends down to the zero isotherm at V_*.

⊠ ⊠

From theorem 4.9, $P \to \infty$ on the compressive branch of the Hugoniot locus. This implies the shock speed goes to infinity since

$$\begin{aligned} \Big[\rho_0(u_s - u_0)\Big]^2 &= \frac{P - P_0}{V_0 - V} \\ &> (P - P_0)/V_0 \to \infty \quad \text{as} \quad P \to \infty \ . \end{aligned}$$

With a similar argument we can obtain the following result for a convex isentrope.

Lemma 4.10.1: Suppose the initial state lies on a convex isentrope. If $\Gamma \leq 2\gamma$ is satisfied everywhere then a pressure increasing shock is entropy increasing, and if $-2 \leq \Gamma$ is satisfied everywhere then an expansive shock is entropy decreasing.

Proof: From the proof of the Bethe-Weyl theorem, the Hugoniot function restricted to the isentrope S_0 satisfies:

$$\tilde{h}(P, S_0) < 0 \ , \quad \text{for} \quad P > P_0;$$
$$h(V, S_0) > 0 \ , \quad \text{for} \quad V > V_0.$$

When $\Gamma \leq 2\gamma$, if $P > P_0$ then $\partial_S \tilde{h} > 0$. Hence, for $P > P_0$ the Hugoniot function $\tilde{h}(P, S)$ can only be zero for $S > S_0$. Similarly, when $-2 \leq \Gamma$, if $V > V_0$ then $\partial_S h > 0$ and the Hugoniot function $h(V, S)$ can only be zero for $S < S_0$.

⊠ ⊠

We can also derive a general result on the asymptotic behavior of the Hugoniot locus.

Lemma 4.10.2: Suppose an EOS is asymptotically regular and $\Gamma \leq 2\gamma$ is satisfied everywhere. Then the compressive branch of the Hugoniot locus has the asymptotic property

$$\liminf_{P \to \infty} S_h(P) = \infty \ .$$

Proof: By theorem 4.9 the compressive branch of the Hugoniot locus can be parameterized by P. From the proof of the Bethe-Weyl theorem, for a given $S_1 > S_0$ the restricted Hugoniot function satisfies $\lim_{P \to \infty} \tilde{h}_{S_1}(P) = -\infty$. Hence, there is a P_1 such that $\tilde{h}(P, S_1) < 0$ for $P > P_1$. When $\Gamma \leq 2\gamma$, $\partial_S \tilde{h} > 0$ for $P > P_0$. Hence, $S_h(P) > S_1$ for $P > P_1$. Therefore, $\liminf_{P \to \infty} S_h(P) = \infty$.

⊠ ⊠

We note that lemmas 4.10.2 and 4.6 imply that $|u| \to \infty$ as $P \to \infty$.

For a non-convex EOS, sonic points can occur on the Hugoniot locus. A sonic shock can be joined with a rarefaction to give a scale invariant composite wave. It turns out that the composite waves are necessary for constructing the wave curve. We next show that a sonic shock corresponds to a local entropy extremum on the Hugoniot locus.

Lemma 4.11: On the Hugoniot locus, at a local entropy extremum

$$-\frac{\Delta P}{\Delta V} = \frac{\gamma P}{V} = -\left.\frac{dP}{dV}\right|_h \ . \tag{4.10}$$

Moreover, the flow is sonic relative to the shock front; *i.e.*,

$$|\sigma - u| = c \ . \tag{4.11}$$

Proof: From Eq. (4.3), at an entropy extremum $\gamma P/V = -\Delta P/\Delta V$. By Eq. (4.8) the flow is sonic. In addition, from Eq. (4.2), at an entropy extremum $dP/dV|_h = \Delta P/\Delta V$. Together these two conditions give Eq. (4.10).

⊠ ⊠

The converse of the previous lemma requires additional restrictions on Γ.

Lemma 4.12: An entropy extremum occurs on the Hugoniot locus if any of the following conditions are satisfied:

$$|\sigma - u| = c \ \text{ or } \begin{array}{ll} \dfrac{\Delta P}{\Delta V} = \left.\dfrac{dP}{dV}\right|_h & ; \\ \dfrac{\gamma P}{V} = -\dfrac{\Delta P}{\Delta V} & \text{and} \quad \Gamma \neq -2\dfrac{V}{\Delta V} \ \text{ or } \ \Gamma \neq 2\gamma\dfrac{P}{\Delta P} \ ; \\ \dfrac{\gamma P}{V} = -\left.\dfrac{dP}{dV}\right|_h & \text{and} \quad \Gamma \neq 0 \ . \end{array}$$

Proof: The first condition follows from Eq. (4.2) and the second condition from Eqs. (4.8) and (4.3). From the thermodynamic relation $V dP = -\gamma P dV + \Gamma T dS$, we obtain

$$\left.\frac{dP}{dV}\right|_h = -\frac{\gamma P}{V} + \Gamma T \left.\frac{dS}{dV}\right|_h \ ,$$

and the third condition follows.

⊠ ⊠

From these lemmas and Eq. (4.9), the Hugoniot locus can be parameterized by V or P in a neighborhood of a sonic point that is not a bifurcation point. This observation allows us to generalize the previous two lemmas. The following generalization will enable us to define a convenient parameterization of the shock Hugoniot and will play a crucial role in determining the wave curve for a non-convex EOS.

Theorem 4.13 (Bethe-Wendroff)**:** Suppose the EOS is asymptotically regular and $-2 \leq \Gamma \leq 2\gamma$ is satisfied everywhere. For any sonic point on the Hugoniot locus, other than the initial state, the following are equivalent: (a) $(\sigma - u)^2 = c^2$; (b) $d\sigma/dV = 0$; (c) $dS/dV = 0$. Moreover, $(\sigma - u)^2 - c^2$, $d\sigma/dV$, and dS/dV vanish to the same order, and the Hugoniot locus is tangent to the rarefaction curve.

Proof: By theorem 4.9, the Hugoniot locus consists of a single curve connected to the initial state. Moreover, there are no bifurcation points on the Hugoniot locus. Conditions (a) and (c) follow from lemmas 4.11 and 4.12.

We recall that the wave speed is given by

$$\left[\rho_0 \cdot (\sigma - u_0)\right]^2 = -\Delta P/\Delta V \ , \tag{2.19}$$

and the particle velocity is given by

$$(\Delta u)^2 = -(\Delta P) \cdot (\Delta V) \ . \tag{2.23}$$

Taking the derivative along the Hugoniot of Eq. (2.19), we find

$$\rho_0^2 \cdot (\sigma - u_0) \cdot \frac{d\sigma}{dV} = \Big(-\frac{dP_h}{dV} + \frac{\Delta P}{\Delta V}\Big)/\Delta V \ .$$

By lemma 4.1, away from the initial state $\Delta V \neq 0$ and $\Delta P \neq 0$. From lemmas 4.11 and 4.12 at a sonic point

$$-dP_h/dV + \Delta P/\Delta V = 0 \ .$$

Therefore, $d\sigma/dV = 0$ and condition (b) is satisfied.

Taking the derivative along the Hugoniot of Eq. (2.23), we find

$$\frac{du_h}{dV} = -\tfrac{1}{2}\,\frac{\Delta V}{\Delta u} \cdot \Big(\frac{dP_h}{dV} + \frac{\Delta P}{\Delta V}\Big) \ .$$

At a sonic point, by lemma 4.11 this reduces to

$$\frac{du_h}{dV} = \pm\Big(-\frac{\Delta P}{\Delta V}\Big)^{\frac{1}{2}} = \pm\rho c \ .$$

From the thermodynamic relation $dE = -P\,dV + T\,dS$, at a sonic point $dE_h/dV = -P_h$ because $dS_h/dV = 0$. Comparing with Eq. (2.13) we find that the Hugoniot locus at a sonic point is tangent to the rarefaction curve.

To show that the specified quantities vanish to the same order, following lemma 2.3 we take repeated derivatives of the Hugoniot function until the first non-vanishing derivative of S is obtained. The first derivative, Eq. (2.27), gives one of the conditions for a sonic point in lemmas 4.11 and 4.12. The second derivative, Eq. (2.28), at a sonic point reduces to

$$2\,T\,\frac{d^2 S_h}{dV^2} = -\Delta V \cdot \frac{d^2 P_h}{dV^2} \ .$$

If the second derivative vanishes then the third derivative, Eq. (2.29), reduces to

$$2\,T\,\frac{d^3 S_h}{dV^3} = -\Delta V \cdot \frac{d^3 P_h}{dV^3} \ .$$

By induction, it can be shown that

Lemma 4.13.1: At a sonic point on the Hugoniot locus, the first non-vanishing derivative of S_h with respect to V is equal to $-\frac{1}{2}\,\Delta V/T$ times the corresponding derivative of P_h.

From the thermodynamic relation, $V\,dP = -\gamma\,P\,dV + \Gamma\,T\,dS$, we obtain

$$\left.\frac{\partial P}{\partial V}\right|_S = V\,\frac{dP_h}{dV} - \Gamma\,T\,\frac{dS_h}{dV} \ .$$

Taking the derivative along the Hugoniot locus, using the relation

$$\frac{d}{dV} = \frac{\partial}{\partial V} + \frac{dS_h}{dV}\cdot\frac{\partial}{\partial S} \ .$$

yields at a sonic point

$$\begin{aligned}\left.\frac{\partial^2 P}{\partial V^2}\right|_S &= V\,\frac{d^2 P_h}{dV^2} - \Gamma\,T\,\frac{d^2 S_h}{dV^2} \\ &= V\cdot\Big(1 + \tfrac{1}{2}\,\Gamma\,\frac{\Delta V}{V}\Big)\frac{d^2 P_h}{dV^2} \ .\end{aligned}$$

We note that the factor $V\cdot(1+\frac{1}{2}\,\Gamma\,\Delta V/V)$ is non-zero when the sonic point is not a bifurcation point. Again by induction, it can be shown that

Lemma 4.13.2: At a sonic point on the Hugoniot locus, the first non-vanishing partial derivative of P with respect to V at fixed S is equal to $V \cdot (1 + \frac{1}{2}\Gamma \Delta V/V)$ times the corresponding derivative along the Hugoniot locus of P_h with respect to V.

Let n be the power of the lowest non-vanishing derivative of P_h; *i.e.*, $(d/V)^n P_h \neq 0$. At a sonic point, $n \geq 2$. From lemma 4.13.1, n is the smallest power such that $(d/dV)^n S_h \neq 0$. By taking repeated derivatives of Eq. (2.19), it follows that n is the smallest power such that $(d/dV)^n \sigma \neq 0$. Similarly, by taking repeated derivatives of Eq. (4.8), it follows that $n-1$ is the smallest power such that $(d/dV)^{n-1}\left[(\sigma-u)^2 - c^2\right] \neq 0$. Therefore, $(\sigma-u)^2 - c^2$, $d\sigma/dV$, and dS/dV vanish to the same order.

⊠ ⊠

We note that the Bethe-Wendroff theorem can be extended to any hyperbolic system of conservation laws. For a proof in the general case see [Wendroff, 1972], [Menikoff & Plohr, 1989, Appendix B] or [Isaacson, Marchesin, Palmeira & Plohr, 1992].

Locally the Hugoniot locus can be parameterized by a single variable which we denote by α. Let the dimensionless parameter α be determined by the relation

$$\begin{aligned} T\,dS &= -\tfrac{1}{2}\frac{\Delta V}{V}\left[\gamma + \frac{V}{P}\frac{\Delta P}{\Delta V}\right] PV\,d\alpha \\ &= -\tfrac{1}{2}\frac{\Delta V}{V}\left[c^2 - (\sigma-u)^2\right] d\alpha\ . \end{aligned} \tag{4.12}$$

At the initial state, both ΔV and $c^2 - (\sigma-u)^2$ vanish. This is compatible with the weak shock limit; *i.e.*, the entropy is third order in shock strength, Eq. (3.16). Away from the initial state, from the Bethe-Wendroff theorem, at a local entropy extremum dS and $c^2 - (\sigma-u)^2$ vanish to the same order. Therefore, the connected branch of the Hugoniot locus is a single valued function of α; *i.e.*, α varies monotonically even when the entropy has a local extremum.

On the Hugoniot locus, the differential of all the variables can be related to the parameter α. From Eqs. (4.3), (2.19) and (2.23) we obtain the following (m, σ and u for a right facing wave):

$$dm = \rho_0 \, d\sigma = \frac{1}{2\,V\,\Delta P}\left[c^2 - (\sigma - u)^2\right] \, m \, d\alpha \ , \tag{4.13}$$

$$dV = -\left[1 + \tfrac{1}{2}\Gamma\frac{\Delta V}{V}\right] \, V \, d\alpha \ , \tag{4.14}$$

$$dE = \left[\frac{\overline{P}}{P} - \tfrac{1}{2}(\gamma - \Gamma)\frac{\Delta V}{V}\right] \, PV \, d\alpha \ , \tag{4.15}$$

$$dP = \left[\gamma - \tfrac{1}{2}\Gamma\frac{\Delta P}{P}\right] \, P \, d\alpha \ , \tag{4.16}$$

$$du = \tfrac{1}{2}\left[\gamma - \Gamma\frac{\Delta P}{P} - \frac{V}{P}\frac{\Delta P}{\Delta V}\right] \, \frac{P}{m} \, d\alpha \ . \tag{4.17}$$

We may choose $\alpha = 0$ to correspond to the initial state (V_0, S_0, u_0). Then from Eqs. (4.14) and (4.16), $\alpha > 0$ corresponds to pressure increasing compressive shocks (the quadrant $\Delta P > 0$, $\Delta V < 0$), while $\alpha < 0$ corresponds to pressure decreasing expansive shocks (the quadrant $\Delta P < 0$, $\Delta V > 0$).

Remark 4.14: Given an incomplete EOS, $P = P(V, E)$, the Hugoniot locus can be determined parametrically by integrating a pair of ODEs, Eqs. (4.14) and (4.15). There are several drawbacks with this approach. First, errors can accumulate from the numerical integration. This could be corrected by using the solution of the ODEs as the initial guess for an iterative solver of a zero of the Hugoniot function. Second, the functions to be integrated depend on γ and Γ, and hence on derivatives of the EOS. For some model EOS, it is not easy or expensive to compute these derivatives accurately. Third, for a single point point on the Hugoniot locus with a given value of a quantity such as P or u, it is computationally expensive to perform the numerical integration.

The differential relations, Eqs. (4.12)–(4.17), can be used to determine derivatives of the state variables along the Hugoniot locus. One example is the slope of the Hugoniot locus in the V–P plane

$$-\frac{V}{P}\left(\frac{dP}{dV}\right)_h = \frac{\gamma - \frac{1}{2}\Gamma\Delta P/P}{1 + \frac{1}{2}\Gamma\Delta V/V} \ . \tag{4.18}$$

This implies that Γ can be determined from measurements of both the sound speed and the shock Hugoniot. In addition, it can be used to determine the asymptotic compression ratio of a strong shock.

Proposition 4.14.1: Suppose an EOS is asymptotically regular and $\Gamma \leq 2\gamma$ is satisfied everywhere. Then as $P \to \infty$, the compression ratio of a shock $V_0/V_h(P)$ approaches a constant.

Proof: By theorem 4.9 the compressive branch of the Hugoniot locus can be parameterized by P. Since $0 < V_h(P) < V_0$, we can define $V_1 = \liminf_{P\to\infty} V_h(P)$ and $V_2 = \limsup_{P\to\infty} V_h(P)$. We need to show that $V_1 = V_2$. If $V_1 < V_2$ then there is a V_* such that $V_1 < V_* < V_2$. Let $P_n > P_0$ be the ascending sequence such that $V_h(P_n) = V_*$. Then $dV_h/dP(P_n)$ must alternate in sign; *i.e.*, proportional to $(-1)^n$. Because $\Gamma \leq 2\gamma$, from Eq. 4.18 with $P > P_0$ the sign of dV_h/dP is minus the sign of $1 + \frac{1}{2}\Gamma\Delta V/V$. From the asymptotic condition (EOS–3), as $P_n \to \infty$

$$1 + \tfrac{1}{2}\Gamma\Delta V/V \to 1 - \tfrac{1}{2}\tilde{\Gamma}_\infty(V_0 - V_*)/V_* \ .$$

If the right hand side is not zero then for sufficiently large P the Hugoniot locus can not cross V_*. Therefore, consistency requires that $1 - \frac{1}{2}\tilde{\Gamma}_\infty(V_0 - V_*)/V_* = 0$ and it follows that

$$\lim_{P\to\infty} \frac{V_0}{V_h(P)} = 1 + \frac{2}{\tilde{\Gamma}_\infty} \ . \tag{4.19}$$

We note, in terms of $\tilde{\gamma}_\infty = \tilde{\Gamma}_\infty + 1$ Eq. (4.19) corresponds to the limiting compression ratio for an ideal gas EOS; $\rho_h/\rho_0 \to (\tilde{\gamma}_\infty + 1)/(\tilde{\gamma}_\infty - 1)$.

⊠ ⊠

We also note that the limiting compression ratio and mass conservation implies in the limit of strong shocks, $u_s/u \to (\tilde{\Gamma}_\infty + 2)/2$.

Remark 4.14.2: The EOS is a function of two variables and that limits can depend on the direction a curve approaches infinity. In particular, along the Hugoniot locus as $P \to \infty$ it follows from the Hugoniot equation that $E_h(P)/(V_0P) \to (\tilde{\Gamma}_\infty + 1)/(\tilde{\Gamma}_\infty + 2) > 0$. In contrast, the asymptotic condition (EOS–1) implies that along an isentrope $E/P \to 0$.

Other important relations can easily be derived from the differential relations. For example, combining Eqs. (4.12) and (4.13) we obtain

$$(-\Delta P \cdot \Delta V)^{\frac{1}{2}} \cdot (-\Delta V/V_0)\, d\sigma = \tfrac{1}{2}\,(\Delta V)^2\, d(m^2) = T\, dS\ . \tag{4.20}$$

We note that $d\sigma$ is proportional to dm. In fact, $dm = \rho_0 d\sigma$. This is not surprising since the mass flux is the Lagrangian wave speed. Furthermore both the mass flux and the wave speed are monotonic if and only if the entropy is monotonic.

4.2 Monotonicity of Hugoniot Locus

The parameteriztion of the Hugoniot locus, which we derived in the previous section, can be used to relate constraints on an EOS to monotonicity properties of the Hugoniot locus. We consider only the connected branch of the Hugoniot locus. It will turn out that the needed monotonicity conditions will imply that the Hugoniot locus is indeed a single connected branch. Since we are not considering reactions, for simplicity we may assume the origin of E has been chosen such that $E_{\min} = 0$.

We begin by analyzing compressive shock waves. From the Hugoniot Eq. (2.22) and (EOS–2) we obtain a bound on ΔV

$$0 < -\Delta V = \Delta E/\overline{P} < 2E/P\ . \tag{4.21}$$

This leads to the following monotonicity relations:

1. **Convex EOS**, $\mathcal{G} > 0$.

   From the Bethe-Weyl theorem, entropy is monotonic. Moreover, by corollary 4.4, the characteristic condition, Eq. (2.36), is satisfied and compressive shock waves are stable in one-dimension. Furthermore, from Eq.(4.20), mass flux and wave speed are monotonic.

2. **Strong condition**, $\Gamma \le PV/E$.

   From Eq. (4.14), the specific volume is monotonic if and only if

$$1 + \tfrac{1}{2}\,\Gamma \frac{\Delta V}{V} > 0\ .$$

From Eq. (4.21) we have

$$1 + \tfrac{1}{2}\,\Gamma \frac{\Delta V}{V} > \begin{cases} 1 - \Gamma \frac{E}{PV} \ , & \text{if } \Gamma \geq 0 \ ; \\ 1 \ , & \text{if } \Gamma < 0 \ . \end{cases}$$

Therefore, the strong condition is sufficient for monotonicity of V. The form of the wave curve, projected in the V–P and u–P planes, is shown in Fig. 4.2A.

3. **Medium condition**, $\Gamma \leq \gamma + \frac{1}{2} PV/E$.

From Eq. (4.15), the specific energy is monotonic if and only if

$$\frac{\overline{P}}{P} - \tfrac{1}{2}\,(\gamma - \Gamma) \frac{\Delta V}{V} > 0 \ .$$

From Eq. (4.21) and $\overline{P}/P > \frac{1}{2}$, we have

$$\frac{\overline{P}}{P} - \tfrac{1}{2}\,(\gamma - \Gamma) \frac{\Delta V}{V} > \begin{cases} \frac{1}{2} + (\gamma - \Gamma) \frac{E}{PV} \ , & \text{if } \Gamma > \gamma \ ; \\ \frac{1}{2} \ , & \text{if } \Gamma < \gamma \ . \end{cases}$$

Therefore, the medium condition is sufficient for monotonicity of E.

From Eq. (4.17), the particle velocity is monotonic if and only if

$$\gamma - \Gamma \frac{\Delta P}{P} - \frac{V}{P} \frac{\Delta P}{\Delta V} > 0 \ .$$

From Eq. (4.21) and $0 < \Delta P/P < 1$, we have

$$\gamma - \Gamma \frac{\Delta P}{P} - \frac{V}{P} \frac{\Delta P}{\Delta V} > \frac{\Delta P}{P} \cdot \left(\gamma + \tfrac{1}{2} \frac{PV}{E} - \Gamma \right) .$$

Therefore, the medium condition is sufficient for monotonicity of both E and u. The form of the wave curve, projected in the V–P and u–P planes, is shown in Fig. 4.2B.

4. **Weak condition**, $\Gamma \leq 2\gamma$.

From Eq. (4.16), the pressure is monotonic if and only if

$$\gamma - \tfrac{1}{2}\,\Gamma\, \Delta P/P > 0 \ .$$

From $0 < \Delta P/P < 1$, we have

$$\gamma - \tfrac{1}{2}\,\Gamma\, \Delta P/P > \begin{cases} \gamma - \frac{1}{2}\,\Gamma \ , & \text{if } \Gamma \geq 0 \ ; \\ \gamma \ , & \text{if } \Gamma < 0 \ . \end{cases}$$

Therefore, the weak condition is sufficient for monotonicity of P. The form of the wave curve, projected in the V–P and u–P planes, is shown in Fig. 4.2C. Theorem 4.9 shows that the weak condition also implies that all compressives shocks lie on the connected branch of the Hugoniot locus.

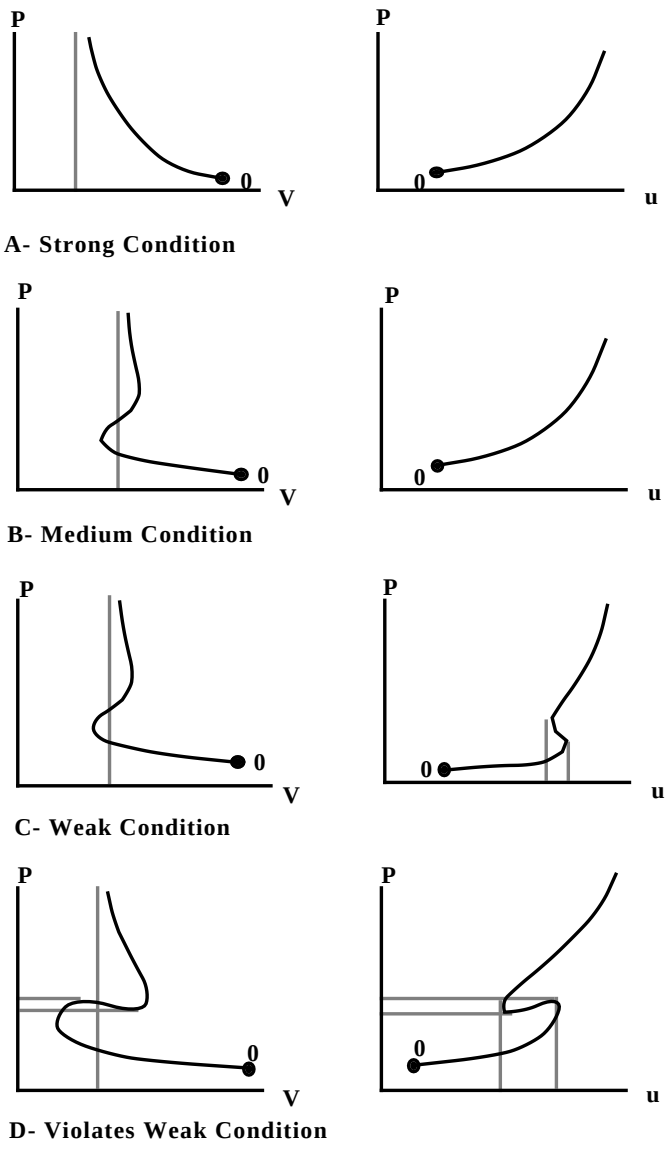

FIGURE 4.2

Form of Hugoniot locus in V–P plane and u–P plane.

The weak and medium conditions were identified in [Smith, 1979], and the strong condition in [Menikoff & Plohr, 1989]. To show that these conditions are related as the names imply we need the following result:

Lemma 4.15 (Smith)**:** Suppose a convex EOS satisfies (EOS–2). If $E_{\min} \geq 0$, then $\gamma > \frac{1}{2}PV/E$ is satisfied everywhere.

Proof: Along an isentrope, the specific energy can be expressed as

$$\begin{aligned} E(V,S) &= E(V_1,S) + \int_V^{V_1} P(V',S)\,dV' \\ &> \int_V^{\infty} P(V',S)\,dV' \\ &> \tfrac{1}{2}P(V,S)\cdot\frac{P(V,S)}{-\partial P/\partial V|_S} = \frac{P\,V}{2\gamma}\ . \end{aligned}$$

The first inequality follows from $E(V,S) \geq E_{\min}$. The second inequality is a consequence of the convexity of the isentrope; the integral is less than the area of a triangle formed by the tangent to the isentrope.

⊠ ⊠

It then follows that

Corollary 4.16: For a convex EOS satisfying (EOS–2) with $E_{\min} \geq 0$, the strong condition implies the medium condition implies the weak condition.

When the strong, medium or weak conditions are satisfied everywhere in thermodynamic state space, the monotonicity properties are global, *i.e.*, everywhere along the Hugoniot locus for any initial state. In this sense, they are sufficient conditions for monotonicity. They are necessary in the following weak sense. If they are violated at some point in state space, then for an initial state along the backwards Hugoniot as $P_0 \to 0$ the Hugoniot locus will loss monotonicity (provided that the zero isotherm isn't reached first). However, for a sufficiently weak shock, the Hugoniot locus is monotonic even at points for which the EOS conditions are violated. Thus, these simplified EOS conditions do not alway imply loss of monotonicity.

Monotonicity of both P and u are needed in order that the solution to any Riemann problem is unique. From the results upto this point we can conclude

Theorem 4.17: For an asymptotical regular convex EOS with $E_{\min} \geq 0$, the medium condition is sufficient for uniqueness of the Riemann problem. Without $E_{\min} \geq 0$, a slightly stronger **modified medium condition**, $\Gamma \leq \gamma$, would be sufficient for uniqueness of the Riemann problem.

We note one example of non-uniquess when the the medium condition is violated. Suppose the weak condition is true and

$$\partial P/\partial u|_S > -\partial P/\partial u|_h \ . \tag{4.22}$$

Then a single shock can split into two waves; a shock of the same family and either a shock or a rarefaction of the opposite family. The wave diagram and the corresponding wave curves are shown in Fig. 4.3.

An ideal gas provides an example of an EOS that satisfies the strong condition. However, monotonicity of V is not typical. As an example consider air. At room temperature, air is composed mostly of diatomic molecules and its EOS is well approximated by an ideal gas with $\gamma = 7/5$. When shock heating causes dissociation and ionization to occur, γ drops below 1.2. For a strong shock in an ideal gas (Ex. 2.7) the compression ratio is $V_0/V_s = (\gamma+1)/(\gamma-1)$. Thus variations in γ from shock heating can lead to local extremum in V_s. Shocks in air strong enough to cause dissociation and ionization occur in applications involving supersonic aircraft and spacecraft re-entry (hypersonic flow).

The equilibrium EOS of a chemically reacting gas can be determined using the principles of statistical mechanics or thermodynamics; *i.e.*, varying the composition to conserve particles and minimize the Gibbs free energy $G(P,T) = E + PV - TS$; see for example, [Zel'dovich & Raizer, 1966] chpt. III.1 or [Anderson, 1989] chpt. 11. The dissociation of a gas can be treated as an equilibrium mixture of thermally perfect gases for the atoms and molecules. The composition is determined from the law of mass action. Similarly, an ionized gas can be treated as an equilibrium mixture of electrons and ions. In this case,

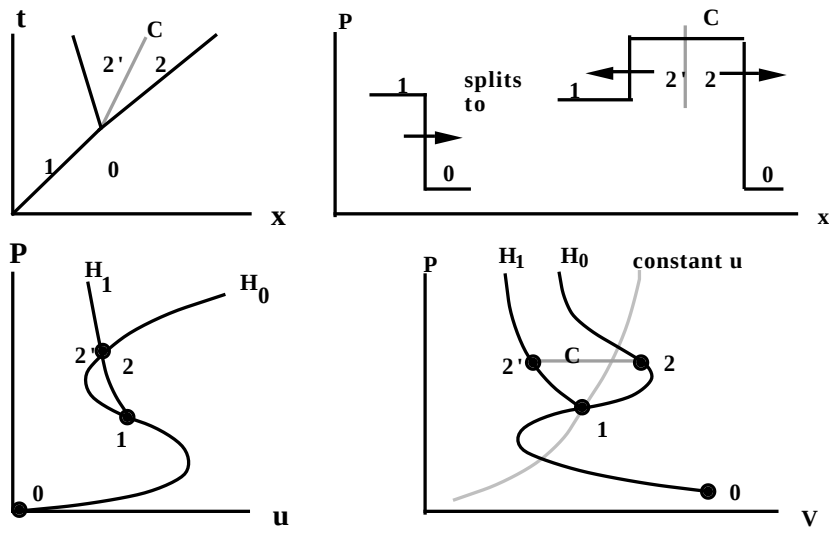

A. Shock splits into 2 shocks

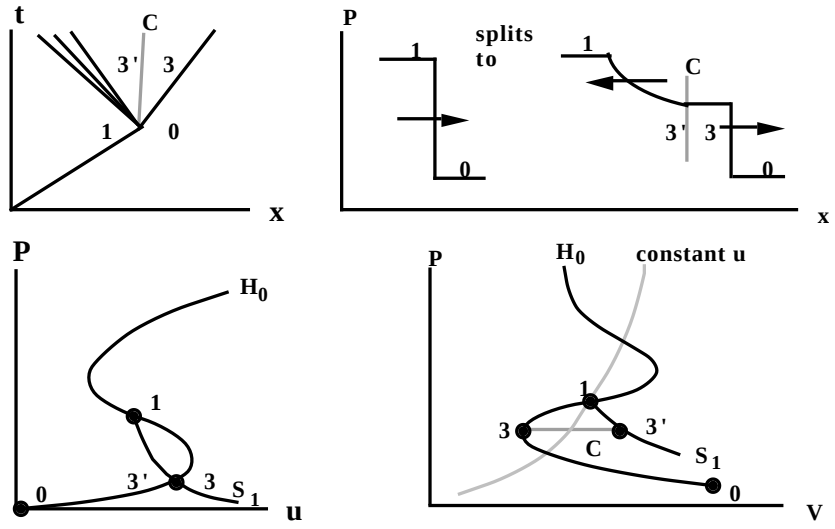

B. Shock splits into shock and rarefaction

FIGURE 4.3

Shock splitting when $\partial P/\partial u|_S > -\partial P/\partial u|_h > 0$.

the law of mass action leads to the Saha equation for the composition. The equilibrium composition and Dalton's law of partial pressures gives a good approximation for the EOS.

It is natural to ask if the medium condition is violated whether the non-uniqueness of the Riemann problem can be resolved. However, instabilities of shock waves raise more serious questions. There are several types of instabilities to consider.

1. 1-D stability.

   The characteristic condition, Eq. (2.35) or Eq. (2.36), is necessary for 1-D stability. As described in Lecture 2, 1-D shock stability is equivalent to having a well behaved interaction between a shock wave and an acoustic wave from either ahead or behind the shock front. For a convex EOS, the Bethe-Weyl theorem implies that compressive shock waves satisfy both the entropy condition and the characteristic criterion. In this case the characteristic condition is sufficient for 1-D stability. For a non-convex EOS we later show that an additional condition is needed.

2. 2-D corrugation stability.

   In shock tube experiments, gases at different pressures are separated with a membrane. It is difficult to break a membrane in a controlled and reproducible manner. Yet after a short distance of travel the shock waves generated are very nearly planar. To understand the stability of a planar shock wave, consider a rippled or corrugated interface. The troughs correspond to diverging waves and the valleys to converging waves. Converging and diverging waves can be analyzed using the 1-D fluid equation with geometric source terms; *i.e.*, cylindrically or spherically symmetric geometry. The speeding up of converging waves and the slowing down of diverging waves tends to stabilize the shock front. The condition for corrugation instability is equivalent to the condition for a shock wave to split into two waves, Eq. (4.22); see *e.g.*, [Fowles, 1993] or [Menikoff & Plohr, 1989, section 6] and reference therein. When the medium condition is satisfied, shock waves are stable to corrugation perturbations.

3. 2-D stability to transverse waves.

   There is another form of 2-D instability in which transverse waves propagate along the shock front. An instability of this form is observed for detonation waves; see [Fickett & Davis, 1979], chapter 7. The conditions for 2-D stability can be expressed as

$$\frac{\Delta P}{m^2} \cdot \frac{dm^2}{dP} > 0 \quad \text{and} \quad \frac{\gamma - (\Gamma+1)\Delta P/P}{\gamma + \Delta P/P} \geq 0 \ ,$$

   see *e.g.*, [Fowles, 1993] or [Menikoff & Plohr, 1989, section 6] and reference therein. For compressive shocks, the first condition implies that entropy increases with pressure. When an EOS satisfies the weak condition, the first condition is equivalent to the characteristic condition. The second condition reduces to [Fowles, 1981]

$$\gamma \geq (\Gamma+1)\Delta P/P \ . \tag{4.23a}$$

   Consequently, a sufficient condition for 2-D stability of a compressive shock is

$$\Gamma \leq \gamma - 1 \ ; \tag{4.23b}$$

   We refer to this as the **stability condition**.

The stability condition is also necessary in the same sense as described for the monotonicity conditions. Weak shocks satisfy Eq. (4.23a). Moreover, the viscous profile of a weak shock is stable, see [Liu, 1986]. The stability condition is related to having a well behaved interaction for an incoming acoustic wave at an angle to the shock front. When the stability condition is violated, the reflection coefficient blows up and an infinitesimal perturbation can generate a finite outgoing wave [Fowles, 1981]. In Lecture 8 on 2-D wave patterns, this is discussed in more detail.

In addition to stability, Eq. (4.23b) implies that the modified medium condition and the weak condition are satisfied. Hence both P and u are monotonic for compressive shocks. Because only compressive shocks occur in the wave curve for a convex EOS, we are led to the important conclusion.

Theorem 4.18: For an asymptotically regular convex EOS, if $\Gamma \leq \gamma - 1$ then every Riemann problem has a unique solution. Moreover, any shock wave in the solution is stable in both 1-D and 2-D.

In fact, Eq. (4.23a), which is both necessary and sufficient for 2-D stability, implies that $dP/d\alpha > 0$ and $du/d\alpha > 0$. Hence, 2-D shock instability would be a problem before the question arises of resolving non-unique solutions of a Riemann problem.

For a non-convex EOS, entropy increasing expansive shocks are need to construct wave curves based on some states. In this case, we will need additional monotonicity properties for the expansive branch of the Hugoniot locus. These properties can be conveniently stated in terms of the parameterization we derived in section 4.1.

Lemma 4.19: Suppose $-2 \leq \Gamma$. Then the expansive branch of the Hugoniot locus has the following properties.

(i) $dV/d\alpha < 0$.

(ii) The state behind the shock is subsonic if and only if $dS/d\alpha < 0$.

(iii) If $dS/d\alpha < 0$ then $dP/d\alpha > 0$ and $du/d\alpha > 0$.

Proof: On the expansive branch of the Hugoniot locus, $\Delta V > 0$.

(i) From Eq. (4.14),

$$dV/d\alpha = -(1 + \tfrac{1}{2}\Gamma \Delta V/V) \cdot V \ .$$

For expansive shocks, $0 \leq \Delta V/V < 1$. When $\Gamma \geq -2$, it follows that $dV/d\alpha < 0$.

(ii) From Eq. (4.12),

$$T dS/d\alpha = -\tfrac{1}{2}(\Delta V/V) \cdot \left[c^2 - (\sigma - u)^2\right] \ .$$

For subsonic flow, $(\sigma - u)^2 < c^2$. Hence, $dS/d\alpha < 0$ if and only if the flow is subsonic. It also follows from Eq. (4.12) that $\gamma + (V/P) \cdot (\Delta P/\Delta V) > 0$ if and only if $dS/d\alpha < 0$.

(iii) From Eq. (4.16), we have

$$\begin{aligned} \frac{1}{P} \cdot \frac{dP}{d\alpha} &= \gamma - \tfrac{1}{2}\Gamma \frac{\Delta P}{P} \\ &= \left(\gamma + \frac{V}{P} \cdot \frac{\Delta P}{\Delta V}\right) - \frac{V}{P} \cdot \frac{\Delta P}{\Delta V} \cdot \left(1 + \tfrac{1}{2}\Gamma \frac{\Delta V}{V}\right) \\ &= \left(\gamma + \frac{V}{P} \cdot \frac{\Delta P}{\Delta V}\right) + \frac{\rho \cdot (\sigma - u)^2}{P} \cdot \left(1 + \tfrac{1}{2}\Gamma \frac{\Delta V}{V}\right) \ . \end{aligned}$$

The first term is positive because of the assumption that $dS/d\alpha < 0$, and the second term is positive because $dV/d\alpha < 0$. Therefore, $dP/d\alpha > 0$.

From Eq. (4.17), we have

$$\begin{aligned}\frac{2m}{P}\cdot\frac{du}{d\alpha} &= \gamma - \Gamma\frac{\Delta P}{P} - \frac{V}{P}\cdot\frac{\Delta P}{\Delta V} \\ &= \left(\gamma + \frac{V}{P}\cdot\frac{\Delta P}{\Delta V}\right) - 2\frac{V}{P}\cdot\frac{\Delta P}{\Delta V}\cdot\left(1 + \tfrac{1}{2}\Gamma\frac{\Delta V}{V}\right) \\ &= \left(\gamma + \frac{V}{P}\cdot\frac{\Delta P}{\Delta V}\right) + \frac{2\rho\cdot(\sigma-u)^2}{P}\cdot\left(1 + \tfrac{1}{2}\Gamma\frac{\Delta V}{V}\right) .\end{aligned}$$

Again each term is positive. Therefore, $du/d\alpha > 0$.

⊠ ⊠

4.3 Wave Curve for Non-Convex EOS

For a non-convex EOS the Hugoniot locus is still well defined. With the condition, $-2 \le \Gamma \le \gamma$, the Hugoniot locus is a single connected curve. Moreover, P and u are monotonic on the compressive branch. However, not all entropy increasing compressive shocks satisfy the characteristic criterion. As a consequence, some shocks are unstable and can not be included in the wave curve. Furthermore, the rarefaction waves only exist upto a point on the isentrope at which $\mathcal{G} = 0$. As a consequence, the rarefaction branch of the wave curve is incomplete. Insufficient waves can give rise to non-existence of a solution to the Riemann problem.

Another complication results from the existence of sonic shocks. This gives rise to additional scale invariant waves that are composites of shock waves and simple waves; either compressive shocks and compressive simple waves, or expansive shocks and rarefaction waves. A composite may consist of (i) a simple wave followed by a shock in which the ahead state is sonic, (ii) a simple wave preceeded by a shock in which the behind state is sonic, (iii) a doubly sonic shock both preceeded and followed by simple waves, or (iv) an alternating sequence of simple waves and doubly sonic shocks possibly starting or ending

with a one sided sonic shock. Typical composites are illustrated in Fig. 4.4.1. Too many waves can give rise to non-uniquess of a solution to the Riemann problem.

In this section, we show that there are just enough stable scale invariant waves for existence and uniqueness of a solution to any Riemann problem. Shock waves that are stable to one-dimensional perturbations must satisfy an extended entropy condition. The E-condition was introduced for scalar hyperbolic equations by Oleĭnik and generalized to hyperbolic systems by [Liu, 1975]. For a right facing wave to satisfy the E-condition, its shock speed must be greater than the speed of any shock that lies on the Hugoniot locus between the initial state and the final state. For the fluid equations, this condition has a simple geometric interpretation in the V–P plane. Let 0 denote the ahead state and 1 denote the behind state. A compressive shock satisfies the E-condition, if and only if the portion of the Hugoniot locus between states 0 and 1 lies below the Rayleigh line (the straight line connecting states 0 and 1). Similarly, an expansive shock satisfies the E-condition if and only if the Hugoniot locus between states 0 and 1 lies above the Rayleigh line.

As a motivation for the E-condition, consider a perturbation in which a compressive shock wave is given a smooth profile. For a non-convex EOS, the characteristic velocity along the profile does not necessarily vary monotonically. Some characteristics converge, steepening a portion of the profile, while other characteristic diverge and spread out a portion of the profile. The converging characteristic lead to the formation of a shock. As the profile evolves, other characteristics impinge on the shock front from behind and increase the shock strength. However, at some point the shock speed may exceed the the characteristic velocity in the remainder of the profile. In this case, the characteristics behind the front can not overtake the shock and a composite forms. As it evolves in time, a composite spreads out and is stable to local perturbations.

The E-condition implies that a shock wave has the property:

$$(u+c)_{\text{behind}} \geq \sigma \geq (u+c)_{\text{ahead}} \ , \quad \text{for right facing wave;} \tag{2.35$'a$}$$

$$(u-c)_{\text{behind}} \leq \sigma \leq (u-c)_{\text{ahead}} \ , \quad \text{for left facing wave.} \tag{2.35$'b$}$$

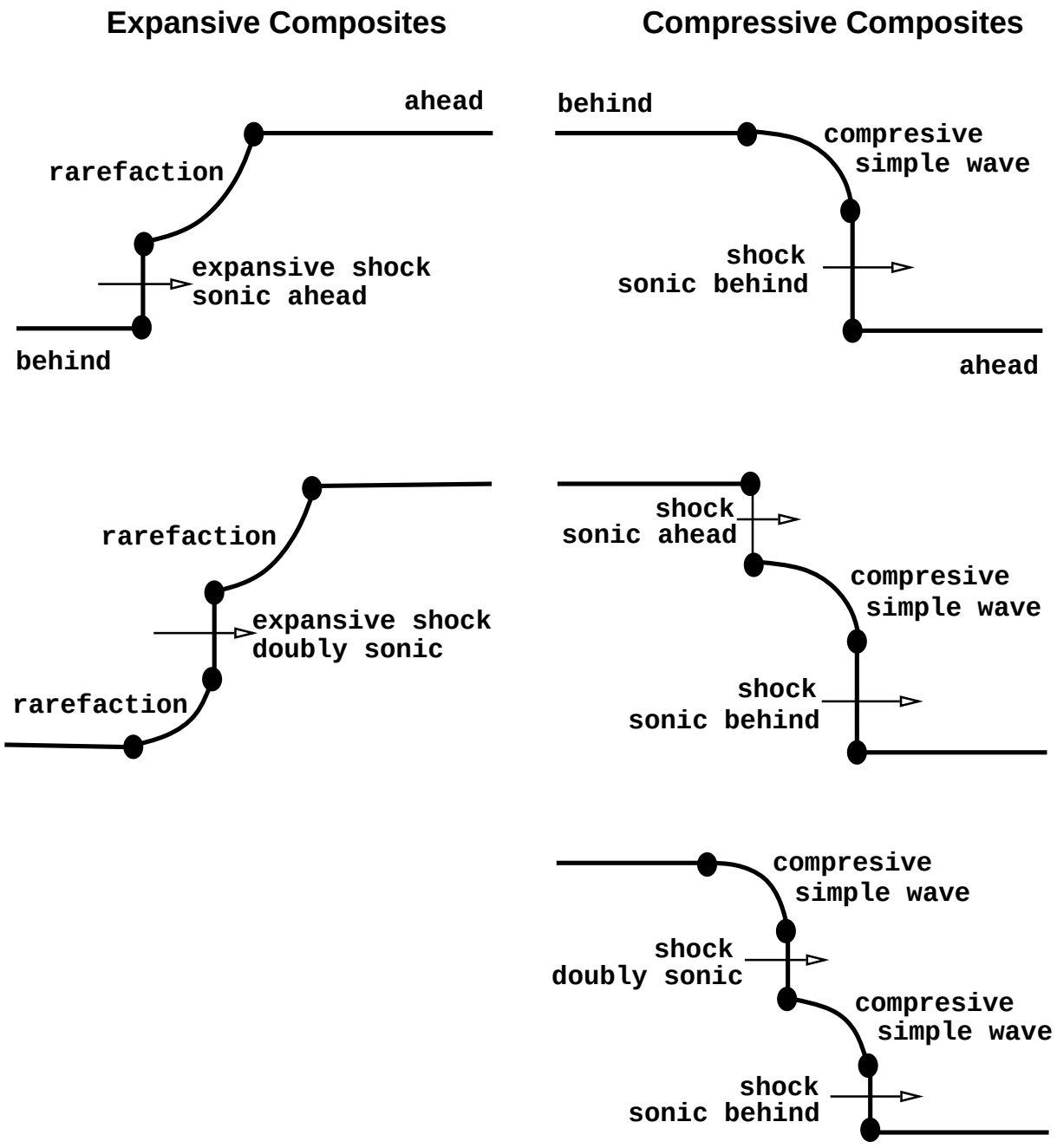

FIGURE 4.4.1

Right facing composite waves in fluid with non-convex EOS. Sketches of pressure profiles that may occur for an initial state with $\mathcal{G}_0 > 0$.

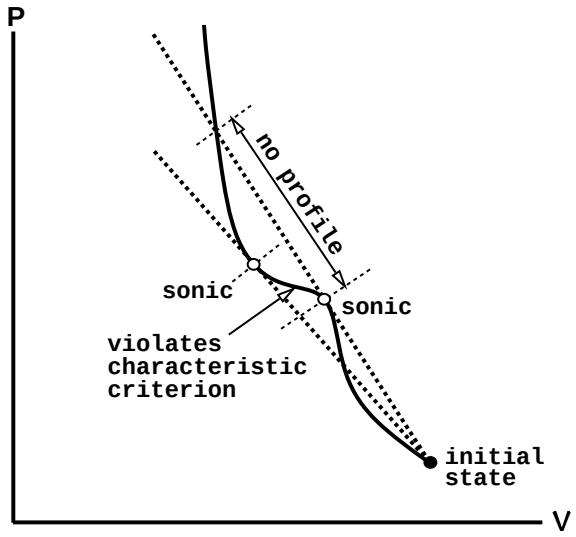

FIGURE 4.4.2

Sketch of Hugoniot locus for a non-convex equation of state. Sonic points are indicated by open circles. The dotted lines are the Rayleigh lines through the sonic points. The Hugoniot locus between the sonic points violates the characteristic criterion. The E-condition is satisfied everywhere on the Hugoniot locus except for the portion marked as corresponding to shocks with no profiles.

Thus, the characteristic condition is satisfied with the strict inequalities replaced by inequalities; *i.e.*, either the state ahead or behind the shock front may be sonic. However, a shock can satisfy the characteristic condition and not the E-condition. In addition, it can be shown that with viscosity and heat conduction steady-state shock profiles exist for only those shocks that satisfy the E-condition. In the regions of phase space in which $\Gamma < 0$, restrictions are required on the Prandtl number (dimensionless ratio of viscosity to heat conduction). We note that the steady-state profiles imply shocks satisfying the E-condition are entropy increasing. Alternatively, as part of the construction of the wave curve, we will show that all shocks satisfying the E-condition are entropy increasing.

Fig. 4.4.2 illustrates the qualitative features of a Hugoniot locus that can arise due to a non-convex EOS. Indicated on the figure are the portion of the Hugoniot locus corresponding to shocks that violate the characteristic criterion, and corresponding to shocks for which viscous, heat conducting profiles do not exist. These complications do not occur for a convex EOS. In this case, (i) all compressive shocks satisfy the E-condition,

(ii) the E-condition and the characteristic condition are equivalent, and (iii) viscous, heat conducting profiles exist for all compressive shocks.

——— To Be Continued ————————-

4.4 EOS with Phase Transition

For all materials, in most of the V–P plane isentropes are convex, *i.e.*, $\mathcal{G} > 0$. Typically, the non-convexity is associated with a phase transition. As seen in Figs. 3.1 and 3.2 a phase transition leads to a mixed phase region in the V–P plane. A general result of thermodynamics for a mixture is that the frozen sound speed is greater than the equilibrium sound speed. In the V–P plane this implies that an isentrope has a kink (discontinuity in slope) at a saturation boundary; *i.e.*, the sound speed in the pure phase is greater than the sound speed in the mixed region. If as V increases the isentrope crosses the saturation boundary from the mixed to the pure phase, then the kink causes the isentrope to be non-convex. In addition, for some materials, isentropes in the pure phase near the critical point are concave. Non-convex isentropes have been observed experimentally for fluids with large specific heats, see [Cramer, 1989].

The **van der Waal** equation of state provides a simple analytic example which displays the qualitative features of a liquid-gas phase transition. The van der Waal equation of state is defined by

$$(P + a/V^2)\,(V - b) = R\,T \ , \tag{4.24}$$

where R is the gas constant, and a and b are parameters which model imperfections in an ideal gas; b represents an excluded volume from a hard core or strong short range repulsive force between atoms or molecules, and a represents a longer range weakly attractive force. With a constant specific heat C_V, the energy is given by (see Ex. 4.4)

$$E = C_V T - a/V \tag{4.25}$$

and the entropy by

$$S = S_0 + C_V \log\left[\frac{(P + a/V^2)\,(V - b)^{\gamma'}}{(P_0 + a/V_0^2)\,(V_0 - b)^{\gamma'}}\right] \ , \tag{4.26}$$

where $\gamma' = 1 + R/C_V$. Note, γ' is the ratio of specific heats and not the adiabatic exponent. When $a = 0$ and $b = 0$, the van der Waal EOS reduces to an ideal γ-law gas EOS.

Next we show that the van der Waal EOS has a mixed phase region. Furthermore, for large heat capacity, γ' is close to 1 and there is a non-convex region near the critical point in the pure phase; see *e.g.*, [Thompson & Lambrakis, 1973] or [Cramer & Sen, 1987]. The isotherms are shown in Fig. 4.4. For low T the isotherms form what is called a van der Waal loop; an anomalous region in which $\partial_V P|_T > 0$. In the anomalous region, the isothermal compressibility is negative and the material is thermodynamical unstable. The boundary of the unstable region $\partial_V P|_T = 0$ is shown as a dotted line and is called the spinodal.

Moreover, along the anomalous isentropes the Gibb's free energy $G = E + P\,V - T\,S$ as shown in Fig. 4.5 is not monotonic. This has the following physical interpretation. For a given T and P, the equilibrium state corresponds to the minimum value of G. Along an isotherm, the curve $G_T(P)$ crosses itself at the phase boundary. The curve defined by the minimum G divides into a pure liquid phase and a pure gas phase. The equilibrium isotherm in the mixed region corresponds to the line $P =$ constant shown in Fig. 4.4. The condition that the gas and liquid Gibb's free energy are equal across the phase boundary, $G(V_l, T) = G(V_g, T)$ and $P(V_l, T) = P(V_g, T)$, corresponds to Maxwell's equal area construction; the shaded area in the V–P plane shown in Fig. 4.5 above and below the equilibrium isotherm are equal. In the mixed region, beyond the liquid saturation boundary is a meta-stable superheated liquid, and beyond the gas saturation boundary is a meta-stable supercooled gas. As the spinodal is approached, the magnitude of a perturbation needed to disturb the meta-stable state decreased towards 0.

At the critical temperature, the isotherm in the V–P plane is tangent to the phase boundary. Thus, the critical point is defined by $\partial_V P|_T = 0$ and $\partial_V^2 P|_T = 0$. For the van der Waal EOS, the critical point occurs at

$$\begin{aligned} P_c &= \frac{a}{27\,b^2}\ , \\ V_c &= 3\,b\ , \\ R\,T_c &= \frac{8\,a}{27\,b}\ . \end{aligned} \tag{4.27}$$

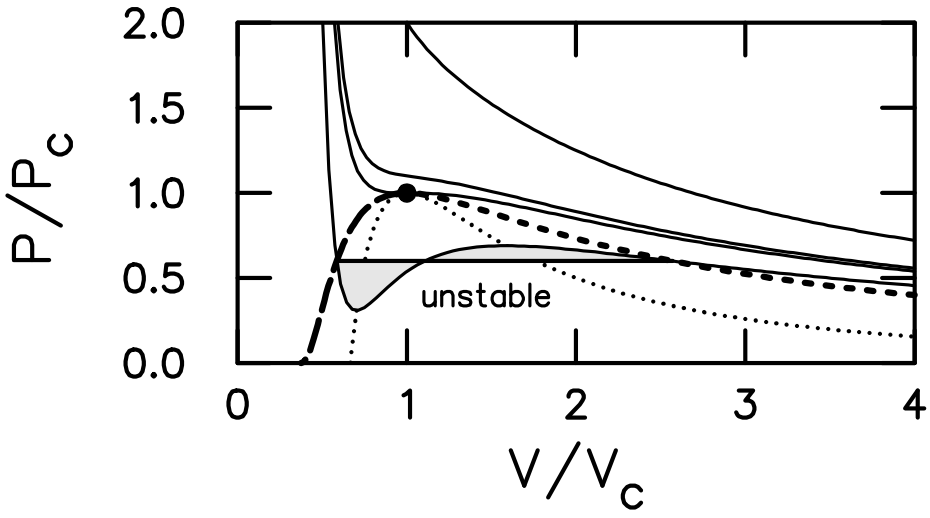

FIGURE 4.4

Isotherms for van der Waal equation of state. Long-dashed and short-dashed lines correspond to the liquid and gas saturation boundaries. The solid circle denotes the critical point. The dotted lines represent the spinodal. Shaded area shows Maxwell's construction for equilibrium isotherm in mixed phase region.

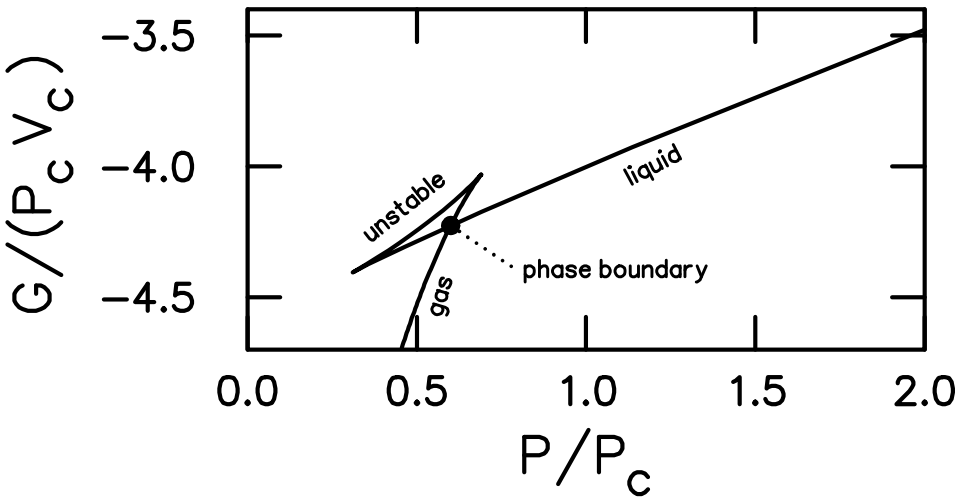

FIGURE 4.5

Gibbs free energy along isotherm through mixed phase region.

Let us scale the thermodynamic variables by their values at the critical point; $\tilde{P} = P/P_c$, $\tilde{V} = V/V_c$, and $\tilde{T} = T/T_c$. The scaled form of the van der Waal EOS

$$\tilde{P} = \frac{8\tilde{T}}{3\tilde{V} - 1} - \frac{3}{\tilde{V}^2} \tag{4.28}$$

is independent of all its parameters. This universality of the form of the EOS near a critical point is known as the principle of corresponding states. In the vicinity of the critical point, the phase boundary and critical exponents determined by the van der Waal EOS corresponds to a mean field approximation; see [Bejan, 1988], chapter 6 sections on corresponding states and critical-point phenomena. The mean field predictions are qualitatively but not quantitatively in agreement with experimental measurements.

In the mixed region, the equilibrium values of the thermodynamic variables are a linear combination of the values of the states at the phase boundary. In particular, the entropy is given in terms of the specific volume by

$$S(V,T) = \frac{[V - V_l(T)]S_g(T) + [V_g(T) - V]S_l(T)}{V_g(T) - V_l(T)} \ , \tag{4.29}$$

where the subscripts g and l denote the values on the saturation boundary corresponding to the gas and liquid respectively. From this it can be shown that the slope of the isentrope in the V–P plane is given by

$$\partial_V P|_S = \frac{(S_g - S_l)/(V_g - V_l)}{\frac{(V-V_l)(d/dT)V_g + (V_g - V)(d/dT)V_l}{V_g - V_l} - \frac{(V-V_l)(d/dT)S_g + (V_g - V)(d/dT)S_l}{S_g - S_l}} \ . \tag{4.30}$$

We note that along the coexistence curve $dP/dT|_{\rm coex} = (S_g - S_l)/(V_g - V_l)$. This is known as the Clausius-Clapeyron relation. The behavior of the isentropes depends on whether the specific heat is large or small.

In the typical case of a low to moderate specific heat, the isentropes are shown in Fig. 4.6 (corresponding to $\gamma' = 2$). In this case all isentropes enter the mixed region from the pure region with V decreasing. Though the isentropes have a kink at the saturation

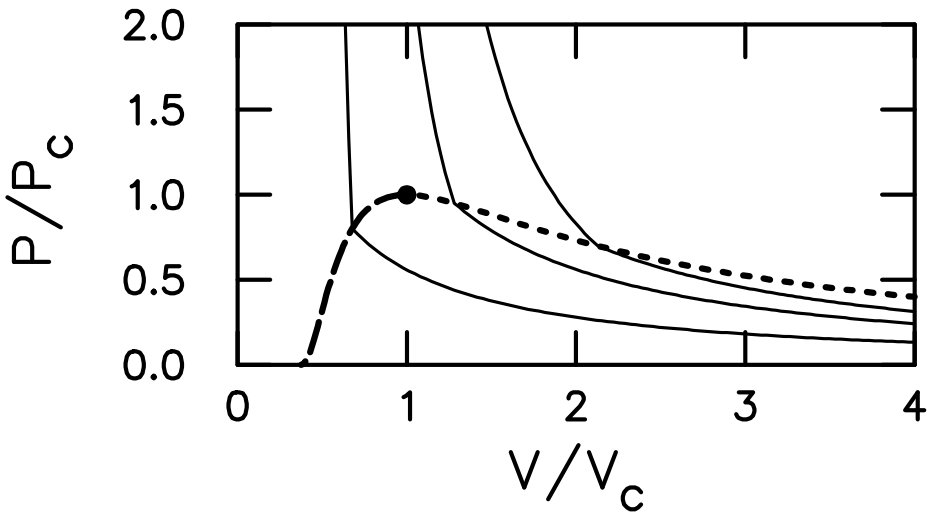

FIGURE 4.6

Isentropes for van der Waal equation of state with $\gamma' = 2$. Long-dashed and short-dashed lines correspond to the liquid and gas saturation boundaries. The solid circle denotes the critical point.

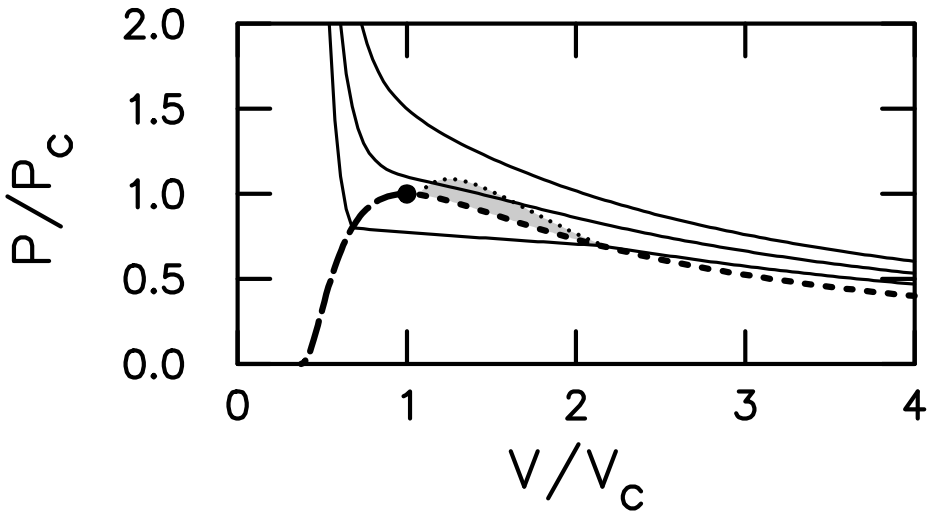

FIGURE 4.7

Isentropes for van der Waal equation of state with $\gamma' = 1.02$. Long-dashed and short-dashed lines correspond to the liquid and gas saturation boundaries. The solid circle denotes the critical point. Shaded area corresponds to pure phase region with $\mathcal{G} < 0$.

boundary, they remain convex. Moreover, as V decreases an isentrope remains in the mixed region. This is possible since $V_g \to \infty$ as $P \to 0$.

Large molecules have a large number of internal vibrational degrees of freedom and can have a large specific heat. The isentropes for this case, as shown in Fig. 4.7 (corresponding to $\gamma' = 1.02$), behave differently. In particular, isentropes with low S cut through the mixed regime while those with large S are entirely in the pure phase. The isentropes that cut through the mixed region are non-convex due to the kink at the gas saturation boundary. Moreover, there is a region in the pure phase near the critical point in which $\mathcal{G} < 0$. This can be explained as follows. The critical isotherm has an inflection point at the critical point. Isotherms slightly above the critical temperature tend to be concave in the neighborhood of the critical point. Using thermodynamic identities, $\partial_V^2 P|_S$ can be expressed as $\partial_V^2 P|_T$ plus other terms proportional to C_V^{-1}; see *e.g.*, [Cramer, 1989]. Thus, for sufficiently large C_V the sign of $\partial_V^2 P|_S$ and $\partial_V^2 P|_T$ are the same, and the isentropes loss convexity near a critical point. This is shown as the shaded region in Fig. 4.7.

Now that we know the structure of the isentropes due to a phase transition, it is natural to ask what effect this has on the equilibrium wave structure. We first consider the rarefaction branch of the wave curve. For the typical case shown in Fig. 4.6 the only anomaly in the isentropes is a convex kink at the saturation boundary. Because of the jump in the characteristic velocity this results in split rarefaction waves; *i.e.*, a composite of two rarefaction waves separated by a constant state. A non-convex kink in the isentrope (as shown in Fig. 4.7 at the gas saturation boundary) has a more significant effect. Since the characteristic velocity is not monotonic, a rarefaction curve can not be continued into a non-convex region of the isentrope. Instead, an entropy increasing rarefaction shock occurs. This leads to a composite wave consisting of a rarefaction wave, doubly sonic rarefaction shock and another rarefaction wave at a higher entropy; see [Zel'dovich & Raizer, 1966] Chpt. XI, sections 19 and 20. It should be emphasized that entropy increasing rarefaction shocks when $\mathcal{G} < 0$ are physical and have been observed experimentally; [Borisov, *et al.*,

1983] and [Thompson, Carofano & Kim, 1986]. These are distinct from the unphysical numerical entropy decreasing rarefaction shocks that can occur in Godunov upwind shock capturing algorithms when approximate Riemann solver are used.

Next we consider the compressive branch of the wave curve. In the V–P plane, the discontinuity in the sound speed results in a discontinuity in the slope of the Hugoniot curve. When the jump in $dP/dV|_h$ results in a decrease in the wave speed, a single shock becomes unstable and split shock waves occur; *i.e.*, a lead shock to a state on the saturation boundary followed by a second shock with a lower wave speed. As the strength of the second shock increases, so does its wave speed. When the wave speed of the second shock catches up with the wave speed of the lead shock, a single shock again becomes stable. The stable portion of the single shock Hugoniot and split shocks form a continuous wave curve. This is a consequence of the following general result.

Lemma 4.20 (Triple Shock Rule)**:** Consider a system of conservation laws $u_t + f(u)_x = 0$. Let u_1, u_2 and u_3 denote three states. If u_1 is connected to u_2 by a shock with speed s, and u_2 is connected to u_3 by a shock with the same speed s, then u_1 is also connected to u_3 by a shock with speed s.

Proof: Exercise 4.2.

We note that not all the unstable shocks are excluded by the characteristic criterion. When there is a non-uniqueness in the structure of the wave curve, it appears that the fastest wave (shock speed or the speed of lead wave for composite) is the most stable and the one that physically occurs.

Similar split waves are common in elastic-plastic flow. The transition at the yield surface between elastic and plastic flow, though changing the material properties irreversibly, has a similar effect on the wave structure as a phase transition; *i.e.*, the characteristic speeds change discontinuously. Typically, a strong wave consists of an elastic precursor followed by a plastic shock. When the plastic shock is sufficiently strong it overtakes the precursor and there is only a single shock wave.

Finally, we consider the effect due to smooth isentropes with $\mathcal{G} < 0$, such as can occur near a critical point as shown in Fig. 4.7. In the V–P plane, this can result in a smooth non-convex Hugoniot curve. At the point when the Hugoniot first losses convexity, the slope of the Rayleigh line and hence the wave speed is a local maximum. By the characteristic criterion, subsequent shocks along the Hugoniot curve are unstable. The unstable shocks can be replaced by stable composites consisting of a sonic shock followed by a compressive wave. An analogous type of composite wave structure occurs in detonations; an underdriven sonic (CJ) detonation wave followed by a rarefaction called a Taylor wave.

As the wave strength increases, the composite wave is expanded by adjoining a second shock after the compressive wave. Again it can be shown that the wave curve formed by the stable portion of the shock Hugoniot and the composites is continuous; see [Wendroff, 1972] or [Menikoff & Plohr, 1989]. The allowable waves satisfy the Oleĭnik-Liu extended entropy condition, [Liu, 1975] and [Liu, 1976]. When the wave structure is non-unique this amounts to selecting the fastest wave. The selection of admissible waves is based on considering which discontinuities have shock profiles and which waves are stable. These considerations are necessary because the standard entropy condition and the characteristic criterion are insufficient to determine a unique weak solution to the fluid equation with a non-convex EOS.

The wave structure is important in determining the solution to a Riemann problem. The solution to the Riemann problem can be determined from the geometric construction using wave curves described in lecture 3. For a non-convex EOS there are too many waves leading to a non-unique wave curve. The non-uniqueness is resolved by excluding the unstable shocks and replacing them with stable composites. This determines a unique solution to the RP. Examples of the wave structure that can occur with non-convex EOS have been calculated in Refs. [Cramer & Kluwick, 1984], [Cramer & Sen, 1987] and [Cramer & Fry, 1993].

For an equilibrium EOS, the wave structure greatly enhances the understanding of fluid flow in applications. Moreover, it serves as an important check on numerical simulations of complicated flows. Some numerical errors result in an artificial wave structure similar to what occurs for a non-convex EOS. Knowing this wave structure enables one to recognize more readily a large class of numerical errors.

4.5 Non-Equilibrium Effects

Strong shock waves generated by high explosives are used to measure material properties in a high pressure and high temperature regime not accessible to static measurements, see [Duvall & Graham, 1977]. These type of measurements for phase transitions (and other applications as well) can be strongly affected by the non-equilibrium response of materials. Though the details are outside the scope of these lectures, in order to understand the range of applicability and limitations of the equilibrium fluid model, the principle non-equilibrium behavior is summarized below.

Physical phenomenon of importance to fluid flow at high temperatures include dissociation of molecules, ionization of atoms and radiation; see *e.g.*, [Zel'dovich & Raizer, 1966], chapter 7. Each process has an associated time scale. When the time scale is small compared to the time scale for the bulk fluid flow, an equilibrium description is usually a good approximation. If the non-equilibrium processes are slow then extra variables and associated rate equations are needed to describe the physical degrees of freedom in the problem. Thus, non-equilibrium phenomena can be modeled in a manner similar to that for reversible chemical reactions (see Ex. 4.5) or multi-phase flow, provided a continuum description is applicable.

Usually the expanded set of equations are hyperbolic and describe a relaxation phenomenon. The wave structure has a hierarchy of characteristics and sub-characteristics; see [Whitham, 1974], chapter 10, and [Liu, 1987]. The characteristics describe the fast time scale or transient acoustic response determined by the 'frozen' sound speeds. The sub-characteristics describe the slow time scale or asymptotic wave behavior determined

by the 'equilibrium' sound speeds. Several types of additional shock wave phenomena can occur:

(i) A partially dispersed shock wave consisting of a discontinuous shock followed by a relaxation layer. The discontinuity satisfies the Hugoniot jump conditions with the frozen EOS and the full wave satisfies the Hugoniot jump conditions with the equilibrium EOS (see Ex. 4.5). In the V–P plane, for an endothermic process (such as ionization or dissociation) the equilibrium Hugoniot is shifted down while for an exothermic reaction the equilibrium Hugoniot is shifted up. As a result, the 'signature' of endothermic process is an increase in the pressure following the lead shock while the 'signature' of a detonation is a decrease in the pressure following the shock. In the exothermic case, the energy release can drive the wave giving rise to a self-sustaining detonation.

(ii) When the frozen sound speed exceeds the equilibrium shock speed the wave is fully dispersed and is continuous. The width of the wave depends on the non-equilibrium time scale. The notion of a shock wave is no longer meaningful when the wave width is large and the gradients in the bulk flow are comparable to those in the dispersed wave. For example, a slowly oscillating small amplitude disturbance gives rise to acoustic waves that fall in this category. In this case, since non-equilibrium effects are dissipative, the sound wave decays in time.

(iii) For a Riemann problem, the early time transient response is based on the frozen wave curve, and the asymptotic response is based on the equilibrium wave curve. Thus, non-equilibrium processes give rise to a time dependent wave structure. A phase transition can be considered as a non-equilibrium process. Thus, a time dependent wave structure can occur when the initial and final state of a wave in the equilibrium theory solution to a Riemann problem are in different phases.

For a description of the above three phenomena in terms of the Hugoniot curve see [Fickett & Davis, 1979], section 4C4, "shock waves in a reactive mixture."

(iv) Non-equilibrium processes can cause shock waves to be unstable. This is well known to occur for detonation waves; see *e.g.*, [Fickett & Davis, 1979], chapter 6. Instabilities of

strong planar shock in argon have also been observed [Glass & Liu, 1978]; see also [Grun *et al.*, 1991]. Even though the wave is unstable the amplitude of the instability can saturate. This is true for detonation waves since the energy density and pressure are too large to support fingering type instabilities of the front. Thus, the wave can be well-behaved on a large length scale and have fluctuation on a short scale akin to turbulence.

Finally, we mention a few application when non-equilibrium effects are important:
(i) Dissociation and ionization of air are quite important for the performance of a jet engine, for hypersonic flow of a supersonic jet and for re-entry of a spacecraft.
(ii) The expansion of a high temperature gas through a nozzle can occur on a shorter time scale than the vibrational relaxation time scale giving rise to population inversion. This is the basis for a gas dynamic laser.
(iii) The flow in a wind tunnel requires very dry air. Otherwise water vapor in the air gives rise to a condensation shock which has an adverse affect on the characteristics of the wind tunnel.
(iv) For magnetically confined fusion, the plasma is optically thin. As a consequence one has to allow for the ions, electrons and radiation to be out of thermal equilibrium.

General references:

1. [Smith, 1979]
2. [Menikoff & Plohr, 1989]

Exercises

4.1 Is V a good choice to parameterize shock Hugoniot?

4.2 Proof the triple shock rule (Lemma 4.20).

4.3 Consider the shock Hugoniot locus in the V–P plane.

A) In the standard case, $\mathcal{G} > 0$ and $\gamma - 1 \geq \Gamma > 0$, show that the slopes of the Hugoniot locus, isentrope and Rayleigh line are related by

$$\frac{-1}{\Delta P/\Delta V} > \frac{-1}{(dP/dV)_S} > \frac{-1}{(dP/dV)_h} \ . \tag{4E.1}$$

B) What is the geometric interpretation of ΔE and Δu? In the strong shock limit $P_1 \to \infty$ show that

$$\frac{\Delta E}{\frac{1}{2}u^2} \to 1 \ . \tag{4E.2}$$

4.4 **A)** Proof the thermodynamic relation

$$\partial_V S|_T = \partial_T P|_V \ . \tag{4E.3}$$

B) Determine the entropy for the van der Waal EOS.

C) Determine the specific energy for the van der Waal EOS.

4.5 Consider the fluid flow equations augmented by one rate process for an energy source term

$$\partial_t \begin{pmatrix} \rho \\ \rho u \\ \rho\left(\frac{1}{2}u^2 + E\right) \\ \rho\lambda \end{pmatrix} + \partial_x \begin{pmatrix} \rho u \\ \rho u^2 + P \\ \rho\left(\frac{1}{2}u^2 + E\right)u + P\,u \\ \rho u \lambda \end{pmatrix} = \begin{pmatrix} 0 \\ 0 \\ \rho\mathcal{R}Q \\ \rho\mathcal{R} \end{pmatrix} \ , \tag{4E.4}$$

where λ is a mass fraction, $\mathcal{R}$ is a rate (mass fraction per unit time), and Q is an energy per unit mass. The variable λ can be associated with a non-equilibrium degree of freedom

for the ionization of an atom, the dissociation or vibrational energy of a molecule, or a chemical reaction. The EOS is assumed to be a function of the internal state variables, $P = P(V, E, \lambda)$.

For a reversible process the rate typically has the form

$$\mathcal{R} = -\big[\lambda - \lambda_{\rm eq}(V, E)\big]/\tau(V, E) \ , \tag{4E.5}$$

where $\lambda_{\rm eq}(V, E)$ is the equilibrium value and $\tau(V, E)$ is the time constant for equilibration. For an explosive, the initial state is assumed to be meta-stable and the reaction is irreversible $\mathcal{R} \geq 0$. Once initiated the reaction runs to completion; *i.e.*, from $\lambda = 0$ (reactants) to $\lambda = 1$ (reaction products).

A) Assume Q is constant. What happens to the fluid equations under the transformation of the EOS

$$\begin{aligned} \widetilde{E} &= E - \lambda Q \ , \\ \widetilde{P}(V, \widetilde{E}, \lambda) &= P(V, E, \lambda) \ . \end{aligned} \tag{4E.6}$$

For a steady partly dispersed shock wave, how is the Hugoniot equation Eq. (2.22) modified?

Assume an ideal gas EOS, $PV = RT$, for an irreversible reaction $A \to B$ that does not change the particle number. Furthermore, suppose the specific heat

$$C_V = R/(\gamma - 1)$$

is constant independent of λ. Then the effective EOS in part (A) for an ideal explosive is given by

$$\begin{aligned} C_V T &= \widetilde{E} + \lambda Q \\ \widetilde{P}(V, \widetilde{E}, \lambda) &= (\gamma - 1)\,(\widetilde{E} + \lambda Q)/V \ . \end{aligned} \tag{4E.7}$$

B) Determine the Hugoniot locus for an ideal explosive. How is $P_h(V)$ affected by the heat release?

C) For $Q > 0$, find the minimum wave speed and the corresponding point on the Hugoniot locus. This point is known as the Chapman-Jouguet or CJ state. In the limit when $P_0 V_0/Q \to 0$ show that

$$\begin{aligned} P_{\rm CJ} &= 2\,(\gamma-1)\rho_0 Q\ , \\ V_{\rm CJ}/V_0 &= \gamma/(\gamma+1)\ , \\ D_{\rm CJ}^2 &= 2\,(\gamma^2-1)Q\ , \\ u_{\rm CJ} &= D_{\rm CJ}/(\gamma+1)\ , \\ c_{\rm CJ} &= \gamma D_{\rm CJ}/(\gamma+1)\ , \end{aligned} \tag{4E.8}$$

where the detonation velocity, denoted by D, is the wave speed.

D) Show that the CJ state is a local entropy minimum, and sonic relative to the wave front. Furthermore, show that the flow behind a wave on the strong branch ($P > P_{\rm CJ}$) is subsonic and on the weak branch ($P < P_{\rm CJ}$) is supersonic.

E) For steady state show that the reaction profile lies on the Rayleigh line. When $Q > 0$, there are two solutions to the Hugoniot jump conditions for wave speeds $\sigma > D_{\rm CJ}$. Which solution is physically admissible.

F) Show for a partly dispersed shock wave: (i) When $Q > 0$, the pressure decreases behind the lead shock. This is characteristic of a detonation wave. (ii) When $Q < 0$, the pressure increases behind the lead shock. This is characteristic of a relaxation wave.

4.6 Assume a shock wave is propagating into a region in which the ahead state is constant. Suppose the shock wave is overtaken from behind by a rarefaction or compressive wave.

A) From the characteristic equations show that the time evolution of the shock strength is related to the spatial gradients behind the shock wave

$$\frac{d\alpha}{dt}\begin{pmatrix} dS/d\alpha \\ [\sigma - u + \rho c^2 (du/dP)_h]\, dP/d\alpha \\ [\sigma - u + V(dP/du)_h]\, \rho c\, du/d\alpha \end{pmatrix} = \begin{pmatrix} (\sigma-u)\partial_x S \\ [(\sigma-u)^2 - c^2]\, \partial_x P \\ [(\sigma-u)^2 - c^2]\, \rho c\, \partial_x u \end{pmatrix}\ , \tag{4E.9}$$

where σ is the wave speed, α is the parameterization of the Hugoniot locus in Eqs. (4.12)–(4.17), and subscript 'h' denotes derivatives along the Hugoniot locus.

B) The vector on the left hand side of the shock change relation has a direction fixed by the Hugoniot locus and magnitude given by the change in shock strength, $d\alpha/dt$. On the other hand, for an initial value problem the spatial gradients on the right hand side can be set independently. Thus, the vectors on the left and right hand side of the shock change equation may not point in the same direction. How is this paradox resolved?

Hint: consider the flow resulting from a rarefaction wave overtaking a shock wave.

Solutions

4.1 For a given initial state, the Hugoniot locus can be parameterized by a single variable. Specific volume is not a good parameterization for three reasons:

(i) The maximum shock compression ratio is finite. Thus, the range of V is limited.

(ii) For strong shocks the shock state is very sensitive to small changes in V.

(iii) In general, only the medium condition is satisfied and the Hugoniot locus is not a single-valued function of V.

It is more convenient to parameterize the Hugoniot locus with wave speed, pressure or particle velocity.

4.2 From the Hugoniot jump conditions

$$-s \cdot (u_2 - u_1) + f(u_2) - f(u_1) = 0 \ ,$$
$$-s \cdot (u_3 - u_2) + f(u_3) - f(u_2) = 0 \ .$$

Adding these equations gives

$$-s \cdot (u_3 - u_1) + f(u_3) - f(u_1) = 0 \ .$$

Hence, there is a shock connecting states u_1 and u_3 with the same wave speed.

4.3 **A)** From Eqs. (2.16) and (2.18)

$$-\frac{\Delta P}{\Delta V} = \Big[\rho_1 \cdot (\sigma - u_1)\Big]^2 \ .$$

From Eq. (1.12)

$$-\left(\frac{dP}{dV}\right)_S = (\rho_1 c_1)^2 \ .$$

When $\mathcal{G} > 0$, by Th. 4.1, the flow behind a physical entropy increasing shock is subsonic, $(\sigma - u_1)^2 < c_1^2$. Hence,

$$-\frac{\Delta P}{\Delta V} < -\left(\frac{dP}{dV}\right)_S .$$

In the standard case, along the Hugoniot locus P and S are monotonically increasing. Moreover, $\partial P/\partial S|_V > 0$ when $\Gamma > 0$. Hence,

$$\frac{-1}{(dP/dV)_S} > \frac{-1}{(dP/dV)_h} .$$

For most of the Hugoniot locus $dP/dV|_h < 0$ and the relation among the slopes can be expressed as by

$$-\Delta P/\Delta V < -(dP/dV)_S < -(dP/dV)_h . \qquad (4S.1)$$

At extremums in V, $(dP/dV)_h$ is discontinuous while $(dV/dP)_h$ is continuous. Consequently, Eq. (4E.1) covers the entire range while Eq. (4S.1) is limited to portion of Hugoniot locus in which V is monotonically decreasing.

B) The Hugoniot equation (2.22) is

$$\Delta E = \tfrac{1}{2}\,(P_0 + P_1)\cdot(V_0 - V_1) .$$

Therefore, ΔE is the area of the trapezoid under the Rayleigh line. From Eq. (2.23)

$$(\Delta u)^2 = (P_1 - P_0)\cdot(V_0 - V_1) .$$

Therefore, $(\Delta u)^2$ is the area of a rectangle. In the strong shock limit, P_0 can be neglected compared to to P_1. The trapezoid degenerates into a triangle which is half of the rectangle. Therefore, in the strong shock limit $\Delta E \sim \frac{1}{2}\,(\Delta u)^2$.

4.4 **A)** The Helmholtz free energy is defined by

$$F(V,T) = E - TS \ .$$

From the thermodynamic relation $dE = -PdV + TdS$ we find

$$dF = -S\,dT - P\,dV \ .$$

The equality of the cross derivatives leads to one of Maxwell's relations

$$\left.\frac{\partial S}{\partial V}\right|_T = \frac{\partial^2 F}{\partial V \partial T} = \left.\frac{\partial P}{\partial T}\right|_V \ .$$

B) The specific heat is given by

$$C_V = \partial_T E|_V = T\partial_T S|_V \ .$$

For the van der Waal EOS

$$\left.\frac{\partial P}{\partial T}\right|_V = \frac{R}{V-b} \ .$$

Therefore,

$$\begin{aligned} dS &= \left.\frac{\partial S}{\partial T}\right|_V dT + \left.\frac{\partial S}{\partial V}\right|_T dV \\ &= C_V \frac{dT}{T} + R\frac{dV}{V-b} \ . \end{aligned}$$

Hence,

$$S = S_0 + C_V \log(T/T_0) + R\log\big[(V-b)/(V_0-b)\big] \ .$$

Using the EOS to eliminate T leads to Eq. (4.26).

C) From the above equation for dS we find

$$\begin{aligned} dE &= T\,dS - P\,dV \\ &= C_V\,dT + \big[RT/(V-b) - P\big]\,dV \\ &= C_V\,dT + \big[RT/(V-b) - P\big]\,dV \\ &= C_V\,dT + a\frac{dV}{V^2} \ . \end{aligned}$$

Integration then gives Eq. (4.25).

4.5 **A)** The transformed system of equations is

$$\partial_t \begin{pmatrix} \rho \\ \rho u \\ \rho\,(\frac{1}{2}u^2 + \widetilde{E}) \\ \rho\lambda \end{pmatrix} + \partial_x \begin{pmatrix} \rho u \\ \rho u^2 + \widetilde{P} \\ \rho\,(\frac{1}{2}u^2 + \widetilde{E})\,u + \widetilde{P}\,u \\ \rho u\lambda \end{pmatrix} = \begin{pmatrix} 0 \\ 0 \\ 0 \\ \mathcal{R} \end{pmatrix} \ . \qquad (4S.2)$$

The first three equations are identical to the usual fluid flow equations. The fourth equation has the form of a rate equation along particle trajectories

$$\frac{d}{dt}\lambda = \mathcal{R} \ . \qquad (4S.3)$$

Thus, by incorporating the heat release in the EOS, the energy source term drops out.

The fluid variables satisfy the standard jump conditions. The same algebraic manipulations that lead to Eq. (2.22) leads to the modified Hugoniot equation

$$E_1 - E_0 = \tfrac{1}{2}\,(P_1 + P_0)\cdot(V_0 - V_1) + Q\cdot(\lambda_1 - \lambda_0) \ . \qquad (4S.4)$$

Because of the source term, the fourth jump equation,

$$-\sigma\Delta[\rho\lambda] + \Delta[\rho u\lambda] = \int \rho\mathcal{R}\,dx \ ,$$

is not an algebraic equation but depends on the wave profile. However, if a steady state wave exists then the state behind the wave must be in equilibrium,

$$\lambda_1 = \lambda_{\rm eq}(V_1, E_1) \ .$$

The Hugoniot equation, the equilibrium condition and the equation of state form a system of three algebraic equations that determine the three variables V_1, E_1, λ_1 for the possible end state of a steady wave.

For an irreversible reaction, $\lambda_0 = 0$ and $\lambda_1 = 1$. The jump conditions then simplify to a single Hugoniot equation

$$E_1 - E_0 = \tfrac{1}{2}\,(P_1 + P_0)\cdot(V_0 - V_1) + Q \ . \qquad (4S.5)$$

Thus, for an explosive, the state behind a detonation wave is determined by the Hugoniot equation. A detonation wave in an explosive is analogous to a shock wave in a non-reactive fluid.

B) From the modified EOS, Eq. (4E.7), and the modified Hugoniot equation, Eq. (4S.5), the Hugoniot locus for an ideal explosive can be derived by similar algebraic manipulations to those used in Ex. 2.7 A to derive the Hugoniot locus for an ideal gas. The result analogous to Eq. (2S.18) is

$$\Delta V = -\frac{V_0 \Delta P - (\gamma - 1)\, Q}{\gamma P_0 + \frac{1}{2}(\gamma + 1)\, \Delta P} \ , \tag{4S.6a}$$

or

$$\Delta P = \frac{(\gamma - 1)\, Q - \gamma P_0 \Delta V}{V_0 + \frac{1}{2}(\gamma + 1)\, \Delta V} \ . \tag{4S.6b}$$

The wave speed is determined by Eq. (2.18)

$$(\rho_0 \sigma)^2 = -\Delta P / \Delta V \ , \tag{4S.7}$$

and the particle velocity by Eq. (2.23)

$$(\Delta u)^2 = -\Delta P\, \Delta V \ . \tag{4S.8}$$

Thus, the Hugoniot locus can easily be parameterized by P or V. From Eq. (4S.6b) the Hugoniot curve $P_h(V)$ is shifted up when the reaction is exothermic, $Q > 0$, and down when the reaction is endothermic, $Q < 0$.

An illustrative case of a Hugoniot locus for an explosive is shown in Fig. 4.8. The branch, $\Delta P > 0$ and $\Delta V < 0$, corresponds to waves which are supersonic with respect to the ahead state (unreacted material). This is known as the detonation branch. Detonation waves are dominated by inertial effects. They are the analog of shock waves for a non-reactive material.

The branch, $\Delta P < 0$ and $\Delta V > 0$, corresponds to subsonic waves. For a non-reactive material, subsonic waves are excluded because the entropy jump across the wave is negative. However, for an explosive, the entropy is increased sufficiently by the reaction for the total entropy jump across the wave to be positive. The subsonic waves form the deflagration branch of the Hugoniot locus for an explosive. Even though deflagration waves satisfy the conservation laws and are entropy increasing, they may not be physically

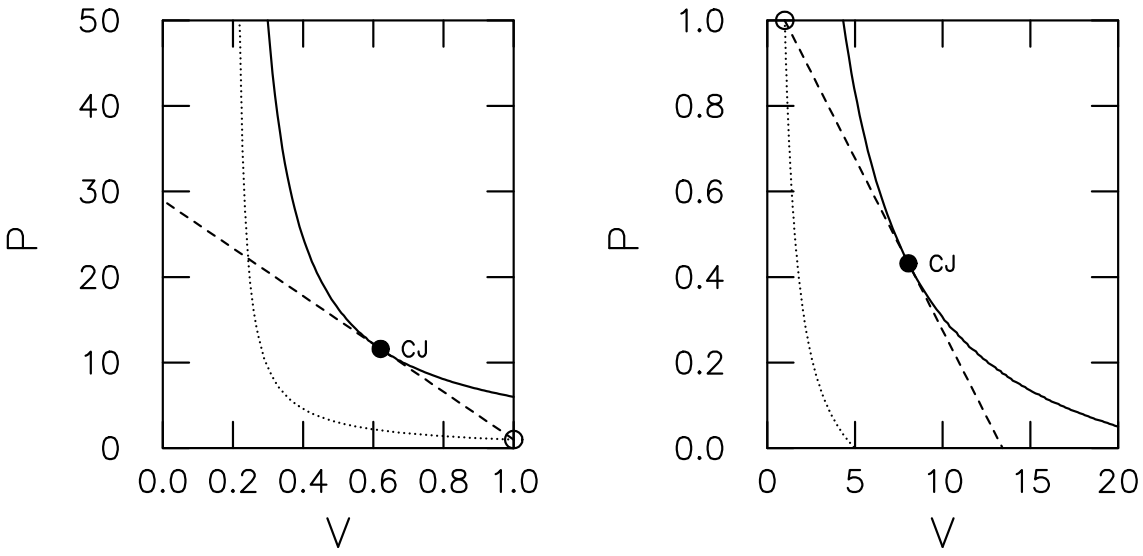

FIGURE 4.8

Hugoniot locus for an ideal explosive; $\gamma = 1.5$, $Q = 10$, $P_0 = 1$ and $V_0 = 1$. The left plot is the detonation branch and the right plot is the deflagration branch. The Hugoniot locus between $V = 1$ and $P = 1$ is excluded because $D^2 = -\Delta P/\Delta V < 0$. The solid curve corresponds to full reaction $\lambda = 1$, and the dotted curve to no reaction $\lambda = 0$. The open circle is the initial state, the solid circle is the CJ state. The Rayleigh line through the CJ state is shown as a dashed line.

admissible. Transport effects, in particular heat conduction, are important for subsonic waves. Usually a wave profile exists for only a single point on the deflagration branch. Since we are neglecting transport effects, deflagration waves are outside the scope of these lectures.

C) Substituting Eq. (4S.6a) for ΔV into Eq. (4S.7) we find

$$(\rho_0\sigma)^2 = \frac{\Delta P \cdot [\gamma P_0 + \frac{1}{2}(\gamma+1)\Delta P]}{V_0\Delta P - (\gamma-1)Q} \ . \qquad (4S.9)$$

A local extremum occurs when

$$\frac{d}{d\Delta P}(\rho_0\sigma)^2 = 0 \ .$$

This leads to the quadratic equation for ΔP

$$(\Delta P)^2 - 2(\gamma-1)\rho_0 Q\Delta P - \frac{2\gamma(\gamma-1)}{\gamma+1}\rho_0 Q P_0 = 0 \ . \qquad (4S.10)$$

The solution on the detonation branch, $\Delta P > 0$, is

$$\Delta P = (\gamma - 1)\,\rho_0 Q \cdot \left[1 + \left(1 + \frac{2\gamma}{\gamma^2 - 1} \cdot P_0 V_0 / Q\right)^{\frac{1}{2}}\right] . \qquad (4S.11)$$

Substituting for ΔP into Eq. (4S.6a) gives

$$\frac{\Delta V}{V_0} = - \frac{\left(1 + \frac{2\gamma}{\gamma^2-1} \cdot P_0 V_0 / Q\right)^{\frac{1}{2}}}{\frac{1}{2}(\gamma + 1)\left[1 + \left(1 + \frac{2\gamma}{\gamma^2-1} \cdot P_0 V_0 / Q\right)^{\frac{1}{2}}\right] + \frac{\gamma}{\gamma-1} \cdot P_0 V_0 / Q} \quad , \qquad (4S.12)$$

and into Eq. (4S.9) yields

$$D_{\rm CJ}^2 / Q = (\gamma^2 - 1) + \frac{(\gamma^2 - 1) + 2\gamma P_0 V_0 / Q}{\left(1 + \frac{2\gamma}{\gamma^2-1} \cdot P_0 V_0 / Q\right)^{\frac{1}{2}}} + \gamma P_0 V_0 / Q \ . \qquad (4S.13)$$

The velocity can be obtained from Eq. (4S.8) and the sound speed from the equation $c^2 = \gamma PV$.

Asymptotically for $P > \rho_0 Q$, the heat release is negligible and an ideal explosive EOS reduces to an ordinary ideal gas EOS. Therefore, asymptotically the wave speed increases with shock pressure. Conversely, as the pressure decreases the first and only local extremum of the wave speed must be a minimum. Consequently, the CJ state has the minimum wave speed. Geometrically, in the V–P plane, the Rayleigh line is tangent to the Hugoniot locus at the CJ state as shown in Fig. 4.8. Because $P_h(V)$ is shifted up for $Q > 0$, the slope of the Rayleigh line is minimum at the CJ state. By Eq. (4S.7) the minimum slope corresponds to the minimum wave speed.

When the heat release is large, the term $P_0 V_0 / Q$ can be neglected and the formulae greatly simplify. The resulting expressions for the CJ state are given in Eq. (4E.8).

D) For an explosive, the Hugoniot locus corresponds to the shock locus for the detonation products with a non-equilibrium initial state. Hence, we can apply results on the local behavior of the Hugoniot locus. From the previous part, the Rayleigh line is tangent to the Hugoniot locus at the CJ state. Moreover, the slope of the Rayleigh line, $m^2 = -\Delta P / \Delta V$,

is a minimum at the CJ state. It follows from Eq. (4.20) that the CJ state is an entropy minimum. From Lemma 4.11 an entropy extemum is also a sonic point. The weak condition is valid for the equation of state (4E.6). From Eq. (4.16) it follows that the parameter α increases with P. Then Eq. (4.12) implies that the flow behind a strong detonation ($P > P_{\rm CJ}$) is subsonic and the flow behind a weak detonation ($P < P_{\rm CJ}$) is supersonic. We note for the deflagration branch a similar analysis can be used to show that (i) the CJ state is an entropy maximum, (ii) the CJ state is sonic, (iii) the flow behind a weak deflagration ($P > P_{\rm CJ}$) is subsonic and the flow behind a strong deflagration ($P < P_{\rm CJ}$) is supersonic. For both the detonation locus and the deflagration locus, the weak branch is defined as lying between the initial state and the CJ state.

Alternatively, for a direct proof that the CJ state is sonic, we start by finding the condition for which the Rayleigh line is tangent to the isentrope.

$$-\frac{\Delta P}{\Delta V} = \frac{\gamma P}{V} \ ,$$

or

$$(V_0 + \Delta V)\,\Delta P = -\gamma\,(P_0 + \Delta P)\,\Delta V \ .$$

Substituting Eq. (4S.6a) for ΔV leads to a quadratic equation for ΔP. The quadratic equation is identical to Eq. (4S.10). Therefore, the condition that the Rayleigh line is tangent to the isentrope is the same as the condition that the wave speed is an extremum. Using Eq. (4S.7), the tangency condition and the mass flux is constant for a steady wave, $\rho_0\sigma = \rho(\sigma - u)$, we obtain

$$[\rho \cdot (\sigma - u)]^2 = (\rho_0\sigma)^2 = (\rho c)^2 \ .$$

Hence, at the CJ state $(\sigma - u)^2 = c^2$.

E) It follow from the jump conditions for mass and momentum, Eqs. (2.17a) and (2.17b) that

$$(\rho_0 D)^2 = m^2 = -\frac{\Delta P}{\Delta V} \ . \tag{2.18}$$

For fixed wave speed, this is the equation of a straight line in the V–P plane. The points on the reaction profile can be parameterized with the value of the mass fraction λ. For a given λ and D, the state is determined by the partially burnt Hugoniot equation; *i.e.*, Eq. (4S.5) with Q replaced by λQ. Consequently, the partially burnt Hugoniot is given by Eqs. (4S.6)–(4S.9) with Q replaced by λQ.

The detonation wave is supersonic relative to the ambient material. When transport effects (viscosity and heat conduction) are neglected, the profile can not consist of the line segment from the initial state to the weak branch of the Hugoniot locus because there is no mechanism for initiating the reaction. Consequently, a detonation wave consists of a lead shock in the reactants followed by a profile which moves along the Rayleigh line from a point on the Hugoniot locus of the reactants to a point on the Hugoniot locus of the reaction products. The shock heating raises the temperature and initiates the reaction. This is the ZND-model which was derived during WW II independently by Zel'dovich, von Neumann and Doering.

An important conclusion of the ZND-model is that points on the strong branch of the Hugoniot locus correspond to admissible waves and the weak branch is unphysical. Because the CJ state is sonic, a rarefaction (known as a Taylor wave) can be adjoined to a CJ detonation to form a composite. This enables compatibility for any back boundary condition with $P < P_{\rm CJ}$. Consequently, the CJ state corresponds to a self-sustaining underdriven detonation wave; *i.e.*, the lead shock initiates the reaction and the energy given off by the reaction drives the lead shock.

The ZND-model is overly simplistic. The fact that it is a good approximation in many cases is an indication of the importance of jump conditions for conservation laws. Additional physical effects not included in the ZND-model can be important but are beyond the scope of these lectures. The ZND-model does illustrate that though the entropy condition is necessary, it is not always sufficient for selecting the physical waves.

F) From part (B) the Hugoniot locus $P_h(V)$ is shifted up when $Q > 0$ and shifted down when $Q < 0$. From part (E) for a given detonation speed the partly dispersed wave profile lies on the Rayleigh line, and extends from the Hugoniot locus with the initial value of λ_0 to the Hugoniot locus with the final equilibrium value of $\lambda_{\rm eq}$. Consequently, when $Q > 0$ the pressure following the lead shock goes down. This is characteristic of a detonation wave. Conversely, when $Q < 0$ the pressure following the lead shock goes up. This is characteristic of a relaxation layer. Relaxation processes, such as ionization or dissociation, have a similar effect on a partly dispersed wave as an endothermic reaction. When the Hugoniot locus is shifted down, there is the additional possibility that the final equilibrium state lies below the Rayleigh line with slope corresponding to the frozen sound speed. In this case, a lead shock is not possible and the wave profile is fully dispersed. In effect, for weak waves the relaxation process provides sufficient dissipation to completely smear out the profile.

4.6 **A)** The derivative

$$\frac{d}{dt_\sigma} = \partial_t + \sigma\partial_x$$

corresponds to the advection of a point behind the shock front. The characteristic equations (1.13) can be written in terms of the advective derivative for the shock front by adding and subtracting terms with ∂_x

$$\begin{aligned} \frac{d}{dt_\sigma}S &= (\sigma - u)\partial_x S \\ \frac{d}{dt_\sigma}P + \rho c\frac{d}{dt_\sigma}u &= (\sigma - u - c)\cdot(\partial_x P + \rho c\partial_x u)\ , \\ \frac{d}{dt_\sigma}P - \rho c\frac{d}{dt_\sigma}u &= (\sigma - u + c)\cdot(\partial_x P - \rho c\partial_x u)\ . \end{aligned} \qquad (4S.14)$$

The state behind the shock lies on the Hugoniot locus and can be parameterized by the shock strength α. Using the chain rule, derivatives behind the shock can be related to

derivatives involving the shock strength; *e.g.*, $(d/dt_\sigma)P = d\alpha/dt \cdot dP/d\alpha$. Behind the shock front Eq. (4S.14) can be expressed as

$$\frac{d\alpha}{dt}\begin{pmatrix} dS/d\alpha \\ (dP/d\alpha)+\rho c\,(du/d\alpha) \\ (dP/d\alpha)-\rho c\,(du/d\alpha)\end{pmatrix} = \begin{pmatrix} \sigma-u & 0 & 0 \\ 0 & (\sigma-u-c) & (\sigma-u-c)\,\rho c \\ 0 & (\sigma-u+c) & -(\sigma-u+c)\,\rho c\end{pmatrix}\partial_x\begin{pmatrix} S \\ P \\ u\end{pmatrix}. \tag{4S.15}$$

Multiplying the left and right hand side by the matrix

$$\tfrac{1}{2}\begin{pmatrix} 2 & 0 & 0 \\ 0 & -(\sigma-u+c) & -(\sigma-u-c) \\ 0 & -(\sigma-u+c) & (\sigma-u-c)\end{pmatrix},$$

and using relations along the Hugoniot locus, such as $du/d\alpha = (dP/d\alpha)\cdot(du/dP)_h$, leads to Eq. (4E.9).

B) Consider a simple wave overtaking a shock wave from behind, see Fig. 4.9. The leading edge of a simple wave is a weak singularity; *i.e.*, the flow is continuous but the derivatives of the flow are discontinuous at the boundary between a uniform region and a simple region. When the leading edge of the simple wave impacts the shock front, the left and right hand side of the shock change relation do not point in the same direction.

In contrast to a Riemann problem, the initial data is not scale invariant. Consequently, the subsequent flow is not scale invariant, and the outgoing waves are not limited to be only shocks, centered-rarefactions and contacts. The shock state is determined by the incoming characteristics from the overtaking wave and the Hugoniot locus for the state ahead of the shock. Therefore, the shock strength will vary continuously in time, and with it the Riemann invariant of the characteristic going through the shock will vary. In the interaction region in which the incident simple wave and the reflected wave overlap, neither Riemann invariant is constant. Thus, the overlap region is non-simple. The leading edge of the reflected characteristic (opposite wave family to the shock) is a weak singularity. If the reflected wave is compressive, then it eventually focuses into a shock. This may

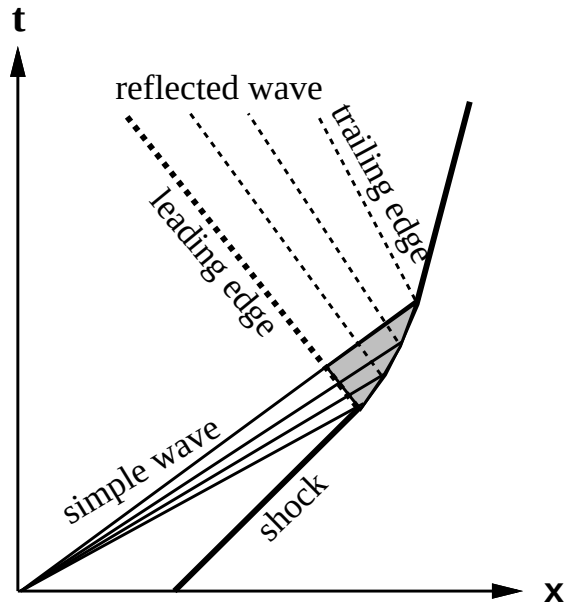

FIGURE 4.9

Overtake of shock wave by simple wave. The thick line is the shock front, the thin lines are the forward characteristics of the incident simple wave, and the dashed lines are the backwards characteristics of the reflected wave. The interaction region in which the waves overlap is shown as the shadded region. The leading edge and trailing edge of the reflected wave are weak singularities. The particle trajectories and entropy wave are not shown.

occur within the interaction region. If the reflected wave is a rarefaction then it leaves the interaction region as a non-centered simple wave. In addition, as the strength of the lead shock varies, the entropy along particle trajectories crossing through it varies. Therefore, between the reflected wave and the shock, there is an entropy wave or smeared out contact.

The initial value problem with an arbitrary gradient in the flow behind a shock results in a qualitatively similar flow consisting of a shock and a weak singularity of the opposite family. The important point is that the incoming characteristic determines the change in the shock strength. The addition of the weak singularity resolves the inconsistency when the vectors on the left and right hand side of the shock change relation are incompatible.

References

ANDERSON, J. D. [**1989**], *Hypersonic and High Temperature Gas Dynamics*, McGraw-Hill, New York.

ARIS, R. [**1989**], *Vectors, Tensors, and the Basic Equations of Fluid Mechanics*, Dover reprint, New York.

ARTOLA, M. and A. MAJDA [**1989**], *Nonlinear Kink Modes for Supersonic Vortex Sheets*, Phys. Fluids A **1**, 583–596.

BEJAN, A. [**1988**], *Advanced Engineering Thermodynamics*, John Wiley, NY.

BEN-DOR, G. [**1992**], *Shock Wave Reflection Phenomena*, Springer-Verlag, NY.

BERGER, M. J. and P. COLELLA [**1989**], *Local Adaptive Mesh Refinement for Shock Hydrodynamics*, J. Comp. Phys. **82**, 64–84.

BETHE, H. [**1942**], *The Theory of Shock Waves for an Arbitrary Equation of State*, Report No. PB-32189, Clearinghouse for Federal Scientific and Technical Information, U. S. Dept. of Commerce, Washington D. C..

BORISOV, A. A., Al. A. BORISOV, S. S. KUTATELADZE and V. E. NAKORYAKOV [**1983**], *Rarefaction Shock Wave Near the Critical Liquid-Vapor Point*, J. Fluid Mech. **126**, 59–73.

BUKIET, B. G., K. S. LACKNER and R. MENIKOFF [**1993**], *Understanding Curved Detonation Waves*, Los Alamos National Laboratory, Report LA-UR-93-1723, Los Alamos, NM.

COLELLA, P. [**1982**], *Glimm's Method for Gas Dynamics*, SIAM J. Sci. Stat. Comp. **3**, 76–110.

COLELLA, P. and L. HENDERSON, [**1990**], *The von Neumann paradox for the diffraction of weak shock waves*, J. Fluid Mech. **213**, 71–94.

COURANT, R. and K. O. FRIEDRICHS [**1948**], *Supersonic Flow and Shock Waves*, Springer Verlag, New York.

COWPERTHWAITE, M. [**1969**], *Relationships between Incomplete Equations of State*, Journal of the Franklin Institute **287**, 379–387.

CRAMER, M. S. [**1989**], *Negative Nonlinearity in Selected Fluorcarbons*, Phys. Fluids **A 1**, 1894–1897.

CRAMER, M. S. and R. N. FRY [**1993**], *Nozzle Flows of Dense Gases*, Phys. Fluids **A 5**, 1246–1259.

CRAMER, M. S. and A. KLUWICK [**1984**], *On the Propagation of Waves Exhibiting both Positive and Negative Non-Linearity*, J. Fluid Mech. **142**, 9–37.

CRAMER, M. S. and R. SEN [**1987**], *Exact Solutions for Sonic Shocks in van der Waals Gases*, Phys. Fluids **30**, 377–385.

DAVIS, W. [**1985**], *Equation of State for Detonation Products*, in Eighth International Detonation Symposium, J. Short, ed., NSWC MP 86-194, Naval Surface Weapons Center, White Oak, Silver Spring, MD, 785–795.

DUKOWICZ, J. K. [**1985**], *A General Non-Iterative Riemann Solver for Godunov's Method*, J. Comp. Phys. **61**, 119–137.

DUKOWICZ, J. K. and B. J. A. MELTZ [**1992**], *Vorticity Errors in Multidimensional Lagranian Codes*, J. Comp. Phys. **99**, 115–134.

DUVALL, G. E. and R. A. GRAHAM [**1977**], *Phase Transitions Under Shock-Wave Loading*, Revs. Mod. Phys. **49**, 523–579.

ELIEZER, S., A. GHATAK and H. HORA [**1986**], *An Introduction to Equation of State: Theory and Applications*, Cambridge Univ. Press, New York.

FICKETT, W. and W. C. DAVIS [**1979**], *Detonation*, Univ. of Calif. Press, Berkeley.

FOWLES, G. R. [**1981**], *Stimulated and Spontaneous Emission of Acoustic Waves from Shock Fronts*, Phys. Fluids **24**, 220–227.

——— [**1993**], *On the Evolutionary Condition for Stationary Plane Waves in Inert and Reactive Substances*, in Shock Induced Transitions and Phase Structures in General Media, J. E. Dunn, R. Forsdick and M. Slemrod, eds., IMA vol 52, Springer-Verlag, New York, 93–110.

Freistühler, H. and E. B. Pitman [**1992**], *A Numerical Study of a Rotationally Degenerate Hyperbolic System. Part I. The Riemann Problem*, J. Comp. Phys. **100**, 306–321.

Friedman, M. P. [**1961**], *A Simplified Analysis of Spherical Blast Waves*, J. Fluid Mech. **11**, 1–15.

Garabedean, P. [**1986**], *Partial Differential Equations*, Chelsea Publishing Co., New York, chap. 2 First order scalar quasi-linear PDEs in 2 indep. variables.

Glass, I. I. and W. Liu [**1978**], *Effects of Hydrogen Impurities on Shock Structure and Stability in Ionizing Monatomic Gases*, J. Fluid Mech. **84**, 55–77.

Glaz, H., P. Colella, I. I. Glass and R. L. Deschambault [**1985**], *A Numerical Study of Oblique Shock Wave Reflections with Experimental Comparisons*, Proc. R. Soc. Lond. **A 398**, 117–140.

Glimm, J. [**1965**], *Solutions in the Large for Nonlinear Hyperbolic Systmes of Equations*, Comm. Pure Appl. Math. **18**, 697–715.

Glimm, J., C. Klingenberg, O. McBryan, B. Plohr, D. Sharp and S. Yaniv [**1985**], *Front Tracking and Two Dimensional Riemann Problems*, Adv. Appl. Math. **6**, 259–290.

Gottlieb, J. J. and C. P. T. Groth [**1988**], *Assessment of Riemann Solvers for Unsteady One-Dimensional Inviscid Flows of Perfect Gases*, J. Comp. Phys. **78**, 437–458.

Grove, J. W. and R. Menikoff [**1990**], *The Anomalous Reflection of a Shock Wave at a Material Interface*, J. Fluid Mech. **219**, 313–336.

Grun, J., J. Stamper, C. Manka, J. Resnick, R. Burris, J. Crawford and B. H. Ripin [**1991**], *Instabilities of Taylor-Sedov Blast Waves Propagating through a Uniform Gas*, Phys. Rev. Letters **66**, 2738–2741.

Harten, A., P. Lax and B. van Leer [**1983**], *On Upstream Differencing and Godunov-Type Schemes for Hyperbolic Conservation Laws*, SIAM Review **25**, 35–61.

Henderson, L. F. [**1988**], *On the Refraction of Longitudinal Waves in Compressible Media*, Lawrence Livermore National Laboratory, Report UCRL-53853, Livermore, CA.

Hornung, H. [**1986**], *Regular and Mach Reflection of Shock Waves*, Ann. Rev. Fluid Mech. **18**, 33–58.

Isaacson, E., D. Marchesin, C. F. Palmeira and B. Plohr [**1992**], *A Global Formalism for Nonlinear Waves in Conservation Laws*, Comm. Math. Phys. **146**, 505–552.

Isaacson, E., D. Marchesin, B. Plohr and B. Temple [**1988**], *The Riemann Problem Near a Hyperbolic Singularity: the classification of Quadratic Riemann Problems I*, SIAM J. Appl. Math. **48**, 1009–1032.

Isaacson, E. and B. Temple [**1992**], *Nonlinear Resonance in Systems of Conservation Laws*, SIAM J. Appl. Math. **52**, 1260–1278.

Jahn, R. G. [**1956**], *The Refraction of Shock Waves at a Gaseous Interface*, J. Fluid Mech. **1**, 457–489.

Jones, D., P. Martin and C. Thornhill [**1951**], *A Note on the Pseudo-Stationary Flow Behind a Strong Shock Diffracted or Reflected at a Corner*, Proc. Roy. Soc. London **A 209**, 238–248.

Kerrisk, J. F. and J. K. Meier [**1992**], *Comparison between Fast Shock Tube Calculations and Tests*, in Shock Compression of Condensed Matter–1991, S. C. Schmidt, R. D. Dick, J. W. Forbes and D. G. Tasker, eds., Elsevier Science Publishing Co., New York, 1049–1052.

Lax, P. [**1957**], *Hyperbolic Systems of Conservation Laws II*, Comm. Pure Appl. Math. **10**, 537–556.

———— [**1972**], *Hyperbolic Systems of Conservation Laws and the Mathematical Theory of Shock Waves*, in Regional Conf. Series Lectures in Appl. Math., Vol. 11, SIAM, Philadelphia.

Leer, B. van [**1979**], *Towards the Ultimate Conservative Difference Scheme. V. A Second-Order Sequel to Godunov's Method*, J. Comp. Phys. **32**, 101–136.

Liu, T.–P. [**1975**], *The Riemann Problem for General Systems of Conservation Laws*, J. Differential Equations **18**, 218–234.

———— [**1976**], *The Entropy Condition and the Admissibility of Shocks*, J. Math. Analysis and Applications **53**, 78–88.

———— [**1979**], *Quasilinear Hyperbolic Systems*, Comm. Pure Appl. Math. **68**, 141–172.

———— [**1986**], *Shock Waves for Compressible Navier-Stokes Equations are Stable*, Comm. Pure Appl. Math. **39**, 565–594.

———— [**1987a**], *Nonlinear Resonances for Quasilinear Hyperbolic Equations*, J. Math. Phys. **28**, 2593–2602.

———— [**1987b**], *Hyperbolic Conservation Laws with Relaxation*, Commun. Math. Physics **108**, 153–175.

Marsden, J. E. and T. J. R. Huges [**1983**], *Mathematical Foundations of Elasticity*, Prentice-Hall, Inc., Englewood Cliffs, NJ.

Marsh, S. P. [**1980**], *LASL Shock Hugoniot Data*, University of California Press, Berkeley.

Marsh, S. P. and T.–H. Tan [**1992**], *Hypervelocity Plate Acceleration*, in Shock Compression of Condensed Matter–1991, S. C. Schmidt, R. D. Dick, J. W. Forbes and D. G. Tasker, eds., Elsevier Science Publishing Co., New York, 1033–1039.

McQueen, R. G. [**1991**], *Shock waves in Condensed Matter*, in High-Pressure Equations of State: Theory and Applications, S. Eliezer and R. A. Ricci, eds., Proceedings of the Enrico Fermi International School of Physics, vol. **CXIII**, Elsevier Science Publishing Co., New York, 101–216.

Meier, J. K. and J. F. Kerrisk [**1992**], *An Introduction to the Fast Shock Tube*, in Shock Compression of Condensed Matter–1991, S. C. Schmidt, R. D. Dick, J. W. Forbes and D. G. Tasker, eds., Elsevier Science Publishing Co., New York, 1045–1048.

Menikoff, R. [**1989**], *Analogies Between Riemann Problem for 1-D Fluid Dynamics and 2-D Steady Supersonic Flow*, in Contemporary Mathematics, W. B. Lindquist, ed., vol. **100**, American Mathematical Society, Providence RI, 225–240, Proceedings of the 1988 Joint Research Conference on Current Progress in Hyperbolic Systems: Riemann Problems and Computations.

———— [**1994**], *Errors when Shock Waves Interact Due to Numerical Shock Width*, SIAM J. Sci. Comput. **15**, 1227–1242.

Menikoff, R., K. Lackner, N. Johnson, S. Colgate, J. Hyman and G. Miranda [**1991**], *Shock wave driven by a phased Implosion*, Phys. Fluids A **3**, 201–218.

Menikoff, R. and K. S. Lackner [**1991**], *Fluid Flow in a supersonic Peristaltic Pump*, in Viscous Profiles and Numerical Methods for Shock Waves, M. Shearer, ed., SIAM, Philadelphia.

———— [**1992**], *Generating Strong Shock Waves with a Supersonic Peristaltic Pump*, in Shock Compression of Condensed Matter–1991, S. C. Schmidt, R. D. Dick, J. W. Forbes and D. G. Tasker, eds., Elsevier Science Publishing Co., New York, 1041–1044.

Menikoff, R. and B. Plohr [**1989**], *Riemann Problem for Fluid Flow of Real Materials*, Revs. Mod. Phys. **61**, 75–130.

More, R. M., K. H. Warren, D. A. Young and G. B. Zimmerman [**1988**], *A New Quotidan Equation of State for Hot Dense Matter*, Phys. Fluids **31**, 3059–3078.

Morris, C. E. [**1991**], *Shock-Wave Equation of State Studies at Los Alamos*, Shock Waves **1**, 213–222.

Morris, C. E., E. D. Loughran, G. F. Mortensen, G. T. Gray and M. S. Shaw [**1990**], *Shock Induced Dissociation of Polyethylene*, in Shock Compression of Condensed Matter–1989, S. C. Schmidt, J. N. Johnson and L. W. Davison, eds., Elsevier Science Publishing Co., New York, 687–690.

Morris, C. E., R. G. McQueen and S. P. Marsh [**1984**], *Mach Disc in Cylindrical Recovery System*, in Shock Compression of Condensed Matter–1983, J. R. Asay, R. A. Graham and G. K. Straub, eds., Elsevier Science Publishing Co., New York, 207–210.

Munz, C.–D. [**1988**], *On the Numerical Dissipation of High Resolution Schemes for Hyperbolic Conservation Laws*, J. Comp. Phys. **77**, 18–39.

Neumann, J. von and R. D. Richtmyer [**1950**], *A Method for the Numerical Calculation of Hydrodynamic Shocks*, J. Appl. Phys. **21**, 232–237.

Noh, W. F. [**1987**], *Errors for Calculations of Strong Shocks Using an Artificial Viscosity and an Artificial Heat Flux*, J. Comp. Phys. **72**, 78–120..

Poirier, J.–P. [**1991**], *Introduction to the Physics of the Earth's Interior*, Cambridge Univ. Press, New York.

Rice, M., R. McQueen and J. Walsh [**1958**], *Compression of Solids by Strong Shock Waves*, in Solid State Physics Vol. 6, F. S. and D. Turnbull, ed., Academic Press, New York, 1–63.

Richtmyer, R. D. and K. W. Morton [**1967**], *Difference Methods for Initial-Value Problems*, Interscience, New York.

Roe, P. L. [**1986**], *Characteristic-Based Schemes for the Euler Equations*, Ann. Rev. Fluid Mech **18**, 337–365.

Schultz, W. D. [**1964**], *Tensor Artificial Viscosity for Numerical Hydrodynamics*, J. Math. Phys. **5**, 133–138.

Sheffield, S. A. and R. L. Gustavsen [**1993**], *Unreacted Hugoniots for Porous and Liquid Explosives*, Los Alamos report, LA-UR-93-2344, APS conference.

Smith, R. [**1979**], *The Riemann Problem in Gas Dynamics*, Trans. Am. Math. Soc. **249**, 1–50.

Smoller, J. [**1983**], *Shock Waves and Reaction Diffusion Equations*, Springer-Verlag, New York.

Strikwerda, J. C. [**1989**], *Finite Difference Schemes and Partial Differencial Equations*, Wadsworth & Brooks, Belmont, Calif..

Thompson, P. A. [**1971**], *A Fundamental Derivative in Gasdynamics*, Phys. Fluids **14**, 1843–1849.

Thompson, P. A., G. C. Carofano and YG. Kim [**1986**], *Shock Waves and Phase Changes in a Large-Heat-Capacity Fluid Emerging from a Tube*, J. Fluid Mech. **166**, 57–92.

Thompson, P. A. and K. C. Lambrakis [**1973**], *Negative Shock Waves*, J. Fluid Mech. **60**, 187–208.

Wendroff, B. [**1972**], *The Riemann Problem for Materials with Non-Convex Equations of State: I Isentropic Flow; II General Flow*, J. Math. Anal. Appl. **38**, 454–466; 640–658.

Weyl, H. [**1949**], *Shock Waves in Arbitrary Fluids*, Commun. Pure Appl. Math. **II**, 103–122.

Whitham, G. B. [**1974**], *Linear and Nonlinear Waves*, J. Wiley, New York.

Zel'dovich, Y. and Y. Raizer [**1966**], *Physics of Shock Waves and High-Temperature Hydrodynamic Phenomena*, Academic Press, New York.

Zucrow, M. J. and J. D. Hoffman [**1977**], *Gas Dynamics, Vol. 2,*, John Wiley, NY.